Photodynamic inactivation of microbial biofilms: impact of Hsp70 expression and non-invasive optical monitoring of oxygen during photodynamic inactivation

Dissertation zur Erlangung des Doktorgrades der Naturwissenschaften (Dr. rer. nat.)

an der Fakultät für Chemie und Pharmazie der Universität Regensburg

vorgelegt von

Fernanda Pereira Gonzales

aus Brazilien

Regensburg, April 2013

Photodynamic inactivation of microbial biofilms: impact of Hsp70 expression and non-invasive optical monitoring of oxygen during photodynamic inactivation

Doctoral Thesis

by

Fernanda Pereira Gonzales

Submitted to the

Faculty of Chemistry and Pharmacy

University of Regensburg

April 2013

Diese Doktorarbeit entstand im Zeitraum von April 2009 bis April 2013 am Institut für Analytische Chemie, Chemo- und Biosensorik, Universität Regensburg.

Die Arbeit wurde angeleitet und begleitet von Prof. Dr. Otto S. Wolfbeis

Promotionsgesuch eingereicht am: 08.04.2013
Kolloquiumstermin: 08.05.2013

Prüfungsausschuß: Vorsitzender: Prof. Dr. Burkhard König

Erstgutachter: Prof. Dr. Otto Wolfbeis

Zweitgutachter: PD Dr. Tim Maisch

Drittprüfer: Prof. Dr. Joachim. Wegener

Table of contents

List of abbreviations and symbols

ABC	ATP binding cassette
AmB	amphotericin B
APDT	antimicrobial photodynamic therapy
ATCC	American Type Culture Collection
BCA	bicinchoninic acid
CDR	*Candida* drug resistance
CFU	colony forming unit
ConA	concanavalin A
EDTA	ethylenediaminetetraacetic acid
EPI	inhibitor of efflux pump
EPS	extracellular polymeric substance
FBS	fetal bovine serum
FKS	glucan synthase genes
GAPDH	glycerinaldehyd-3-phosphat-dehydrogenase
H_2O_2	hydrogen peroxide
HO*	hydroxyl radical
HRP	horseradish peroxidase
ICU	intensive care units
ISC	intersystem crossing
LPS	lipopolysaccharides
MB	methylene blue
MDR	multidrug resistance
MFS	major facilitator super family
MIC	minimum inhibitory concentrations
MRSA	methicillin-resistant *Staphylococcus aureus*
MTT	(3-(4,5-dimethylthiazol-2-yl)-2,5-diphenyltetrazolium bromide,
MW	molecular weight
NaN_3	sodium azide
NPe6	mono-L-aspartyl chlorin-e6
OD	optical density
$^1O_2$	singlet oxygen
O^{2-}	superoxide anions
ROS	reactive oxygen species
SDB	sabouraud Dextrose Broth
TB	toluidine Blue
PBS	phosphate buffered saline
PH-II	photofrin
PS	photosensitizer
Pt-TFPP	platinum(II)-5,10,15,20-tetrakis(2,3,4,5,6-pentafluorophenyl porphyrin
SDA	sabouraud dextrose agar
SDS	sodium dodecyl sulfate
SnET2	tin etio-purpurin
TMPyP	(5,10,15,20-Tetrakis(1-methyl-4-pyridyl)-21H,23H-porphine, tetra-p-tosylate salt)
TBS-T	tris-buffered saline tween

THF   tetrahydrofuran
TSB   tryptic soy broth
Φ_Δ quantum yield

1. Introduction

1.1 Aim of the study

The frequency of opportunistic fungal infections has considerably increased in the last 20 years and they currently represent a global health problem [2]. This increasing incidence of fungal infection is directly related to the growing number of immunocompromised individuals, resulting from medical advances in healthcare, such as the introduction of newer methods for hematopoietic stem cell transplantation, the evolution of organ transplantation practices, and the use of novel immunosuppressive agents [3].

An epidemiological study in the United States showed that the number of sepsis cases caused by fungal organisms increased by 207 % between 1979 and 2000 [4]. In the United States, the incidence of bloodstream infections varies between 0.28 to 0.96 per 1.000 patients admissions, and 0.2 to 0.38 in Europe, whereas in Latin America these rates vary between 1.2 and 5.3 [5].

The most frequently diagnosed fungal infections are caused by *Candida albicans, Cryptococcus neoformans,* and *Aspergillus fumigatus*. These pathogens can cause skin and mucous membrane infections or invasive fungal infections, particularly in immunocompromised patients. In these patients, invasive fungal infections are often associated with high morbidity and mortality [6, 7].

Fungal infections are difficult to treat successfully. The number of antifungal agents available to treat this kind of infections is limited. In fact, it took 30 years for the newest class of antifungal drugs, the echinocandins, to progress from bench-to-beside.

and they are the newest class of antifungal agents available since 2001 [8]. The gold standard therapy for many invasive fungal infections is amphotericin B (AmB), which was discovered nearly 50 years ago. The emergence of antifungal resistance has also decreased the efficacy of conventional therapies. In addition, treatments are time-consuming and thus demanding on health care budgets. Current drugs have only a limited spectrum of action and toxicity, and drug interactions are common. Furthermore, fungal and mammalian cells share many structures and metabolic pathways, limiting the design of drugs that selectively target cells from human hosts [9].

For these reasons, effective alternatives are required to treat fungal superficial and localized infections, mainly in immunocompromised patients, which are highly susceptible to infections, due to their highly compromised immune system. A promising alternative is antimicrobial Photodynamic Therapy (aPDT), originally developed for the treatment of skin tumors [10]. APDT combines a photoactive molecule, termed photosensitizer, light, and oxygen to produce cytotoxic reactive oxygen species (ROS), such as singlet oxygen or oxygen radicals, which are able to eliminate pathogens [11].

Therefore, the photodynamic action of the new porpyhrine-derivative photosensitizer, XF-73 was investigated against both planktonic and biofilm growing *C. albicans*. The efficacy of aPDT was compared to the efficacy of Amphotericin B (AmB). Furthermore, the mechanism of action of XF-73-aPDT in *C. albicans* biofilms was investigated.

The mechanisms of resistance to aPDT are not completely elucidated, and heat shock proteins overexpression is a mechanism of resistance, whereby cells could develop resistance to aPDT. Therefore, the role of heat shock protein 70 (Hsp70) expression by *C. albicans* was investigated regarding their protecting properties against oxidative stress, caused by aPDT. In addition, a new optical sensor technology was used

to monitor in a non-invasive manner the oxygen concentration in *C. albicans* and *S. epidermidis* biofilms during aPDT, which could be a new possibility to improve the efficacy of aPDT. In the future, this therapy might either substitute or act as coadjuvant in the conventional antimicrobial therapy.

1.2 History of Antimicrobial Photodynamic Therapy

Antimicrobial Photodynamic therapy (APDT) was first reported in 1900 by Oskar Raab in Munich. He observed that the protozoan *Paramecium caudatum* was killed after staining with acridine orange and subsequent exposure to light under certain wavelengths [12]. Additional experiments showed that oxygen was also essential in the photodynamic action, because antibacterial activity of fluorescent dyes against the facultative anaerobic species *Proteus vulgaris* could not be demonstrated in the absence of oxygen. Fig. 1 shows the results of the first antimicrobial photodynamic experiment using the photosensitizer (PS) eosin in combination with sun light to kill *Streptococcus* bacteria. In 1903, H. von Tappeiner and A. Jesionek treated skin tumours with topically applied eosin and white light. This phenomenon was coined "photodynamic action"[13].

With the discovery of antibiotics, starting with penicillin in 1929 followed by the golden age of antibiotics, in the 1950's, when one-half of today's commonly used drugs were discovered, aPDT lost its attention. At this time, many experts believed that the problematic with infectious diseases is over. But the widespread and sometimes inappropriate use of antibiotics, the use of antibiotics in the food and farming industries led all soon to the appearance of antibiotic resistant strains [14]. In fact, resistant strains

started to be reported already in 1955, four years after penicillin was available on the

market [15].

To date, approximately 70% of bacteria, which cause hospital acquired

infections, are resistant to at least one antibiotic used to treat them, and some organisms

are resistant to all approved antibiotics and can only be treated with experimental and

potentially toxic drugs [16].

$+++$ sehr reichliches Wachstum,
$++$ reichliches Wachstum,
$+$ geringes Wachstum,
L einzelne Kolonien,
0 kein Wachstum.

I. Versuche am Tageslichte.

1. Versuch mit Streptokokken.

26. I. Streptokokkenbouillon wird ungefärbt, mit Eosin bzw. Erythrosin gefärbt dunkel und am Lichte 1, 3 und 6 Stunden lang exponiert. Lichtverhältnisse: hell, keine Sonne.

Dauer d. Exposition	1 Stunde		3 Stunden		6 Stunden		Kontroll nicht exponiert	
Wachstum am . .	1. Tag	2. Tag	1. Tag	2. Tag	1. Tag	2. Tag	1. Tag	2. Tag
Bouillon ungefärbt	+++	+++	+++	+++	+++	+++	+++	+++
Bouillon mit Eosin gefärbt	++	++	0	0	0	0	+++	+++
Bouillon mit Ery- throsin gefärbt .	++	++	0	0	0	0	+++	+++

Fig. 1. First antimicrobial photodynamic experiment (1905) using eosin combined with day light to kill *streptococci*. Adopted from: [17]

The increasing threat of microbial resistance has highlighted aPDT as a

promising alternative treatment for localized and superficial infections [18]. Currently,

in many countries aPDT is an approved additional therapy for the treatment of

periodontal disease, dental infections and infected leg ulcers. In the future, it has the

potential to become the standard therapy for infectious localized and superficial

diseases. In this way, effective systemic agents can be withheld for more life-

threatening infections.

1.2.1 **Mechanism of action**

After a photosensitizer (PS) absorbs a photon of light of an appropriate wavelength, this molecule will be promoted from its ground state to the excited singlet state, which is short lived with a half-life between 10^{-6} and 10^{-9} s [19, 20]. Then, the PS can return to the ground state, by emitting a photon as light energy (fluorescence) or heat. Alternatively, the molecule may convert via intersystem crossing (ISC) to the triplet state. The triplet state PS has lower energy than the singlet state, but it has a longer lifetime (10^{-3} s). The PS in the triplet state can return to the ground state by a phosphorescence process (P) or interact with oxygen by two mechanisms: (Fig. 2).

In the **type I mechanism**: the triplet state PS can transfer electrons to surrounding biomolecules producing radicals, like superoxide anions (O^{2-}) and hydroxyl radical (HO*). These radicals can further react with oxygen to generate hydrogen peroxide (H_2O_2). All of them are able to attack cellular targets [21, 22]. In **type II mechanism** there is a transfer of energy from the excited triplet state PS to the oxygen, producing the electronically excited and highly reactive singlet oxygen ($^1O_2$), which is able to react to cell membranes, peptides, and nucleic acids (Fig. 2) [23]. However, DNA damage seems not to be the main cause of cell death, since *Deinococcus radiodurans*, which is known to have a very efficient DNA repair mechanism, is readily killed by the photodynamic process [24]. The photodynamic mechanism damages fungal cells by generation of reactive oxygen species (ROS), which can perforate cell walls and membranes. Furthermore, when the PS is taken up intracellularly, ROS generated by light excitation induce photodamage to internal cell organelles. All these oxidizing processes lead to a final cell death [21, 25].
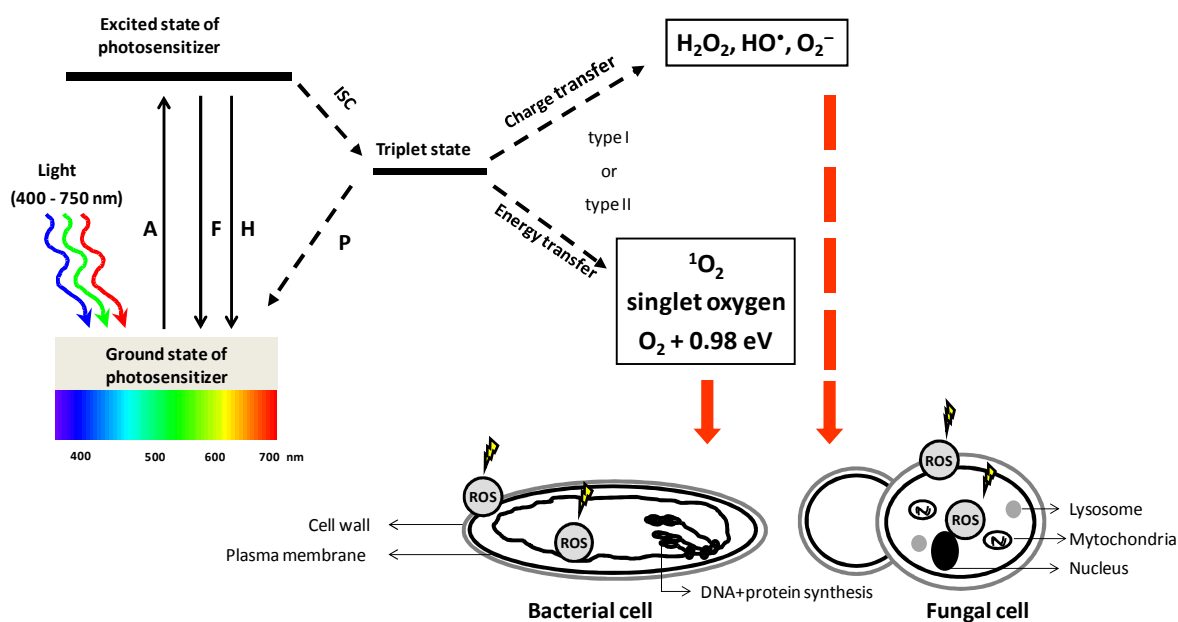
Fig. 2: Schematic illustration of mechanism of action of aPDT: Generation of ROS can follow two alternative pathways after light activation by a given PS. Upon absorption (A) of a photon by the ground state PS, the excited state of the PS is formed. The excited state is short-lived and can undergo intersystem crossing (ISC) to a long-lived triplet state or, alternatively, can return to the ground state by fluorescence emission (F) or heat (H) or both. In the triplet state the PS can return to the ground state by phosphorescence (P) or interact with oxygen by two mechanisms: Type I: Generation of superoxide anions (O_2^-), hydroxyl radical (HO^*) and hydrogen peroxide (H_2O_2) by charge transfer from the excited PS. Type II: The triplet state of PS can directly undergo energy exchange with triplet ground state oxygen, leading to the formation of singlet oxygen, $^1O_2$. The generated ROS rapidly react with their environment, depending on the localization of the excited PS: microorganism walls, lipid membranes, peptides, and nucleic acids.

1.2.2 Susceptibility of pathogens to aPDT

Differences in the cell wall structure and cell size account for the different pattern of susceptibility to aPDT between different microbial cells, like bacteria and fungi (Fig. 3). Cationic PSs are the predominant type of all current PS employed in aPDT. The mechanism of action of positive charged PSs may be the "self-promoted uptake pathway", where the cationic molecules displace the divalent cations, Ca^{2+} and Mg^{2+} on the outer membrane and bind to lipopolysaccharides (LPS), increasing the permeability of the outer membrane to cationic PSs [11, 26].

The cytoplasmic membrane of Gram-positive bacteria is surrounded by an outer wall composed of peptydoglican, lipoteichoic and teichoic acids, with no significant amount of lipids or proteins. This peptidoglycan network is thick but relatively porous, allowing photosensitizer, independently of their charge, to cross (Fig. 3 A). In contrast, the outer layer of Gram-negative bacteria is a highly complex multilayered structure, consisting of a periplasmic space, containing enzymes and other components, a few layers of peptidoglycan and an additional lipid membrane, containing strongly negatively charged lipopolysaccharides (LPS), lipo-proteins and proteins with porin function (Fig. 3 B). Thus, the outer layer of Gram-negative bacteria represents a very effective permeability barrier between the cell and its environment, tending to restrict the binding and penetration of many photosensitizer structures. The efficacy of aPDT against Gram-negative bacteria can be increased by the addition of biological or chemical molecules, *e.g.* polymyxin B or Ethylenediaminetetraacetic acid (EDTA), which are known to be membrane disrupting agents [27].

Cells of fungi like *C. albicans* are even more resistant to aPDT than Gram-positive and Gram-negative bacteria (Fig. 3 C). They are enveloped by a thick cell wall, composed of glucan, mannan, and chitin and have a nuclear membrane, protecting the nucleus and acting as a barrier either to the penetration of photosensitizers or the reactive oxygen species formed during the treatment. The presence of nuclear membrane also restricts the mutagenic potential from aPDT. Besides, fungal cells are larger than bacterial cells, presenting more targets to be damaged; consequently the amount of reactive oxygen species necessary to kill yeasts is much greater than the amount necessary to kill bacteria [1, 28].
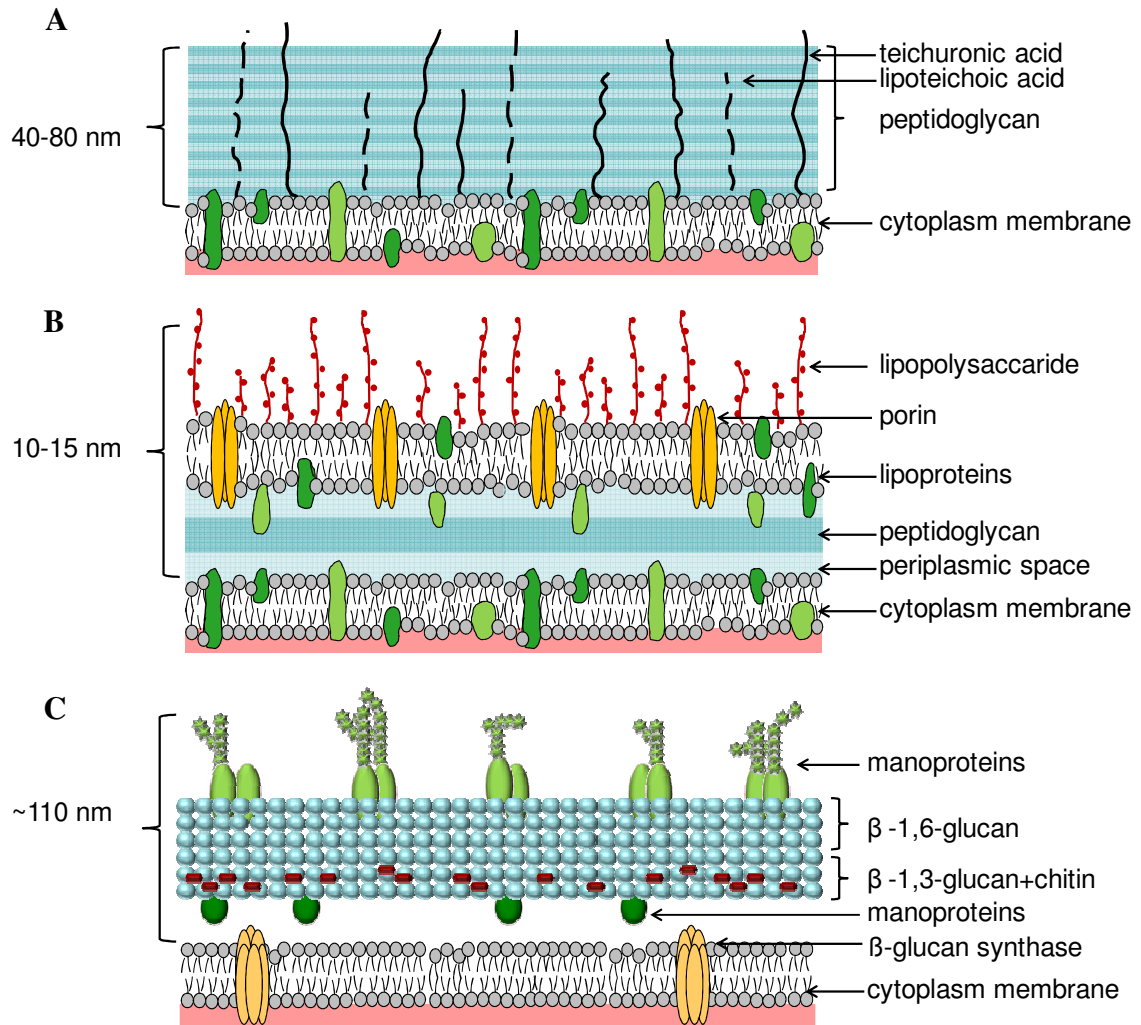
Fig. 3. Cell wall of A) Gram-positive bacteria, B) Gram-negative bacteria and C) fungal cells. Modified from reference [29]

1.2.3 **Irradiation parameters**

To achieve maximum treatment efficacy, one of the most important factors concerning the choice of the light source is that the emission spectrum of the used light source matches the absorption spectra of the PS used. In addition, sufficient light intensity should be delivered at the site where the PS-loaded pathogen is localized, like the skin or mucosal surfaces. Light of longer wavelength (>500 nm) have a deeper penetration in biological tissues. Therefore, it is important to find an agreement with regard to the penetration depth of light, the absorption spectrum of the PS used, and the location sites of the pathogen [30].

Irradiation parameters depend on the application of interest. Decolonization of microorganisms growing on the surface of the skin, affecting just the stratum corneum, will be inactivated by blue light (~400 nm). In deeper infections where microorganisms colonize the stratum corneum and hair follicles, red light (~600 nm) is necessary. Power outputs for light sources in a PDT are usually in the range of 10–100 mW cm^{-2}, with total light doses between 10 and 200 J cm^{-2}. One crucial point in light dosimetry is to avoid thermal effects by the light itself, when light doses above 100 mW cm^{-2} are needed for an efficient aPDT [21].

1.2.4 **Photosensitizers**

There are additional criteria that a given PS should fulfill: (I) efficacy against several classes of microorganisms at relatively low concentrations and low light fluence, (II) no dark toxicity, (III) selectivity for microbial cells over human cells, (IV) hydrophilic properties and electric positive charges, due to the penetration in the microbial cell wall, (V) high extinction coefficients to efficiently absorb blue or red light and (VI) high triplet and singlet oxygen quantum yields [31]. There are several PSs used to photoinactivate microbial cells, most of them belonging to three chemical groups: phenothiazines, porphyrins and phthalocyanines.

1.2.4.1   Phenothiazines

Phenothiazinium dyes have been employed in medical practice for over 100 years [32]. As a consequence, the toxicity of these dyes is well documented and they are the only PSs clinically used in aPDT so far (Table 1).

Table 1. Some antimicrobial photosensitizers available on the market worldwide. Adopted from ref: [33]

Photosensitizer	Infections treated	Country	Company
Phenotiazine derivatives	Periodontal disease	Canadá	Periowave
Phenotiazine derivatives	Dental infection	Germany	Helbo
Methylene blue	Dental infection	Brazil	Aptivalux
Phenotiazine derivatives	Dental infection	UK	DenFotex
Phenotiazine derivatives	Infected leg ulcers	UK	Photopharmica

Phenothiazinium PSs are planar, tricyclic, aromatic molecules, presenting intrinsic positive charge and blue color with an intense absorption between 600 and 680 nm. The most used phenothiazines in aPDT are methylene blue (MB) and Toluidine Blue (TBO) (Fig. 4 A and 4 B, respectively). MB has a molecular weight (MW) 319.85 g mol^{-1} and a quantum yield of $\Phi_\Delta = 0.52$ [34]. It is used in the sterilization of blood products, since this PS has a high chemical affinity to the nucleic acids, which denotes its potential to application against virus, including HIV, hepatitis B and C [35, 36]. TBO has a MW of 305.83 g mol^{-1}. It is predominantly used in the treatment of oral infections, for sterilizing dental cavities and root canals, and for treating periodontitis [37].

A   **B**
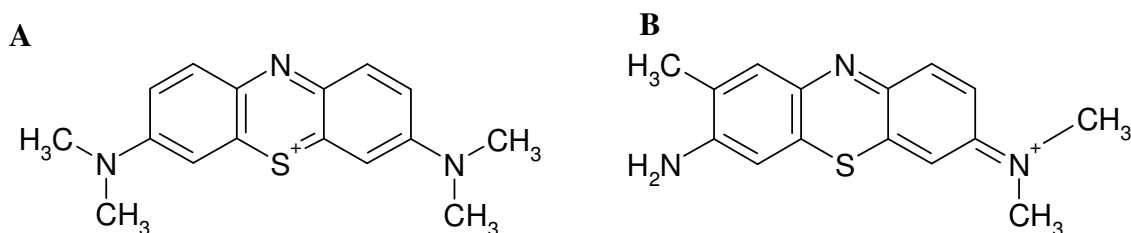
Fig. 4. Chemical structure of A) Methylene Blue and B) Toluidine Blue O

1.2.4.2   Porphyrins

Porphyrins are a group of naturally occurring intensely colored compounds, involved in a number of biologically important roles, like oxygen transport and photosynthesis, and have applications in a number of fields, ranging from fluorescence imaging to medicine. They are composed of four pyrrole rings, linked through four methine bridges (Fig. 5) [38]. Porphyrins have a strong absorption band around 400 nm (Soret band), but further absorption peaks between ~500-700 nm (Q-bands). So, a large number of porphyrins derivatives with different side groups have been synthesized, presenting higher absorption bands in the far red spectral region [39].
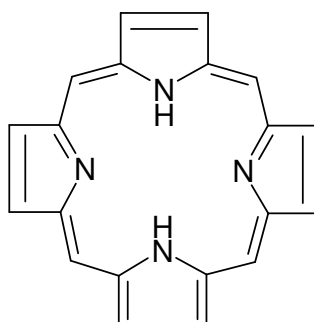
Fig. 5. Chemical structure of a porphyrin

1.2.4.3   TMPyP

TMPyP (5,10,15,20-Tetrakis(1-methyl-4-pyridyl)-21H,23H-porphine, tetra-p-tosylate salt) possesses four positive charges on the peripheral pyridinium rings and a molecular weight of 682.2 g mol^{-1} (Fig. 76). It is a well-known PS, which, besides the positive charges, has a high singlet oxygen production quantum yield of $\Phi\Delta = 0.77$ [40]. Furthermore, TMPyP has been shown to be an effective PS against *C. albicans* planktonic cells. These cells underwent 5 log$_{10}$ decrease inactivation, when incubated for 30 min with TMPyP and then irradiated for 30 min with an applied dose light of 90 J cm^{-2} [41]. Photoaction of TMPyP was also tested against *C. albicans* planktonic cells,

immobilized on agar surfaces. First of all, cells were treated with TMPyP in solution for 30 min and then placed on an agar surface. Then cells were illuminated for 30 min (90 J cm^{-2}). No colony formation on the agar surface was observed, for cells treated with 5 µM TMPyP. In the second condition, *C. albicans* cells were grown as a lawn on the agar surface with TMPyP impregnated in a small area. Cultures were kept in the dark for 30 min, allowing binding of TMPyP to cells. After this period, plates were illuminated for 30 min [42]. Growth of *C. albicans* cells was not detected in the area, treated with 4.5 nmol of TMPyP. Therefore, photoaction of TMPyP led to cell death on the agar surface. These results indicate that photodynamic inactivation of cells, growing *in vivo* as localized *foci* of infection, on skin or on an accessible area to be irradiated, might also be possible [42]. Furthermore, a later study, made by the same group, showed that the photokilling of *C. albicans* cells by TMPyP seems to be mainly mediated by singlet oxygen [43].
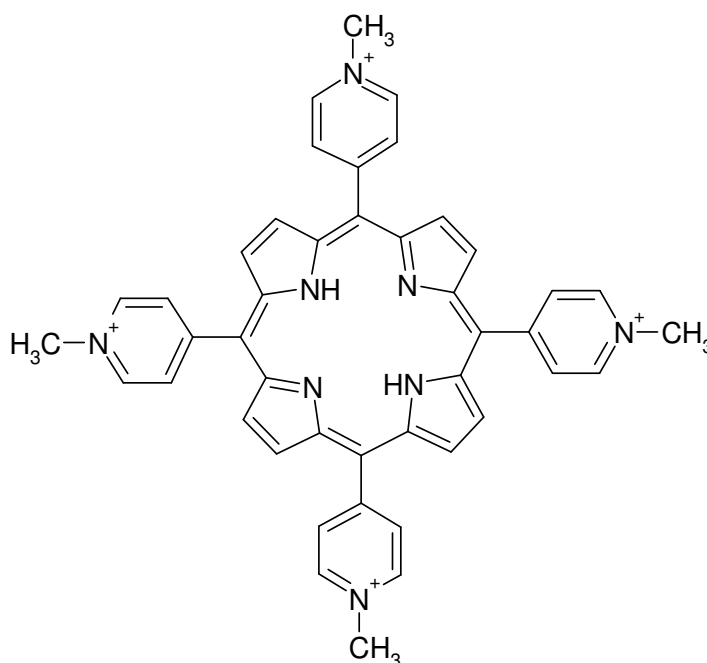
Fig. 6: Chemical structure of TMPyP

1.2.4.4   XF-73

XF-73 also belongs to the porphyrin-based class of photosensitizers, containing two

positive charges, being oppositely connected via a propyl chain to the ring system (Fig.

7) [44]. It has a MW of 694.81 g mol^{-1} and a singlet oxygen quantum yield of $\Phi\Delta = 0.57$

(singlet oxygen production quantum yield of XF-73 was measured in our laboratory,

according to the reference [40].) This PS was originally developed during a European

Union project, entitled "Dynamicro", for the development of a photodynamic treatment

to eradicate and control the current spread of infectious antibiotic resistant

microorganisms in humans (Destiny Pharma, UK).
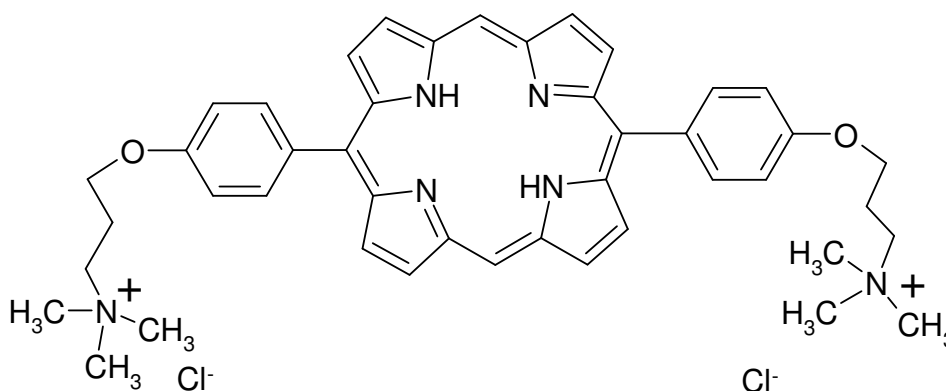
Fig. 7: Chemical structure of XF-73

So, the charges have a high mobility to interact with cell walls of

microorganisms [44]. So far XF-73 has shown a very high efficacy (reduction of >5

log$_{10}$) to kill bacteria of all known photosensitizers [45].

1.2.4.5   Phthalocyanines

Phthalocyanines consist of four pyrrolic rings, connected via nitrogen bonds (Fig. 8).
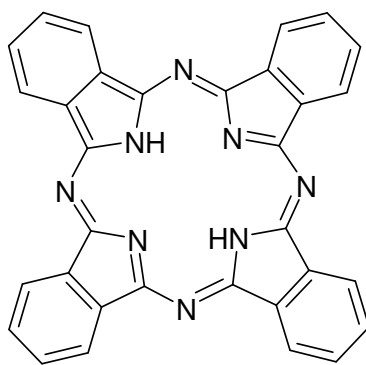
Fig. 8: Chemical structure of a phthalocyanine

These PSs have higher absorption in the far-red region of the spectrum (650-700 nm) and consequently optimal tissue penetration by light [46] . The addition of central metal ions, like Zn^{2+} (zinc phthalocyanine) or Al^{3+} (aluminium phthalocyanine), produce long triplet states and enhance their singlet oxygen production [47]. A recent study showed successful photoinactivation of *C. albicans* biofilms, using two different phthalocyanines PSs. There, biofilms were incubated for 1.5 h with 6 µM of a gallium phthalocyanine (GaPc) and a zinc phthalocyanine (ZnPc). Then they were irradiated with red light (635 nm). An applied dose of 50 J cm^{-2} caused ~5 log_{10} decrease of cell survival. The authors suggest that the susceptibility of *C. albicans* biofilms to aPDT with these two PSs are a potential value for treatment of denture associated infections in the future [48].

1.2.5 Reactive oxygen species: Singlet oxygen

Singlet oxygen is believed to be the main factor responsible for photodynamic action [49, 50]. This highly reactive oxygen species has a lifetime in biological systems as short as 10^{-6} s, and, consequently, limited diffusivity (<0.02 µm), which may enhance localized response, without damaging host tissues [51].

Multiple cellular targets are available for the photo-oxidative effect caused by singlet oxygen, including inactivation of enzymes and other proteins and peroxidation

of lipids, leading to the lyses of cell membranes, lysosomes, and mitochondria [25]. Thus, singlet oxygen, generated by the excitation of PSs, is a non-specific oxidizing agent, and there is so far no cellular defense against it [21]. Antioxidant enzymes, such as peroxide dismutase, catalase, and peroxidase, protect microbial cells against some oxygen radicals, but not against singlet oxygen, which even inactivates some antioxidant enzymes, for instance catalase and superoxide dismutase [52].

1.2.6 Mechanisms of resistance to aPDT

So far the potential mechanisms of resistance to aPDT are the general mechanisms of drug resistance and may be associated to active efflux, altered drug uptake or altered intracellular trafficking of the photosensitizer [53]. It was reported that phenothiaziniumbased PSs, such as MB, are substrates of multidrug resistance (MDR) pumps in both Gram-positive and in Gram-negative bacteria [54]. The authors proposed that specific MDR inhibitors could be used in combination with phenothiazinium salts to enhance their photokilling efficacy [54]. The ability to photoinactivate biofilm bacteria was also significantly enhanced when using an inhibitor of efflux pump (EPI) with MB [55].

ATP-binding cassette (ABC) transporters and major facilitator super family (MFS) in *C. albicans* can affect the killing effect of aPDT using MB and red light. *C. albicans* strains overexpressing MFS system showed a slightly protective effect of MB-aPDT phototoxicity, showing 1.5 $\log_{10}$ less reduction than parental cells. The effect of ABC overexpression was more prominent when compared with MFS overexpression in protecting against MB-mediated aPDT. Mutants overexpressing ABC transporters were resistant to aPDT killing, whereas the parental cells showed 5 $\log_{10}$ of killing under the same experimental conditions. The phototoxic effect of MB could be potentiated by the

ABC inhibitor verapamil, but not by the MFS inhibitor INF271. The authors suggested that the inhibition of fungal cell death, caused by the combination of aPDT-MB with MFS inhibitor may be explained by the hypothesis that the MFS channel can also serve as an uptake mechanism for MB [18].

However, PSs with molecular weights above 600-700 Da does not serve as substrate to efflux pumps, since porins exclude compounds above this molecular mass. Repetitive treatments of *Staphylococcus aureus* with a phthalocyanine derivative, which have a molar weight >1.300 Da did not induce the development of resistance. The authors supposed that larger PS molecules could not be internalized by the bacteria cells and that the PS molecules should accumulate in the superficial portions of the bacterial structures. Like that, the photodynamic action would promote oxidative damage at the exterior of the cell, causing cell wall or membrane disruption and consequent bacteria lyses [56].

Overall, the potential mechanisms of microorganisms to achieve resistance against aPDT, described above, are related to the PSs. In addition, antioxidant enzymes like superoxide dismutases and peroxidases protect cells against hydroxyl radicals, superoxide anions and hydrogen peroxide, which are ROS formed by the type I mechanism of action of aPDT. However, to date, no cellular defense against singlet oxygen is known (type II mechanism), which is proposed to be the predominant ROS formed during aPDT [21].

Heat shock proteins (Hsps) are a class of functionally related proteins, involved in the folding and unfolding of cellular proteins. These proteins are over expressed upon oxidative stress from the environment enabling microorganisms to survive such "stress situations" [57]. Therefore, the expression of Hsp might be increased upon the oxidative damage, caused by aPDT, preventing aggregation and refolding proteins, and thus can

be a mechanism, whereby microbial cells could become resistant to aPDT [58, 59]. The Hsps DnaK and GroEL were upregulated in *Escherichia coli* and *Enterococcus faecalis* after aPDT-mediated by TBO. Consequently, *E. coli* survival was improved by 2 $\log_{10}$ and *E. faecalis* by 4 $\log_{10}$. Combination of aPDT with an inhibitor of the HSP DnaK did not significantly potentiate the effect of aPDT in both microorganisms [60].

For *C. albicans* so far, it is not known, whether HSPs are upregulated after photodynamic treatment and also whether the overexpression of HSPs can protect *C. albicans* cells from the oxidative damage, caused during aPDT. But induction of heat shock response may not be enough to avoid cell death, since aPDT is a multihit process and many cellular sites can be damaged by the ROS, generated during the treatment [61].

1.2.7 **Microbial biofilms**

Biofilms are structured microbial communities, characterized by sessile cells that are attached to natural (living tissues, natural aquatic systems) or abiotic moist surfaces (indwelling medical devices, industrial or potable water system piping) and embedded in a extracellular polymeric substance (EPS), such as glycoproteins and polysaccharides, produced by these cells itself (Fig. 9). The EPS, one of the distinguishing characteristics of biofilms, is made of polymeric substances, comprising polysaccharides, proteins, glycopeptides, lipids, lipopolysacharides and other materials that serve as a scaffold, holding the biofilm together [62, 63].
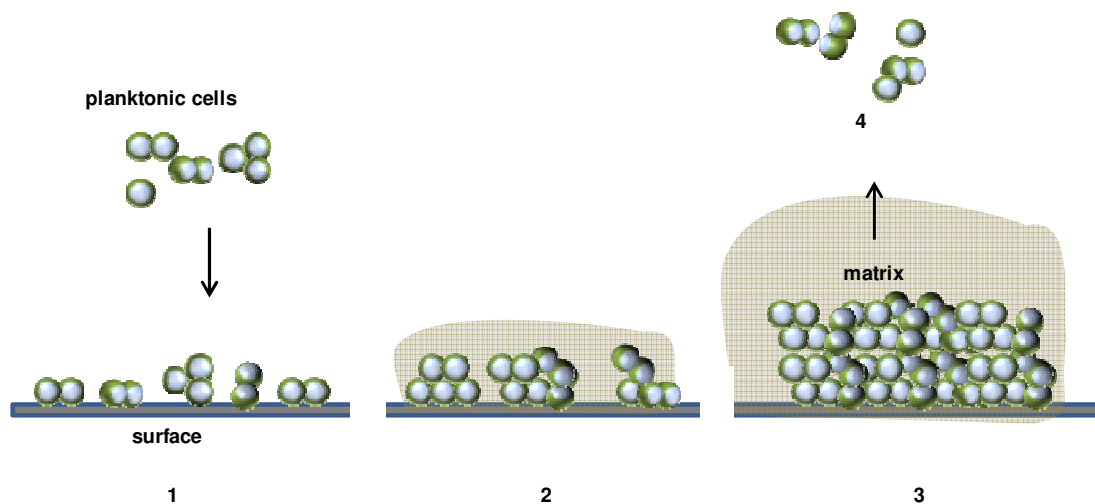
Fig. 9. Biofilm formation: 1. Biofilm formation starts with the adherence of planktonic cells (free floating cells) to a biotic or abiotic surface; 2. The attached cells start to multiply, form microcolonies and produce the EPS. 3. Microbial cells produce a large amount of EPS and the microbial groups increase in size and thickness; 4. In the final stage of biofilm formation, cells may detach and form new biofilms or dispersing infections.

Cells in a biofilm state show a distinct phenotype from those of their free-living planktonic counterparts by production of the EPS, reduced growth rates, and the up- and down-regulation of specific genes [63]. They constitute a unique niche for microbial growth, where these cells, attached to a surface and encased in the EPS, are protected from the action of antimicrobial agents and host cells [64]. Furthermore, biofilm is an organized community of cells, which are highly interactive and release molecule compounds termed autoinducers to communicate between them in a process called quorum sensing. This phenomenon regulates the number of microbial population and controls competition for nutrients. It has important implications in the infectious process, particularly for dissemination and for the establishment of distal sites of infection [65, 66]. *C. albicans* biofilms produce farnesol as a quorum sensing molecule, which blocks the yeast-to-hyphal conversion, required for biofilm formation [67].

The National Institutes of Health [68] states that 80% of all human microbial infections are caused by microorganisms (bacteria or fungi), growing in a biofilm state,

representing a serious problem in health care [68]. Of particular concern is the increased resistance of biofilms to antimicrobial agents compared to their planktonic counterparts. Microbial cells growing in a biofilm can tolerate antimicrobial agents at concentrations 10–1000-times higher than needed to kill genetically equivalent planktonic microbial cells, and are also resistant to phagocytosis, making biofilms extremely difficult to eradicate from living hosts [69, 70]. In addition, biofilms can also act as reservoirs for persistent sources of infection in a host [71, 72].

There are multiple mechanisms, which account for biofilm increased resistance, when compared to their planktonic counterparts. These mechanisms vary with the microorganisms present in the biofilm, and the drug being applied. One mechanism of biofilm resistance to antimicrobial agents is the failure of an agent to penetrate the full depth of the biofilm due to the presence of the EPS. This structure can act as a physical barrier, thereby inhibiting drug diffusion to the cells within the biofilm and reducing the concentration of the drug, reaching the cells in the biofilm. Another hypothesis is that the EPS may slow the diffusion of the drugs within the biofilm, permitting enough time for microbial cells to upregulate drug resistance genes [73]. Another contributing factor might be that the cells within the biofilm have very slow growth rates as a consequence of nutrient deprivation, particularly at the base of the biofilm [74]. Biofilms may also harbor persister cells, which are cells that account for 0.1-1 % of the biofilm population and exhibit multidrug tolerance [75]. Upregulation of genes, coding for efflux pumps proteins, may also be a mechanism, whereby biofilms can resist the action of antimicrobial agents [76].

Another mechanism that may account for biofilm resistance might be the role of cross-resistance. Mild forms of stress prepare cells for subsequent stress conditions of a different nature. So, biofilm-grown cells live in a nutrient-poor, hypoxic environment

and these suboptimal growth conditions may result in increased tolerance to various forms of stress [62]. The interaction of these facts may lead to a decreased susceptibility of the biofilms to antimicrobial agents. Therefore, antimicrobial drugs with just one single mechanism of action, as the ones used routinely, are unlikely to be effective against biofilms.

Biofilms not only tend to be more resistant to antimicrobial agents, but also to withstand host immune defenses. Antibodies and leucocytes have limited penetration into the biofilm. Like that cells within the biofilm remain hidden from antibodies and complement factor recognition, and thus from subsequent phagocytosis. This may result in the oxidative burst of phagocytes, leading to inflammation and destruction of nearby tissues [77].

1.2.8 **Antifungal drugs**

The important antifungal drugs, currently used in the treatment of fungal infections, can be divided into 3 different classes, as follows: (i) polyene macrolides that lead to an alteration of membrane functions (amphotericin B [AmB] and its lipid formulations); (ii) azole derivatives that inhibit the 14α lanosterol demethylase, a key enzyme in ergosterol biosynthesis (ketoconazole, fluconazole, itraconazole, and voriconazole); and (iii) 1,3-β-glucan synthase inhibitors (echinocandins) [78].

Of these three classes of antifungal agents, only AmB and the echinocandins have shown *in vitro* activity against *C. albicans* biofilms [79, 80]. But even when using these drugs, biofilm infections caused by *C. albicans*, are extremely difficult, if not impossible to eradicate [80, 81]. In Latin America, amphotericin B (AmB) continues to be the antifungal drug, most commonly used for the treatment of invasive fungal infections, followed by fluconazole. Echinocandins and other AmB formulations are rarely used, because of their higher cost [5].

1.2.8.1   Polyenes

The polyene antifungal agents owe their name to the presence of alternating conjugated double bonds that constitute a part of their macrolide ring structure. The polyene antibiotics are all products of *Streptomyces* species. These drugs bind strongly to ergosterol, forming pores through the membrane, leading to the disruption of the osmotic integrity of the membrane, with leakage of intracellular potassium and magnesium, and also the disruption of oxidative enzymes in target cells, causing cell death [82, 83]. AmB can also induce oxidative stress in fungi cells, due to formation of ROS like superoxide, hydroxyl radicals and hydrogen peroxide, disrupting cell membrane and leading to cell death through membrane lipid peroxidation [84].

AmB is considered the gold standard for the treatment of many invasive or life-threatening fungal infections and has been the mainstay of antifungal therapy for over 50 years (Fig. 10). This can be explained by the fact that, besides the wide spectrum of action of AmB, resistance to polyenes is rare, and this in part due to the severe host toxicity, limiting the long-term use of these class of drugs [8, 85]. Resistance to polyenes is related to mutation in fungal ergosterol biosynthetic pathway, leading to accumulation of other sterols in the fungal membrane, which have less binding affinity for AmB [83]. Concurrent or previous therapy with azoles might also lead to AmB resistance, by altering the sterol type or the content in the membrane [78, 86]. In addition, catalase activity is also involved in resistance to AmB, leading to decreased cell susceptibility towards oxidative damage, caused by AmB [87].

The use of this agent is limited by significant drug host toxicity, such as renal dysfunction, which is likely due to the structural similarities between ergosterol and cholesterol in the mammalian cell membrane [85, 88]. Consequently, lipid formulations of AmB have been developed and they greatly reduce nephrotoxicity of the parental

drug. But the acquisition cost of these compounds are considerably more expensive than conventional AmB, ranging from 10 to 20 fold higher in cost per dose [89].
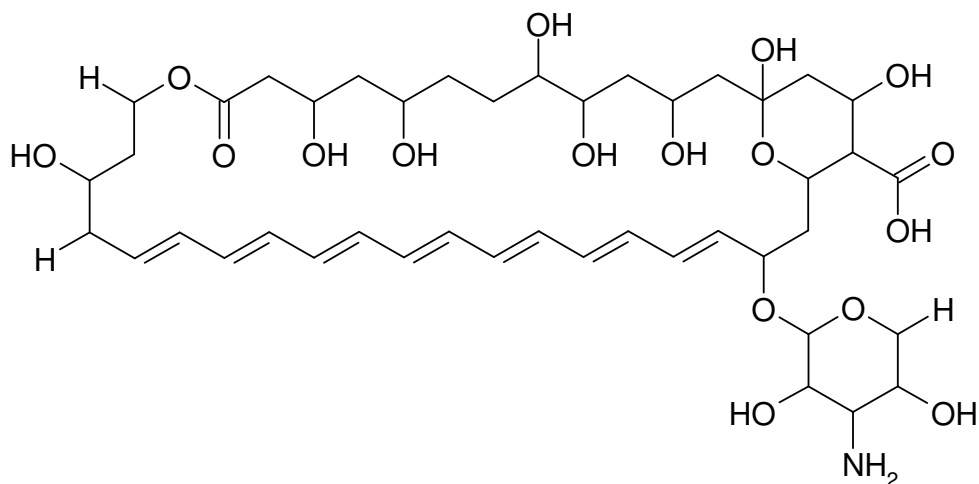
Fig. 10. Chemical structure of Amphotericin B

1.2.8.2   Azoles

The azole antifungal agents are the most widely used class of antifungals in the clinic [90]. They have a ring made of five atoms containing either two or three nitrogen molecules (the imidazoles and the triazoles respectively) [91]. They act by inhibiting the ergosterol biosynthetic enzyme 14α lanosterol demethylase, causing a block in the production of ergosterol and the accumulation of toxic sterols, culminating in a severe fungal membrane stress and inhibition of fungal growth [90, 92-94]. The fungistatic nature of azoles drugs contributes to the development of resistance in clinical isolates from immunocompromised hosts [95]. Approximately 81 % of patients with AIDS are estimated to be colonized with azole-resistant strains [96].

Another potential limitation of the azole antifungal drugs is the frequency of their interactions with drugs that are used in chemotherapy or in AIDS treatment, because they are metabolized via similar pathways in the liver, resulting in a decrease of azole concentration, or even in toxicity of the coadministered drug [97]. Fluconazole

(Fig. 11), the most suitable azole for the treatment of superficial candidiasis and disseminated candidiasis, is used for prevention of candidiasis in intensive care units (ICU). The extensive use of fluconazole as prophylaxis in ICU patients became the leading cause of colonization of *Candida*-non-*albicans* species and increasing resistance to antifungal drugs [68, 98, 99].
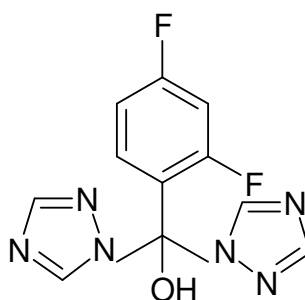
Fig. 11: Chemical structure of fluconazole

Resistance to azoles can occur by mutations that modify the target molecule or by the upregulation of multidrug efflux pumps coded for by multidrug resistance (MDR) or *Candida* drug resistance (CDR) genes [100, 101]. Besides, long-term use can cause life-threatening liver toxicity [102].

1.2.8.3 Echinocandins

The echinocandins are semisynthetic lipopeptides produced via chemical modification of natural products of fungi [101]. This class of drug inhibits the synthesis of 1,3-ß-D-glucan, an essential component of the fungal cell wall, comprising 30%–60% of the fungal cell wall in *Candida* sp [101]. This leads to depletion of glucan polymers in the fungal cell, resulting in cell rupture and death. This is the first class of antifungal agents that target the fungal cell wall, the ideal target for the therapeutic treatment of fungal pathogens of humans, since mammalian cells do not have cell walls [92, 94, 103, 104].

Echinocandins are highly effective against *Candida* spp, including azole-resistant strains, and also against *Candida* growing biofilm cells [105]. However, their

high price may limit their use as initial therapy for patients with fungemia (fungal infections in the bloodstream) [106] and clinical resistance attributed to point mutation in glucan synthase (FKS) genes coding for β-1,3-glucan-synthase has been reported in some *Candida* spp. [107].

2 Photodynamic inactivation of *Candida albicans* biofilms

2.1 Introduction

C. albicans is a commensal organism in healthy individuals, colonizing several niches of the human body in the skin and mucosal surfaces, such as the oral cavity, the gastrointestinal tract, and the genitourinary tract of 30–70% of healthy individuals at any given moment [92, 108]. Both the normal bacterial flora of mucosal surfaces and epithelial layers act as physical barriers, as well as a functional immune system, maintaining the commensal phase of *C. albicans* colonization [109]. However, an imbalance between the host immunity and this opportunistic fungus may trigger infections of the skin, nails, and mucosal epithelia. In severely immunocompromised patients, the fungus can penetrate through epithelial layers into deeper tissues, reach the bloodstream, and disseminate within the body, infecting internal organs (invasive candidiasis), like heart, brain, kidney, and liver (Fig. 12) [5-7].

C. albicans is the major fungal pathogen of humans. It is the predominant fungal species, found on oral mucosal layers, in vaginal infections, and in invasive bloodstream infections [62]. This microorganism is responsible for 90%–100% of mucosal infections and for 50%–70% of episodes of candidemia (bloodstream infection caused by *Candida* spp) [110-113].

In the United States, *Candida* spp. are the fourth most common cause overall of bloodstream infections, and they rank fourth to seventh in Europe [114-116]. In

multicenter studies, conducted in Brazil and in Mexico, it has been found that 4% of

nosocomial bloodstream infections are caused by *Candida* spp [117].
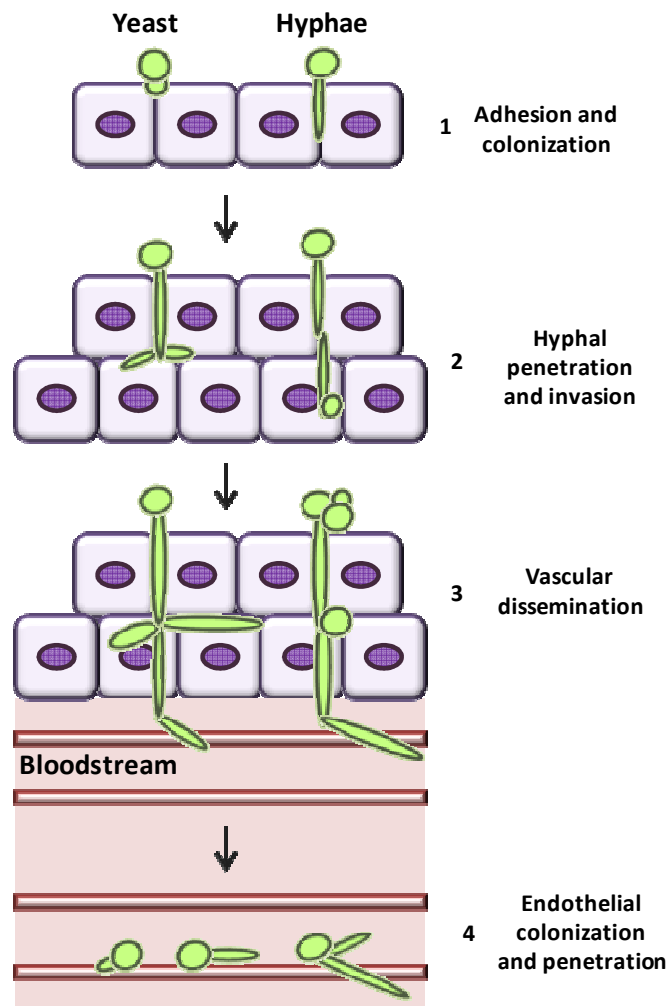
Fig. 12: The steps of tissue invasion by *Candida albicans*: (1) adhesion to the epithelium; [118] epithelial penetration and invasion by hyphae; [119] vascular dissemination, which involves hyphal penetration of blood vessels and seeding of yeast cells into the bloodstream; and, (4) finally, endothelial colonization and penetration during disseminated disease. Adopted and modified from reference [108].

In immunocompromised patients, vaginal, esophageal, oropharyngeal, and urinary

tract candidiasis are very frequent. In HIV patients, oropharyngeal candidiasis is a

major cause of morbidity. Oral candidiasis may also lead to esophageal candidiasis, an

even more distressing complication [120]. Oropharyngeal candidiasis affects 15-60 %

of patients with haematologic or oncologic malignancies during the period of

immunosuppression [121], 7-48 % of patients infected with HIV, and over 90 % of those in advanced stage of the disease. In severely immunocompromised patients, relapse rates are high (30-50 %), usually occurring within 14 days of treatment cessation [122, 123].

Bloodstream infections by *C. albicans* are difficult to diagnose because of its nonspecific signs and symptoms, delaying appropriate treatment and resulting in substantial morbidity and mortality. The mortality rate, related to invasive candidiasis, can be up to 61%. Usually, an excess length of hospital stay of 30 days ist required, making the treatment more expensive [6, 8, 9].

The fact that *C. albicans* is the most common human fungal pathogen can be explained by its ability to survive in different environments in the host organism [52]. *C. albicans* has developed specialized virulence factors to rapidly adapt itself to local growth conditions, cause diseases, and overwhelm the host defense systems [9]. The ability to switch between unicellular yeast growth forms and a filamentous form is an important virulence trait (Fig. 13). Yeast cells are suited for dissemination in the bloodstream to target organs, whereas hyphae are invasive and allow *C. albicans* to firmly anchor and penetrate host epithelial and endothelial cells, damaging them through the release of hydrolytic enzymes and initiating candidiasis. Furthermore, hyphae cells can escape from phagocyte cells after host internalization [124].

Yeasts   **Hyphae**
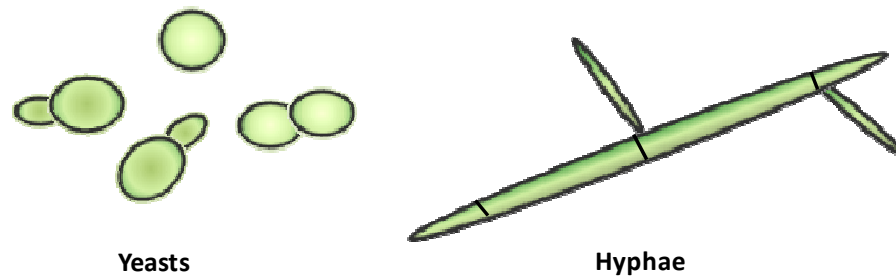
Fig. 13. *C. albicans* **has ability to grow as unicellular budding yeast or in filamentous hyphal forms.**

Mutants that are unable to undergo morphogenesis are often attenuated in virulence [9, 10, 11]. Other virulence factors of *C. albicans* include secretion of hydrolytic enzymes such as proteinases, phospholipases enzymes, which enhance adhesion and facilitate invasion by destroying host cells [125], and adhesion to host cells and tissues by expression of cell surface glycoproteins, called adhesins [126]. But the major virulence factor in *C. albicans* pathogenensis is the formation of biofilms in host tissue surfaces (Fig. 14) [127].

Fig. 14. Superficial infections of skin and mucosal membranes, caused by *Candida albicans*. Fig. 10-1: Oral candidiasis. Adopted from [114]. Fig. 10-2: Chronic mucocutaneous candidiasis. Adopted from [128]. Fig. 10-3: *C. albicans* soft tissue infection. Adopted from [118].

Considering the substantial excess mortality due to candidemia and the difficulties encountered in administering early and effective antifungal therapy, prevention of epithelial cell invasion by *C. albicans* and its subsequent spread through the bloodstream is absolutely essential [6].

2.1.1 *Candida albicans* biofilms

C. albicans is the main responsible fungal species for biofilm formation. It has the ability to produce biofilms on almost any medical device [129, 130], for instance blood and urinary catheters, on prosthetic devices, like heart valves, voice prostheses, and

denture surfaces [62], as well as on human epithelial surfaces, such as the gastrointestinal, the bronchial [129], the genital tract and the skin [131].

Most cases of candidiasis at both mucosal and systemic sites are caused by biofilm-grown *C. albicans* cells [132]. In addition, this phenotype is less susceptible to antifungal agents, compared to its planktonic counterparts, and it can be up to 2000 times more resistant to the effects of antimicrobial agents [66, 133].

The morphological heterogeneity is a unique feature of *C. albicans* biofilms and results in complex three-dimensional biofilm architecture [134]. They exhibit a highly heterogeneous architecture, composed of yeast and hyphae cells, and the fungal-derived EPS, which is comprised of polysaccharides, mainly ß-1,3 glucans, and proteins. Basically, biofilm formation proceeds over a period of 24–48 h, where adherent yeast cells are transformed to well-defined cellular communities, encased in the EPS [135]. *C. albicans* biofilm formation starts with: 1. Attachment of yeast cells to a biotic or abiotic surface. 2. Initial attachment is followed by hyphae formation and production of EPS. 3. The biofilm becomes a thick layer of EPS enveloping an intricate network of yeasts and hyphaes. 4. Cells are released from the biofilm, spreading into the environment and forming new biofilms or dispersing infections (Fig. 15) [136].
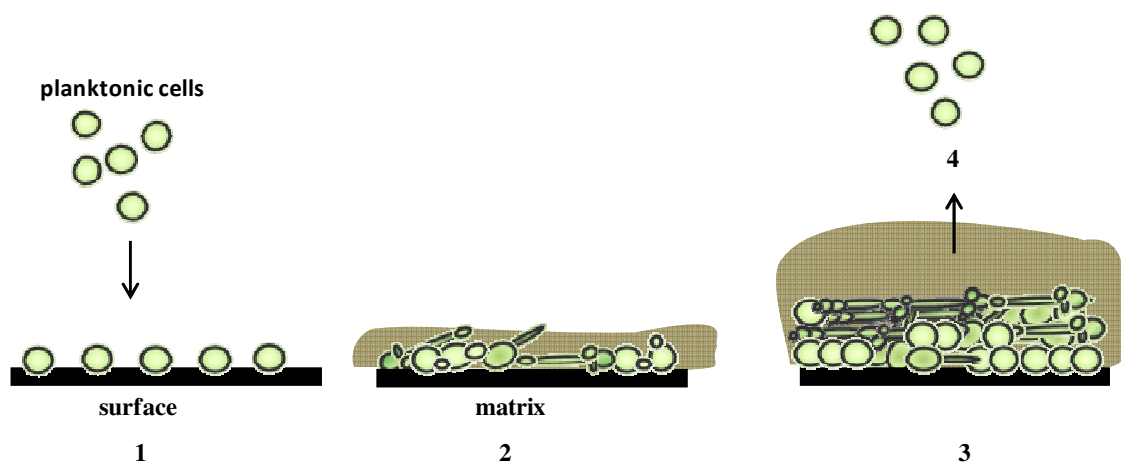
Fig. 15. Biofilm development of *Candida albicans*: 1. *Candida albicans* biofilm formation starts with the adherence of planktonic cells to a surface. 2. Initial attachment is followed

by hyphae formation and production of EPS. 3. The biofilm becomes a thick layer of EPS enveloping an intricate network of yeasts and hyphaes. 4. Cells are released from the biofilm, spreading into the environment and forming new biofilms or dispersing infections

There are multiple hypotheses to explain, why *C. albicans* biofilms are much more resistant to antifungal drugs than planktonic cultures. In addition to the factors, already mentioned for microbial biofilms, such as presence of EPS, slow growth rate, overexpression of drug efflux pumps, and presence of persister cells, *C. albicans* biofilms have been reported to show decreased content of ergosterol and diminished levels of ergosterol biosynthetic gene expression [76, 137]. These changes in membrane sterol composition during biofilm formation might explain resistance to drugs such as AmB and the azoles, which target sterols and sterol biosynthesis [138]. The elevated levels of ß-1,3 glucan levels in the cell wall and biofilm EPS of *C. albicans*, in response to environmental signals, may physically interact with antifungal drugs and inhibit the penetration to the site of action [139].

Thus, a clear need exists for an effective nonantibiotic treatment, mainly against cells, growing as a biofilm. Biofilms are the leading cause of microbial infections in humans and represent a serious problem in health care [140]. Therefore, in this study the photodynamic action of a new porphyrine derivative XF-73 against *C. albicans* planktonic and biofilm cells was investigated and the results were compared with the photodynamic action of the standard PS TMPyP, regarding uptake, phototoxicity and mechanism of action.

2.2 Material and Methods

2.2.1 Strains of *C. albicans*

One to three colonies of *C. albicans* (ATCC-MYA-273, LGC Standards GmbH, Germany) were picked up from agar plates with a sterile inoculating loop, transferred to culture tubes containing 5 mL of Sabouraud Dextrose Broth (SDB) (Sigma Chemical Co., St. Louis, Mo), and cultured overnight. When the cultures reached the stationary phase of growth, the cells were harvested by centrifugation (200 g, 5 min) and washed once with Dulbecco's phosphate-buffered saline (PBS without Ca^{2+} and Mg^{2+}; PAA Laboratories GmbH, Austria). For experiments with planktonic cells, approximately 5×10^7 cells mL^{-1} were prepared in PBS.

2.2.2 Formation of *C. albicans* biofilm

Different conditions were tested to find the optimal conditions to form *C. albicans* biofilms. Planktonic cells were diluted at different densities: 10^4 to 10^7 cell mL^{-1} and in different fetal bovine serum (FBS; PAN Biotech, Aidenbach, Germany) concentrations: 25% to 100% FBS diluted in PBS. The incubation times of these suspensions were varied between 24 and 48 h. The best condition found to form the biofilms, used in this study, were: *C. albicans* planktonic cells diluted to 10^6 cells mL^{-1} in 25% of FBS and 200 µL were added to sterile flat-bottomed 96-well polystyrene plates (Costar® 96 Well Clear Flat Bottom, TC-treated microplate, Corning Incorporated, Corning, New York, USA), incubated at 37 °C for 24 h without shaking. This set up was used for further experiments.

The cell density of 10^6 cells mL^{-1} provided an optimal recovery rate of 10^5 cells mL^{-1}. All tested concentrations of FBS induced robust biofilm formation (data not

showed). 25% of FBS was used, since porphyrins are known to bind serum proteins [141] and increasing FBS concentrations may reduce the attachment/uptake of the PSs by microbial cells, due to the nonspecific binding of PSs molecules to serum proteins. Biofilms incubated for 48 h became too fragile to permit manipulation. So 24 h biofilms were used in the study (Fig. 16).
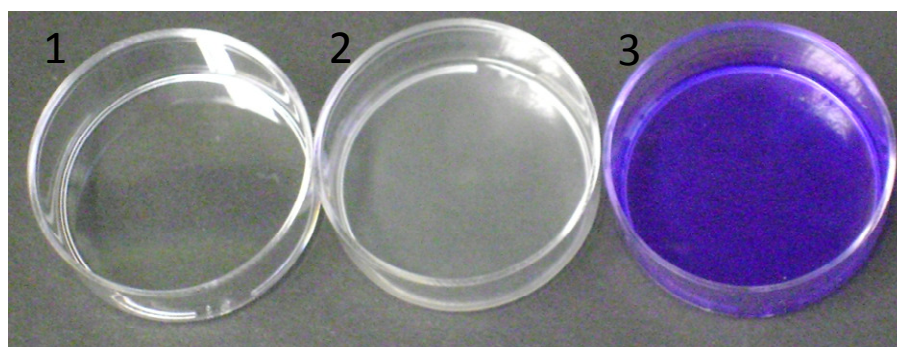
Fig. 16. Biofilm growing cells, used in this study: 1. Empty plate, the 2. Plate containing biofilm growing cells and 3. Plate containing biofilm growing cells stained by 5% of crystal violet. Crystal violet stains the biofilm EPS and the cells within the biofilm.

2.2.3 Photosensitizers and light source

The photosensitizer 5,10,15,20-Tetrakis(1-methyl-4-pyridyl)-21H,23H-porphine, tetra-p-tosylate salt (TMPyP) was purchased from Sigma Aldrich (Taufkirchen, Germany), purity 97%. The dicationic 5,15-bis-[4-(3-Trimethylammoniopropyloxy)-phenyl]-porphyrin (XF-73), was synthesized by Xiangdong Feng (Solvias Company, Basel, Switzerland) and kindly provided by Destiny Pharma Ltd. (Brighton, United Kingdom).

Both photosensitizers were dissolved in bidistilled water at a concentration of 500 µM, passed through a 0.22 µm pore-size filter, and stored at 4°C until usage. The irradiation of the samples was performed using an incoherent light source (UV236) $\lambda_{em} = 418 \pm 20$ nm), provided by Waldmann GmbH (Schwenningen, Germany) (Fig. 17). The maximal fluence rate at the level of the irradiated samples was 13.4 mW cm^{-2}. Planktonic cells were irradiated for 15 min (12.1 J cm^{-2}) and biofilms for 60 min (48.2 J cm^{-2}).
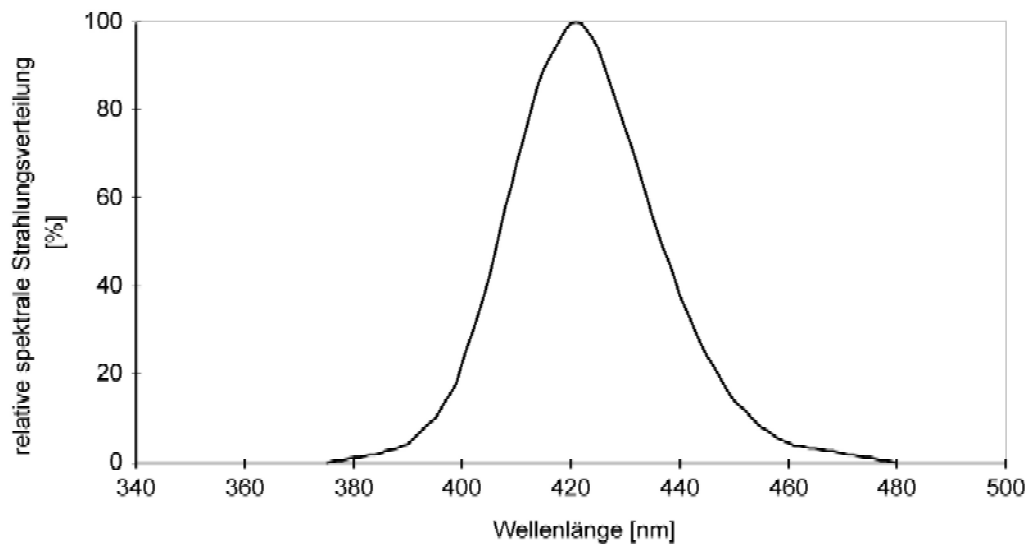
Fig. 17. Spectral emission of the light source with an emission peak at 418 nm (blue).

2.2.4 **Binding assay**

Planktonic and biofilm cells were incubated in the dark with increasing concentrations of the PSs for 60 and 120 min respectively. The cells were washed twice to remove unbound PSs molecules. The pellet was lysed with Sodium Dodecyl Sulfate (SDS) 2% overnight at 37°C. Cell lysates were centrifuged for 5 min at 37 °C and the spectra of TMPyP and XF-73 in the supernatant was measured by absorbance spectroscopy using a Beckman DU640 spectrophotometer (Beckman Instruments GmbH, Munich, Germany).

2.2.5 **Localization of XF-73 and TMPyP in *C. albicans***

To determine the localization of TMPyP in *C. albicans* planktonic cells and the localization of XF-73 in *C. albicans* biofilms, *C. albicans* planktonic cells were incubated with 1 μM of TMPyP for 15 min and washed once with PBS. *C. albicans* biofilms were incubated with 100 μM of XF-73 for 1 h and washed once with PBS. Thereafter, the distribution of TMPyP and XF-73 was examined by fluorescence

microscopy (Zeiss Axiotech, Goettingen, Germany) using an appropriate dual band filter set (Omega Optical, Brattleboro, VT, USA) for excitation (405nm ± 40 nm) and emission (λ_{em}600nm longpass). Light microscopy images were done in parallel. Fluorescence images were superimposed onto the corresponding light microscopy image using an image processing program (Image-Pro Plus 5.0; Media Cybernetics, Silver Spring, MD, USA).

2.2.6 Photodynamic inactivation of *C. albicans* planktonic cells

Cells submitted to aPDT were incubated in the dark with different concentrations of the PSs (0 to 2µM) for 15 min under agitation. 200 µL of cell suspension were transferred to sterile flat-bottomed 96-well polystyrene and illuminated for 15 min (13.4 mW cm^{-2}, 12.1 J cm^{-2}). Illumination was done from the bottom side of the 96-well plate to avoid refraction of the light in the cell culture media. Controls included: *C. albicans* cells kept in the dark and not treated with PS (normal control), *C. albicans* cells exposed just to the light (light control), and *C. albicans* cells treated just with the PS (dark control). Immediately after treatment, fungal viability was monitored by the colony forming unit assay (CFU assay).

2.2.7 Photodynamic inactivation of *C. albicans* biofilm cells

After 24 h of incubation, the biofilms were washed once to remove loosely attached cells. The cells were incubated with increasing concentrations of the PSs for 4 h in the dark at 37°C. Thereafter, cells were illuminated for 60 min (13.4 mW cm^{-2}, 48.2 J cm^{-2}). Then, the biofilms were detached from the bottom of the well by scraping the bottom of the microplate with a pipette tip. Afterwards, they were transferred to an Eppendorf tube containing 1 mL of PBS. The cells were then placed in an ultrasonic water-bath chamber with a frequency of 35 kHz (Qualilab USR30H, Merck Eurolab GmbH,

Bruchsal, Germany) and vigorously vortexed (REAX top, Heidolph Instruments GmbH & Co. KG, Schwabach, Germany) for 1 min each procedure. Thereafter, sensitivity of *C. albicans* biofilms to aPDT was determined by CFU assay.

2.2.8 Photodynamic inactivation of *C. albicans* cells resuspended from biofilms

Additional experiments were made to assess the susceptibility of *C. albicans* cells, which were resuspended from preformed biofilms. Twenty four hours old biofilms were washed twice, detached from the well microplate by scrapping, and transferred to an Eppendorf tube with 1 mL of PBS. The cells were then placed in an ultrasonic water-bath chamber with a frequency of 35kHz (Qualilab USR30H, Merck Eurolab GmbH, Bruchsal, Germany) and vigorously vortexed (REAX top, Heidolph Instruments GmbH & Co. KG, Schwabach, Germany) for 1 min each procedure. This procedure was done for disrupting the biofilm structure and getting individual cells of *C. albicans* into the suspension. Thereafter, the sensitivity of *C. albicans* cells to aPDT was evaluated as stated above for the experimental set up for planktonic cells.

2.2.9 Amphotericin B activity against *C. albicans* planktonic and biofilm cells

Planktonic cells were incubated with 0; 0.1; 1; 5, 10, 50 and 100µg mL^{-1} of AmB, for 30 min concerning the overall photodynamic treatment time (15 min incubation with PS + 15 min illumination). Biofilms were incubated with 0; 0.1; 1, 10; 50 and 100 µg mL^{-1} of AmB for 5 h (4 h incubation with PS + 1 h illumination). Besides, planktonic and biofilm cells were also incubated with AmB for 24 h, which is the standard time for the

susceptibility tests of *C. albicans* planktonic cells *in vitro*. Fungal viability was monitored by the CFU assay.

2.2.10 Colony forming unit assay

The colony forming unit assay (CFU assay) was used to estimate the viable number of microbial cells after phototoxic treatments. For this, ten-fold serial dilutions in SBD were made and aliquots of 0.1 mL were seeded onto Sabouraud Dextrose Agar (SDA) and cultured for 48 h at 37°C. Thereafter, the number of surviving colonies was counted (CFU mL^{-1}).

2.2.11 Multi-channel 3D fluorescent microscopy images

Biofilms were formed, as described before (section 2.2.2), using cell culture dishes of the size of 35×10 mm^2 (Cellstar, Frickenhausen, Germany). Biofilms were stained with a live/dead biofilm viability kit (Molecular Probes, Eugene, OR, USA). The kit contains two nucleic acid intercalators, membrane-permeable Syto-9 and membrane-impermeable propidium iodide. Living cells are stained green and dead cells stained orange-red. The final concentrations of dyes were as follows: 0.01 mM for Syto-9, 0.06 mM for propidium iodide. Additionally, 200 µg mL^{-1} of Concanavalin A (ConA)-Texas Red conjugate (Molecular Probes, Eugene, OR, USA) was used to stain the biofilm EPS in red. Fluorescence microscopy was performed using a Zeiss Observer Z1 inverted fluorescence microscope with ApoTome (Zeiss) and AxioVision software (v 4.6.2.0, Zeiss, Jena, Germany) using appropriate filter-sets for excitation and emission of Con A (λ_{ex}590nm/λ_{em}615nm), SYTO 9 (λ_{ex}485nm/λ_{em}500nm), and propidium iodide (λ_{ex}535nm/λ_{em}617nm).

Light microscopy images were done in parallel. Fluorescence images were superimposed onto the corresponding light microscopy image using an image processing program AxioVision software.

2.2.12 Singlet oxygen luminescence signal from biofilms, incubated with XF-73

The biofilms were formed, as already described, for phototoxic experiments (section 2.2.2) in cell culture dishes (35×10 mm^2). The biofilms were incubated after formation with 100 μM of XF-73 for 1 h and previous to the detection of $^1O_2$ luminescence the cells were either non-washed or washed with pure H_2O once. After incubation, the biofilms were excited with a frequency doubled Nd:YAG-Laser (PhotonEnergy, Ottensoos, Germany) with a wavelength $\lambda = 532$ nm, power output P = 50 mW, repetition rate f = 2 kHz, and with a pulse energy of E = $2.5 \cdot 10^{-5}$ J. Every sample was irradiated with 40.000 laser pulses, which equals an irradiation time of 20 s. The spot size of the excitation laser covered an area of 7 cm^2 using an optical lens in regard to the size of the dishes. The $^1O_2$ luminescence was directly detected by time resolved measurements at 1270 nm (LOT Oriel GmbH, Darmstadt, Germany, 30 nm FWHM filter) in near-backward direction with respect to the exciting beam. An infrared-sensitive photomultiplier tube (PMT, R5509-42, Hamamatsu Photonics Deutschland GmbH, Herrsching, Germany) with an additional 950 nm cut-off-filter (Omega Opticals, Photomed GmbH, Seefeld, Germany) was used. The time resolved luminescence signals were fitted based on the Levenberg-Marquardt-algorithm, as described previously [143]. These experiments were done in collaboration with the Dipl.-Phys. Ariane Felgenträger, Department of Dermatology, University Hospital Regensburg.

2.2.13 **Data analysis**

All results are shown as medians, including 25% and 75% quartiles, which were calculated from the values of at least 3 independent experiments. Each experiment was conducted in triplicates using Prism 4 for Windows (GraphPad Software Inc. San Diego, CA, USA). The calculation (reduction of CFU mL^{-1}) was referred to the untreated, so called dark controls, which were neither incubated with TMPyP or XF-73 nor illuminated. In Figs. 19-27, medians on or below the green or red horizontal line represent ≥99.9% or ≥99.999% efficacy of fungal killing, corresponding to at least three or five magnitudes of log_{10} reduction compared to the respective matching untreated controls (no light and no photosensitizer). A reduction of at least three magnitudes of log_{10} of viable median numbers of *C. albicans* was stated as biologically relevant with regard to the guidelines of hand hygiene [144, 145].

2.3 Results

The photodynamic efficacy of both XF-73 and TMPyP in combination with blue light against *C. albicans* planktonic and biofilm cells was investigated.

2.3.1 Absorption and fluorescence spectra

The absorption spectrum of TMPyP and XF-73 consists of a typical absorption spectrum of a porphyrin, showing a Soret band at 418 nm, and Q bands at 516, 551, 592, and 648 nm in H_2O [146]. The Figs. 18 and 19 show the concentration-dependent absorption of TMPyP and XF-73 respectively.
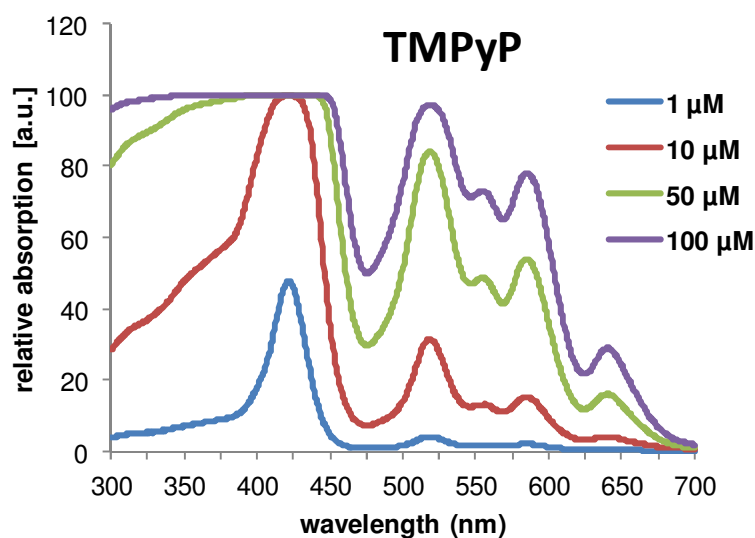
Fig. 18: Absorption spectra of TMPyP in H_2O in the range between 300 and 700 nm (Soret band and Q-bands I-IV) at different concentrations.
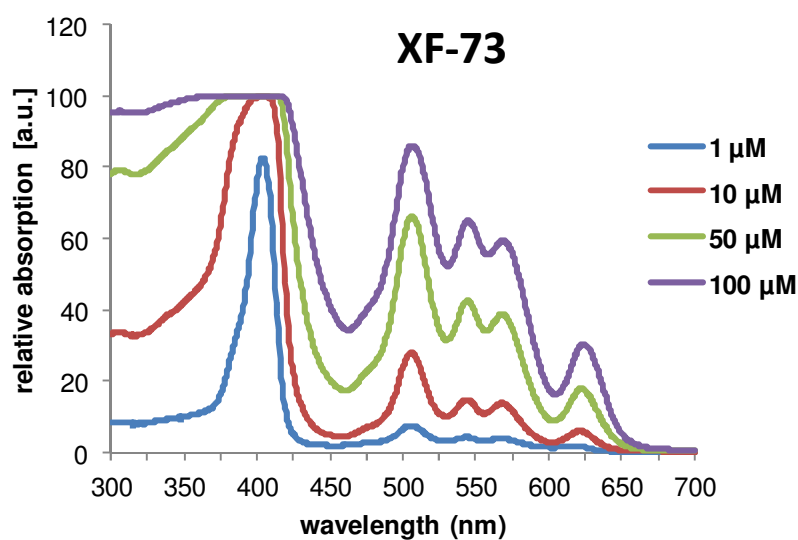
Fig. 19: Absorption spectra of XF-73 in H₂O in the range between 300 and 700 nm (Soret band and Q-bands I-IV) at different concentrations.

2.3.1 **Fluorescence microscopy of TMPyP and XF73 in *C. albicans***

Fluorescence microscopy was used to visualize TMPyP and XF73 uptake/binding by *C. albicans* cells. Fig 20 B shows a clear distribution of TMPyP around the cell wall and inside of *C. albicans* planktonic cells. For XF73, the same distribution was detected in planktonic cells (data not shown).
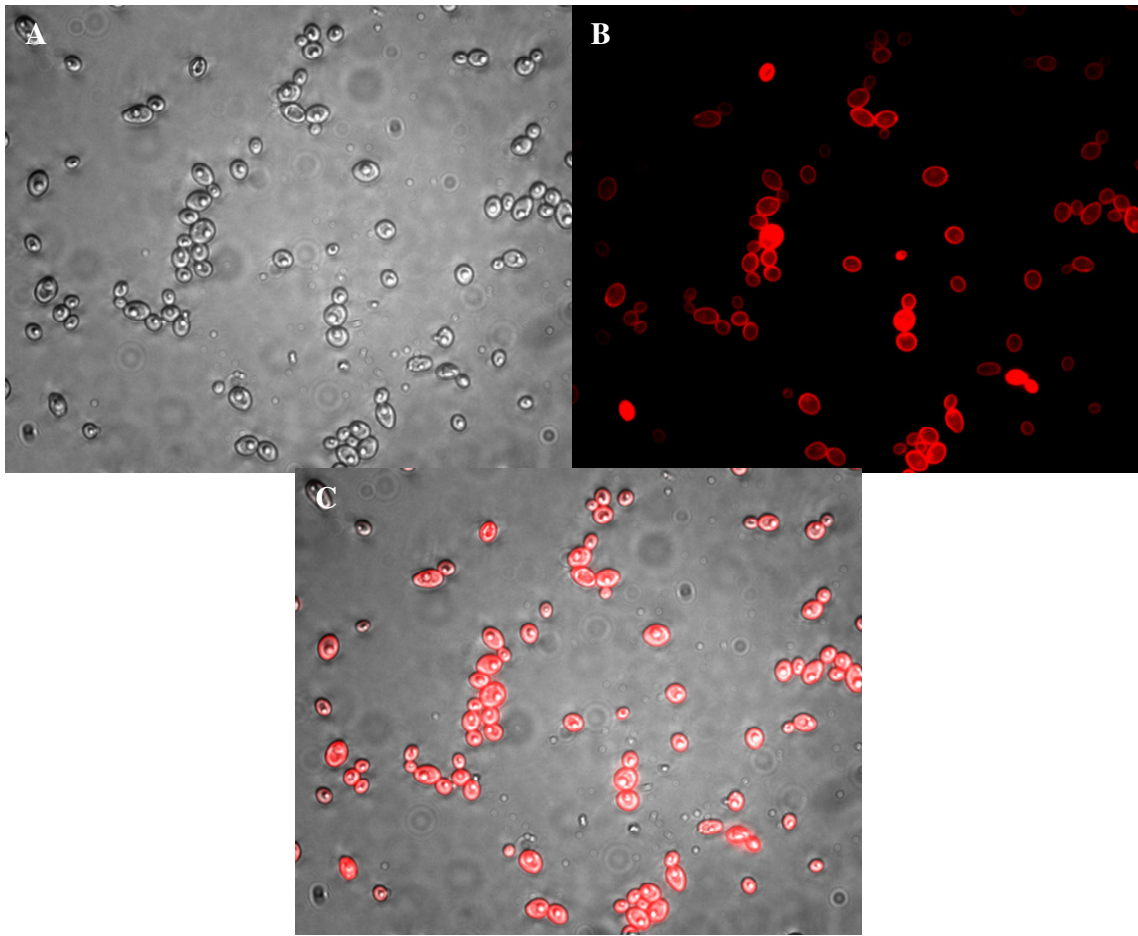
Fig. 20. Localization of TMPyP in *C. albicans* planktonic cells. *C. albicans* planktonic cells were incubated for 15 min with TMPyP. The distribution of TMPyP was examined by fluorescence microscopy. A) shows *C. albicans* biofilms incubated with TMPyP that were imaged by brightfield microscopy; B) shows *C. albicans* biofilms incubated with TMPyP that were imaged by fluorescence microscopy; C) shows the overlay of the brightfield image (A) and the fluorescence image (B). (×40 objective).

Fig 21 B shows the distribution of XF73 in *C. albicans* biofilms. XF73 fluorescence signals were detected in both yeast and hyphae of *C. albicans*. For TMPyP, fluorescence signals were also detected in both yeast and hyphae cells (data not shown).
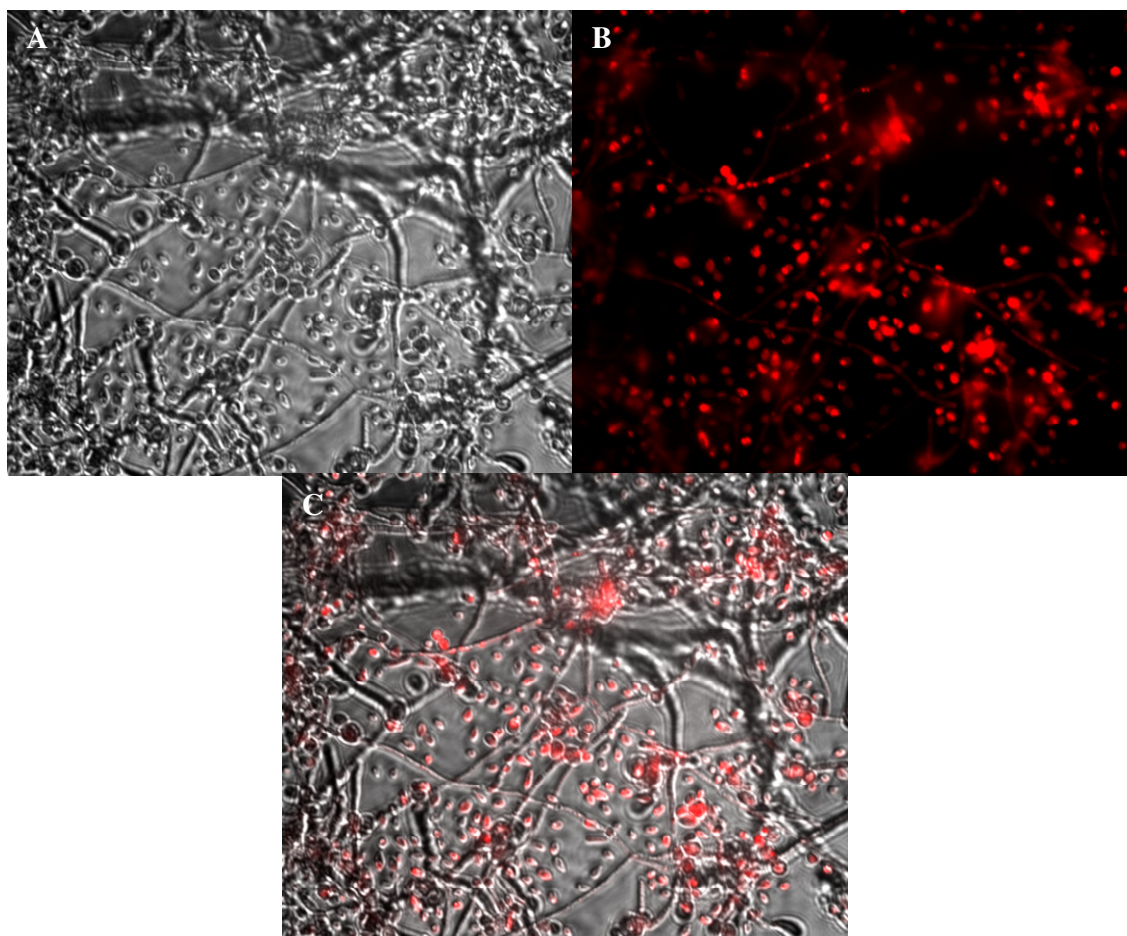
Fig. 21. Localization of XF-73 in *C. albicans* biofilms. *C. albicans* biofilms were incubated for 15 min with XF-73. The distribution of XF-73 was examined by fluorescence microscopy. A) shows *C. albicans* biofilms incubated with XF73 that were imaged by brightfield microscopy; B) shows *C. albicans* biofilms incubated with XF73 that were imaged by fluorescence microscopy; C) shows the overlay of the brightfield image (A) and the fluorescence image (B). (×20 objective).

2.3.2 Binding experiments

The efficacy of aPDT depends on the amount of PS, attached or uptaken by the cells, because singlet oxygen, generated by aPDT, has a short diffusion rate and the localization of the PS in the cell is supposed to be the first target of aPDT. Therefore, the binding of both PSs to the cells was determined. XF-73 attached better to both cell phenotypes than TMPyP. XF-73 attached better to planktonic cells than biofilm. On the other hand, attachment of TMPyP to both cell phenotypes was almost the same (Fig. 22 and 23).
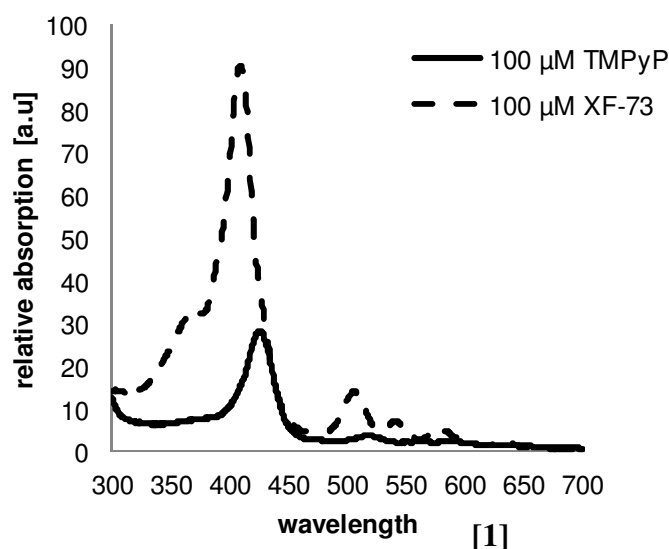
Fig. 22. Binding of XF-73 (dashed) and TMPyP (solid line) in *C. albicans* planktonic cells. *C. albicans* planktonic cells were incubated for 60 min with each PS. The relative absorption of the PSs in the supernatant was measured by absorbance spectroscopy.
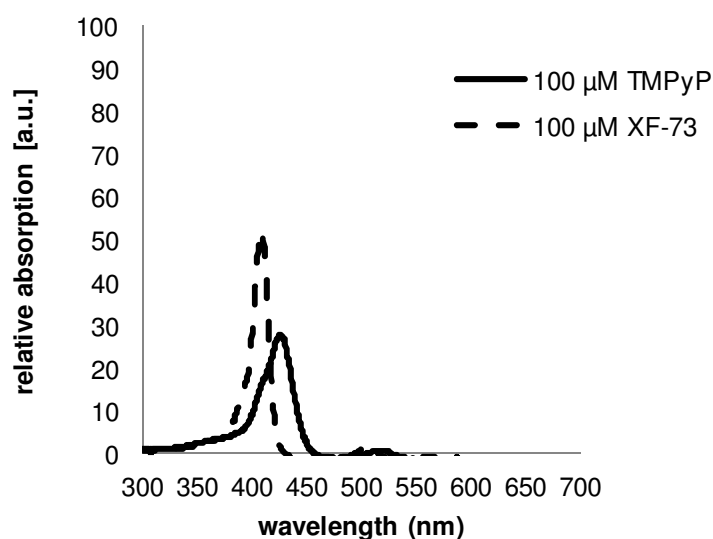
Fig. 23. Binding of XF-73 (dashed) and TMPyP (solid line) in *C. albicans* biofilm cells. *C. albicans* biofilms were incubated for 120 min with each PS. The relative absorption of the PSs in the supernatant was measured by absorbance spectroscopy.

2.3.3 **Photodynamic inactivation of *C. albicans* planktonic cells**

Incubation of planktonic cells for 15 min with 2 μM of TMPyP, followed by irradiation with blue light (12.1 J cm^{-2}), caused a 6 log$_{10}$ cell inactivation (Fig. 24), whereas only 0.5 μM of XF-73 was necessary to reach the same killing values (Fig. 25). No dark

toxicity towards *C. albicans* planktonic cells was detected with the highest PSs concentrations used. Furthermore, light alone did not show any significant toxicity toward *C. albicans*.
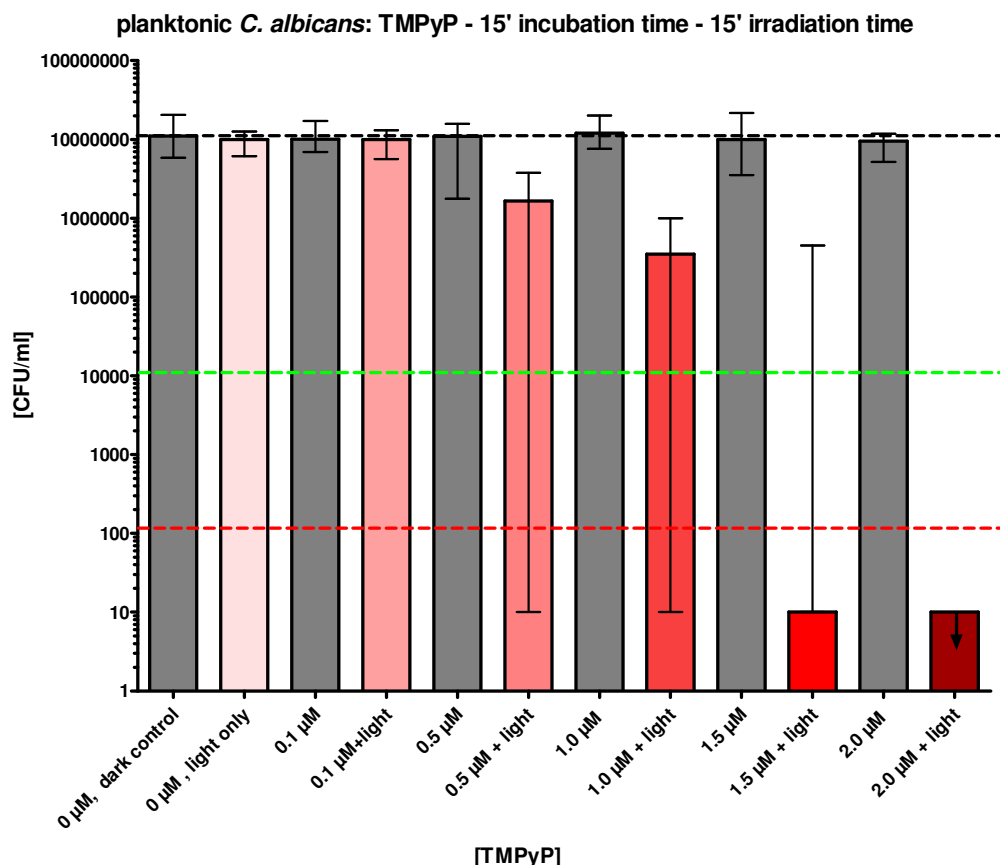
Fig. 24. APDT treatment of *C. albicans* planktonic cells. *C. albicans* planktonic cells were incubated with different concentrations of TMPyP for 15 min. The samples were irradiated with 12.1 J cm^{-2}. A CFU assay was performed immediately after aPDT, and surviving colonies were counted 24 h later. Black dashed line: baseline CFU/ml; green dashed line: reduction of 3 log$_{10}$ steps in viable *C. albicans* (reduction 99.9%); red dashed line: reduction of 5 log$_{10}$ steps in viable *C. albicans* (reduction 99.999%). (n = 3 experiments; median ± interquartile range). The arrow marks the lower detection limit of the CFU assay.
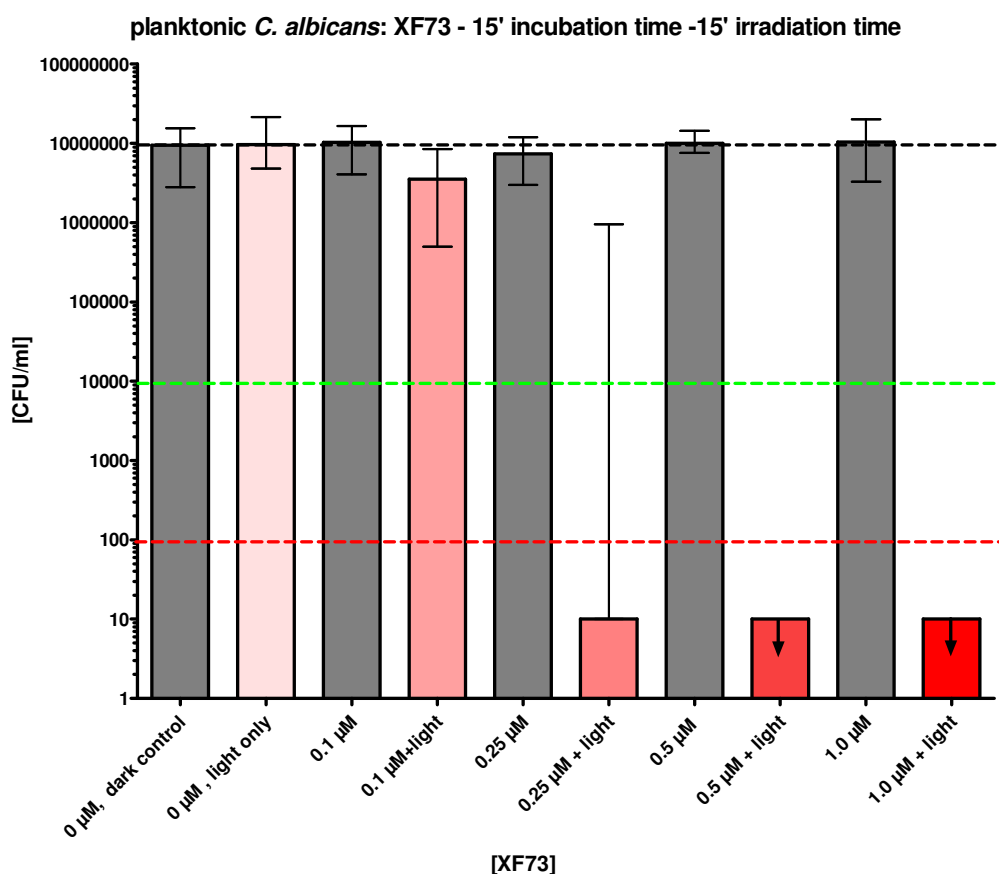
Fig. 25. APDT treatment of *C. albicans* planktonic cells. *C. albicans* planktonic cells were incubated with different concentrations of XF-73 for 15 min. The samples were irradiated with 12.1 J cm^{-2}. A CFU assay was performed immediately after aPDT, and surviving colonies were counted 24 h later. Black dashed line: baseline CFU/ml; green dashed line: reduction of 3 $\log_{10}$ steps in viable *C. albicans* (reduction 99.9%); red dashed line: reduction of 5 $\log_{10}$ steps in viable *C. albicans* (reduction 99.999%). (n = 3 experiments; median ± interquartile range). The arrows mark the lower detection limit of the CFU assay.

2.3.4 Photodynamic inactivation of *C. albicans* biofilm cells

For both PSs, higher PSs concentrations and light doses, as well as longer incubation times with the PSs were necessary to kill biofilm cells compared to planktonic cells. Incubation of the biofilms for 4 h with different concentrations of the PSs, followed by illumination with a light dose of 48.2 J cm^{-2}, caused a decrease in viability. TMPyP at a concentration of 50 µM exhibited a photodynamic killing efficacy of 5 $\log_{10}$ (Fig. 26). At this concentration, a dark toxicity was observed (2.3 $\log_{10}$). In contrast, only 1 µM of

XF-73 caused the same photokilling rate as TMPyP, without causing dark toxicity in the cells (Fig. 27). Light alone, did not have an effect on cell viability.
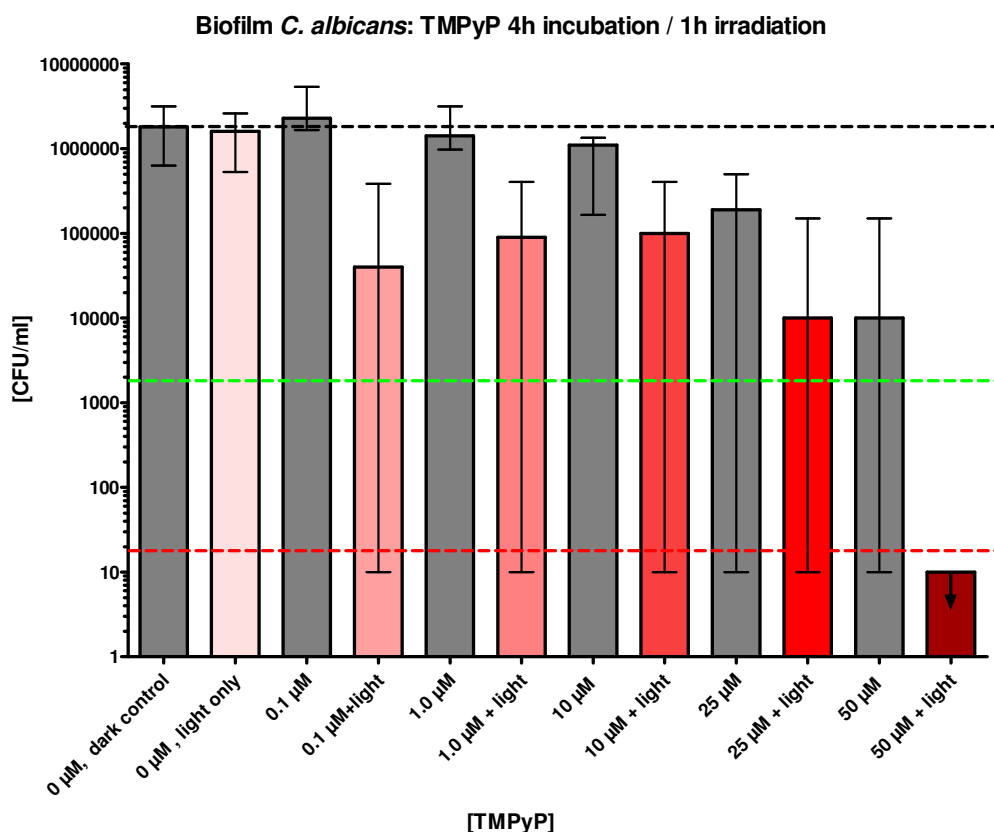
Fig. 26. APDT treatment of *C. albicans* biofilm cells. *C. albicans* biofilm cells were grown on the surface of 96 well plates for 24h. After incubation with different concentrations of TMPyP for 4 h, the samples were irradiated with 48.2 J cm^{-2}. A CFU assay was performed immediately after aPDT, and surviving colonies were counted 24 h later. Black dashed line: baseline CFU/ml; green dashed line: reduction of 3 log$_{10}$ steps in viable *C. albicans* (reduction 99.9%); red dashed line: reduction of 5 log$_{10}$ steps in viable *C. albicans* (reduction 99.999%). (n = 3 experiments; median ± interquartile range). The arrow marks the lower detection limit of the CFU assay.

Fig. 27. APDT treatment of *C. albicans* biofilm cells. *C. albicans* biofilm cells were grown on the surface of 96 well plates for 24h. After incubation with different concentrations of XF-73 for 4 h, the samples were irradiated with 48.2 J cm^{-2}. A CFU assay was performed immediately after aPDT, and surviving colonies were counted 24 h later. Black dashed line: baseline CFU/ml; green dashed line: reduction of 3 log$_{10}$ steps in viable *C. albicans* (reduction 99.9%); red dashed line: reduction of 5 log$_{10}$ steps in viable *C. albicans* (reduction 99.999%). (n = 3 experiments; median ± interquartile range). The arrows mark the lower detection limit of the CFU assay.

To determine whether the biofilm EPS is responsible for the increased resistance of biofilms, retarding the diffusion or excluding the PS within the cells, experiments were done with cells disrupted from the biofilm. These cells were then detached by scraping the microplate wells, resuspended in PBS, followed by sonication and vortexing to create a suspension of planktonic cells. Thus, these cells presumably have lost most of their EPS, since the EPS is responsible for keeping the organized structure of the biofilm. The results showed that resuspended biofilm cells were more susceptible to aPDT with XF-73 than intact biofilm populations (Fig. 28), suggesting that the EPS might play a role in aPDT resistance.
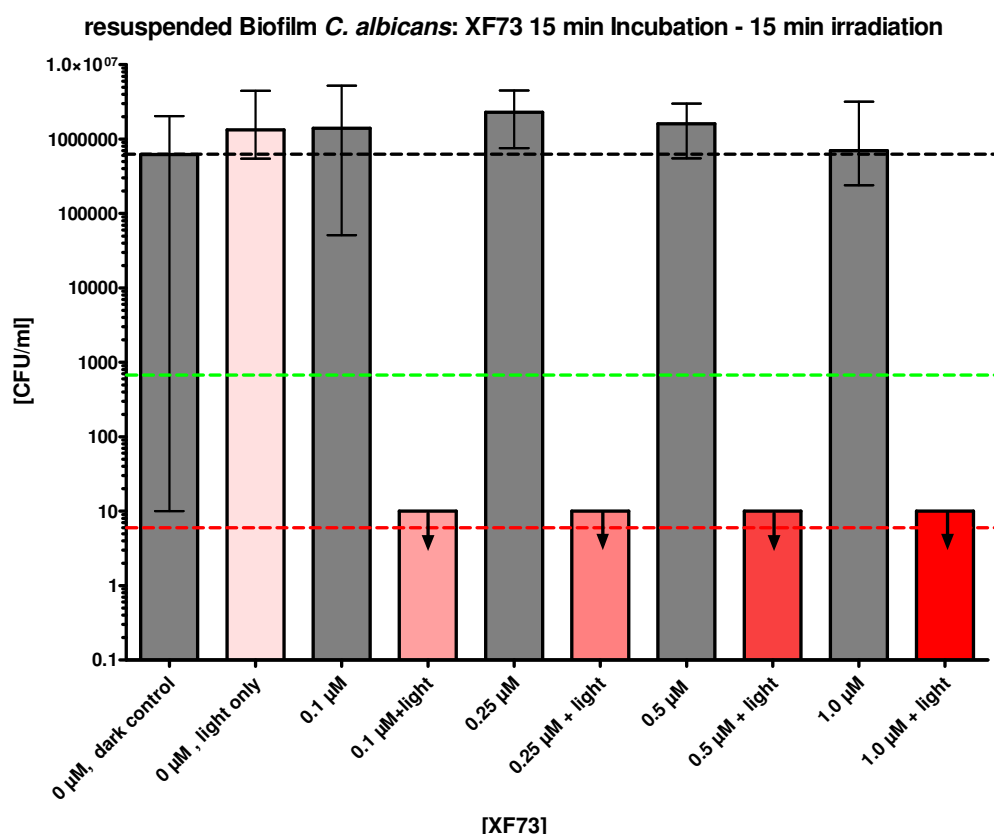
Fig. 28. APDT treatment of *C. albicans* cells resuspended from biofilms. *C. albicans* cells were disrupted from the biofilms with the tip of a pipette. The cells were then transferred to an Eppendorf tube with 1 mL of PBS, sonicated and vortexed for 1 min each, incubated with different concentrations of XF-73 for 15 min and irradiated with 12.1 J cm^{-2}. A CFU assay was performed immediately after aPDT, and surviving colonies were counted 24 h later. Black dashed line: baseline CFU/ml; red dashed line: reduction of 3 log$_{10}$ steps in viable *C. albicans* (reduction 99.9%); green dashed line: reduction of 5 log$_{10}$ steps in viable *C. albicans* (reduction 99.999%). (n = 3 experiments; median ± interquartile range). The arrows mark the lower detection limit of the CFU assay.

2.3.5 Amphotericin B activity against *C. albicans* planktonic and biofilm cells

To compare the action of AmB with aPDT, *C. albicans* planktonic and biofilm cells were treated with AmB for the same time period as aPDT. Planktonic cells, incubated for 30 min with AmB, were not killed with a concentration as high as 100 µg mL^{-1} of AmB (Fig. 29 A). Planktonic cells were killed with AmB only after a treatment time of 24 h with 2.5 µg mL^{-1} of the drug (Fig. 29 B).

A

B
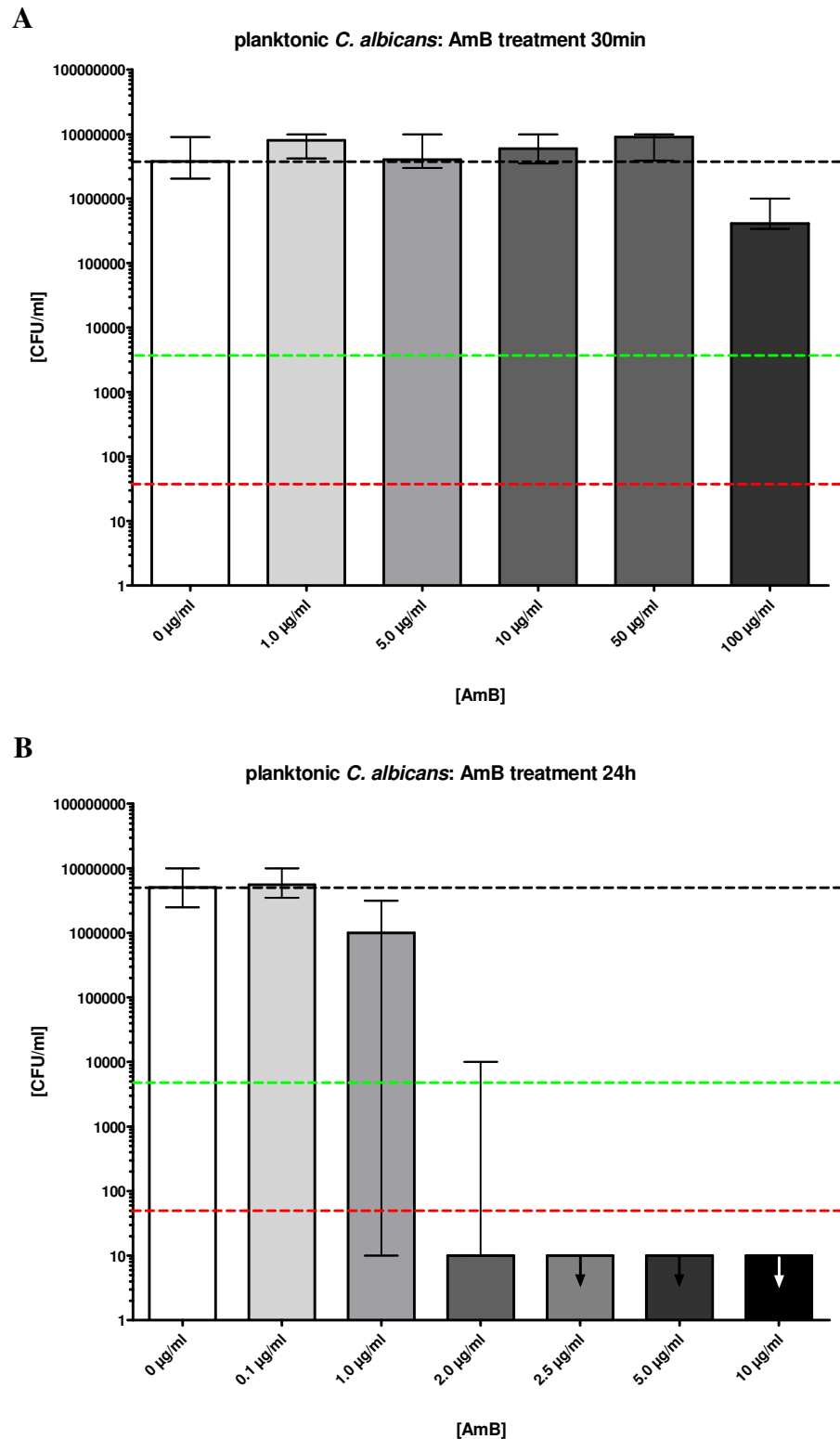
Fig. 29. AmB treatment of *C. albicans* planktonic cells. *C. albicans* planktonic cells were incubated with different concentrations of AmB for (A) 15 min and (B) 24 h. A CFU assay was performed immediately after aPDT, and surviving colonies were counted 24 h later. Black dashed line: baseline CFU/ml; green dashed line: reduction of 3 $\log_{10}$ steps in viable *C. albicans* (reduction 99.9%); red dashed line: reduction of 5 $\log_{10}$ steps in viable *C. albicans* (reduction 99.999%). (n = 3 experiments; median ± interquartile range).

Biofilms, treated with AmB for the same time period as aPDT (5 h), were killed with 50 µg mL^{-1} (Fig. 30) and biofilms, incubated with AmB for 24 h, were killed with 10 µg mL^{-1}(Fig. 31).
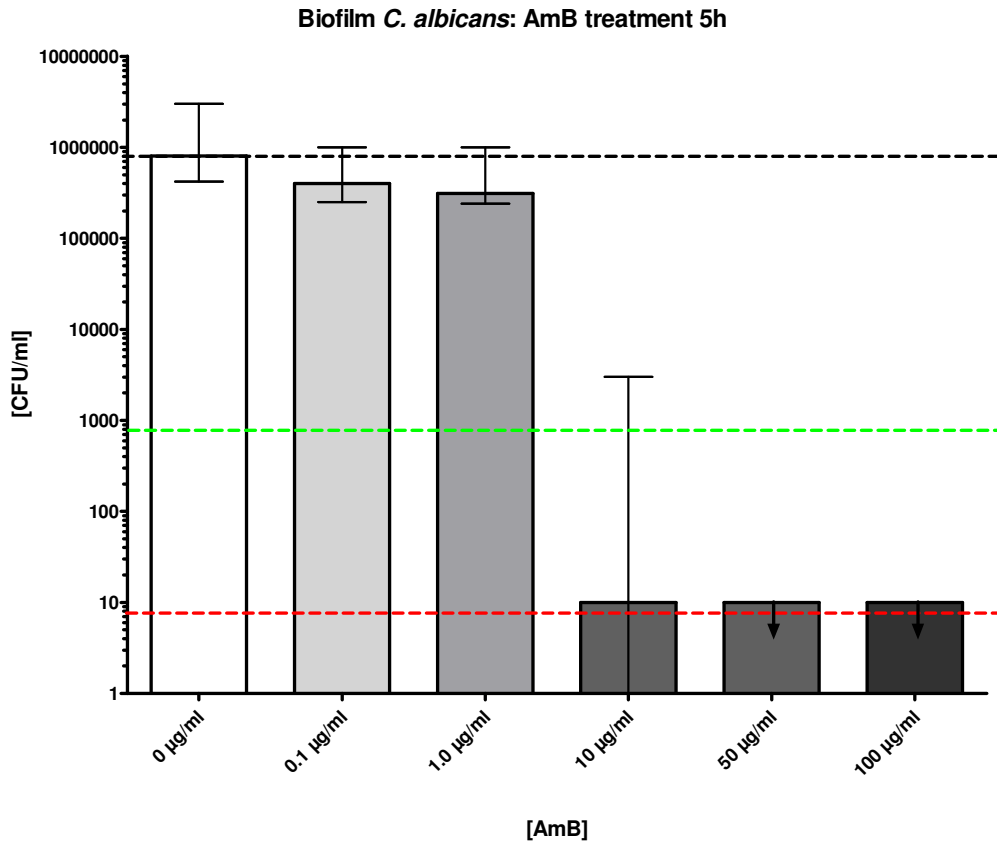
Fig. 30. AmB treatment of *C. albicans* biofilm cells. *C. albicans* biofilm cells were grown on the surface of 96 well plates for 24h. *C. albicans* biofilm cells were incubated with different concentrations of AmB for 5 h. A CFU assay was performed immediately after aPDT, and surviving colonies were counted 24 h later. Black dashed line: baseline CFU/ml; green dashed line: reduction of 3 log$_{10}$ steps in viable *C. albicans* (reduction 99.9%); red dashed line: reduction of 5 log$_{10}$ steps in viable *C. albicans* (reduction 99.999%). (n = 3 experiments; median ± interquartile range). The arrows mark the lower detection limit of the CFU assay.

Biofilm *C. albicans*: AmB treatment 24h
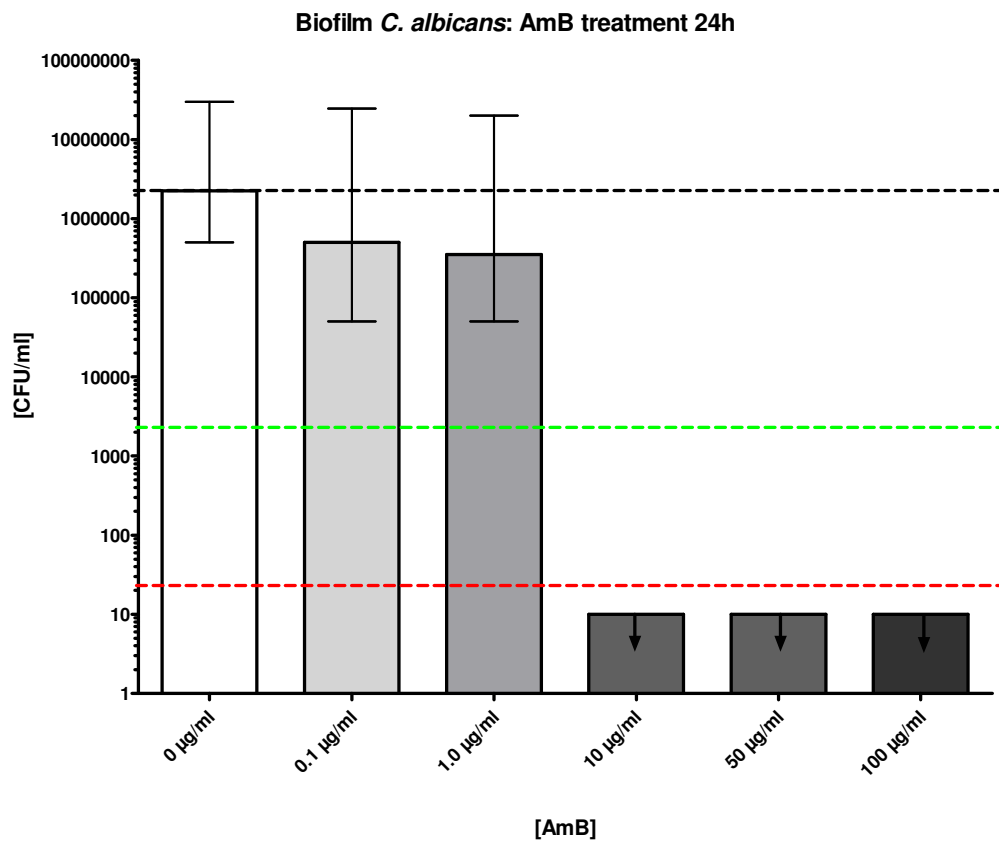
Fig. 31. AmB treatment of *C. albicans* biofilms. *C. albicans* biofilms were grown on the surface of 96 well plates for 24h. *C. albicans* biofilm cells were incubated with different concentrations of AmB for 24 h. A CFU assay was performed immediately after aPDT, and surviving colonies were counted 24 h later. Black dashed line: baseline CFU/ml; green dashed line: reduction of 3 $\log_{10}$ steps in viable *C. albicans* (reduction 99.9%); red dashed line: reduction of 5 $\log_{10}$ steps in viable *C. albicans* (reduction 99.999%). (n = 3 experiments; median ± interquartile range). The arrows mark the lower detection limit of the CFU assay.

### 2.3.6 Multi-channel 3D fluorescent microscopy images

Fluorescence images confirmed that biofilms, used in this study, were composed of a mixture of yeasts, and hyphae. The live/dead staining kit was used to distinguish between living (green stained), and dead *C. albicans* cells (red stained) within the biofilm. 24 h old biofilms were stained and the fluorescence intensities of the live/dead staining were evaluated. The evaluation of 3 independent biofilms showed that 95 +/- 5% of living *C. albicans* cells can be detected within the biofilms. Fig. 32 shows

exemplarily the fluorescence distribution of a live/dead staining of a biofilm with living

(green-stained) and dead (red-stained) *C. albicans* cells.
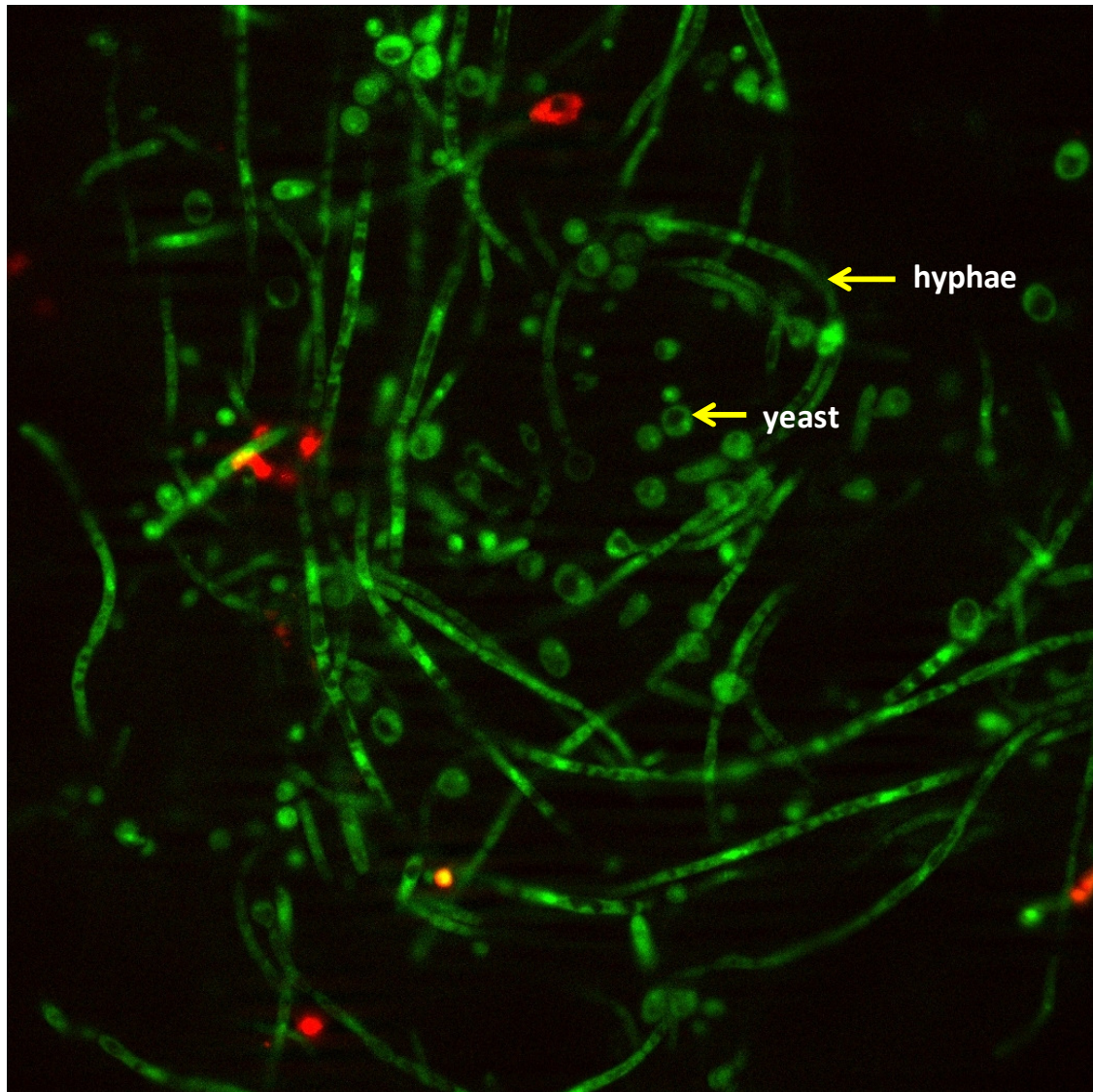
Fig. 32. Fluorescence image of *C. albicans* biofilm labeled with live/dead staining: Fluorescence image of a 24 h old biofilm composed of yeasts and hyphae cells. Biofilms were stained with live/dead biofilm viability kit, where Syto 9 labeled live cells in green and Propydium iodide labeled dead *C. albicans* cells in red (×40 objective).

In addition, the presence of the EPS, a defining characteristic of biofilms, was

confirmed by staining it with ConA-Texas Red conjugate. (Fig. 33).
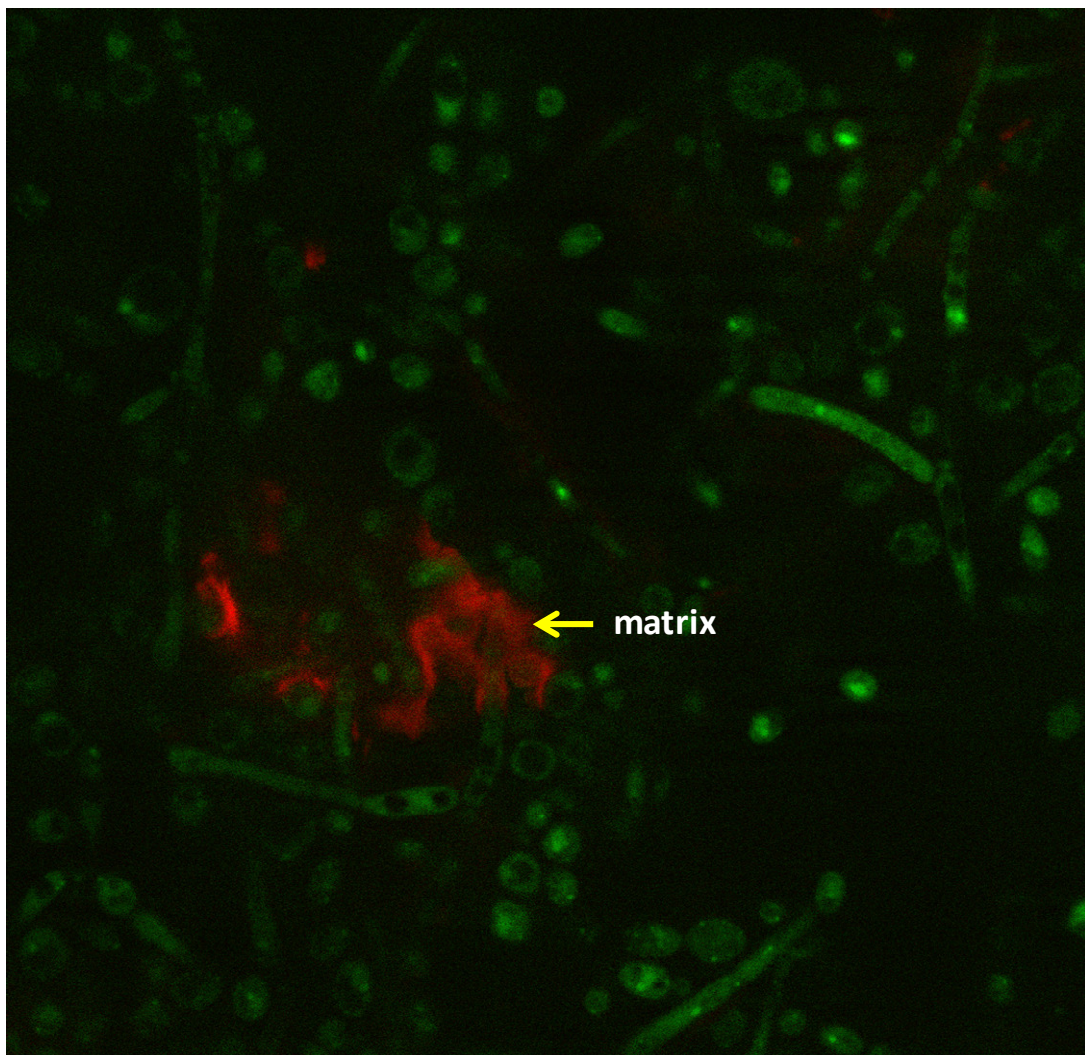
Fig. 33. Fluorescence image of *C. albicans* EPS labeled with Concanavalin A (ConA)-Texas Red conjugate. Fluorescence image of a 24 h old biofilm stained with Syto 9 (fungi cells stain in green) and ConA labeled EPS in red (×40 objective).

2.3.7 Singlet oxygen luminescence signal from *C. albicans* biofilm cells incubated with TMPyP and XF-73

The spectrally resolved $^1O_2$ luminescence signal observed in *C. albicans* biofilm cells, incubated with TMPyP and XF-73, was detected at 1270 nm, which is characteristic for $^1O_2$ luminescence.

This indicates that TMPyP and XF-73 act as photosensitizers against *C. albicans* biofilm via the intermediacy of $^1O_2$. The decay time of the $^1O_2$ luminescence of the washed incubated biofilms is in the range of µs with $t_{TMPyP,1} = (4.88 \pm 0.5)$ µs, $t_{TMPyP,2} = (2.09 \pm 0.2)$ µs and $t_{XF-73,2} = (6.61 \pm 0.7)$ µs. The $^1O_2$ luminescence signal showed a smaller intensity, when the biofilm was incubated with TMPyP and subsequently washed (Fig. 34), compared to the XF-73 (Fig. 35). No rise time of $^1O_2$ could be fitted for XF-73 activated by light in *C. albicans* biofilms. Singlet oxygen is the most important ROS formed during aPDT. Therefore it was investigated, whether $^1O_2$ could be responsible for the XF/TMPyP photodynamic killing in *C. albicans* biofilms.
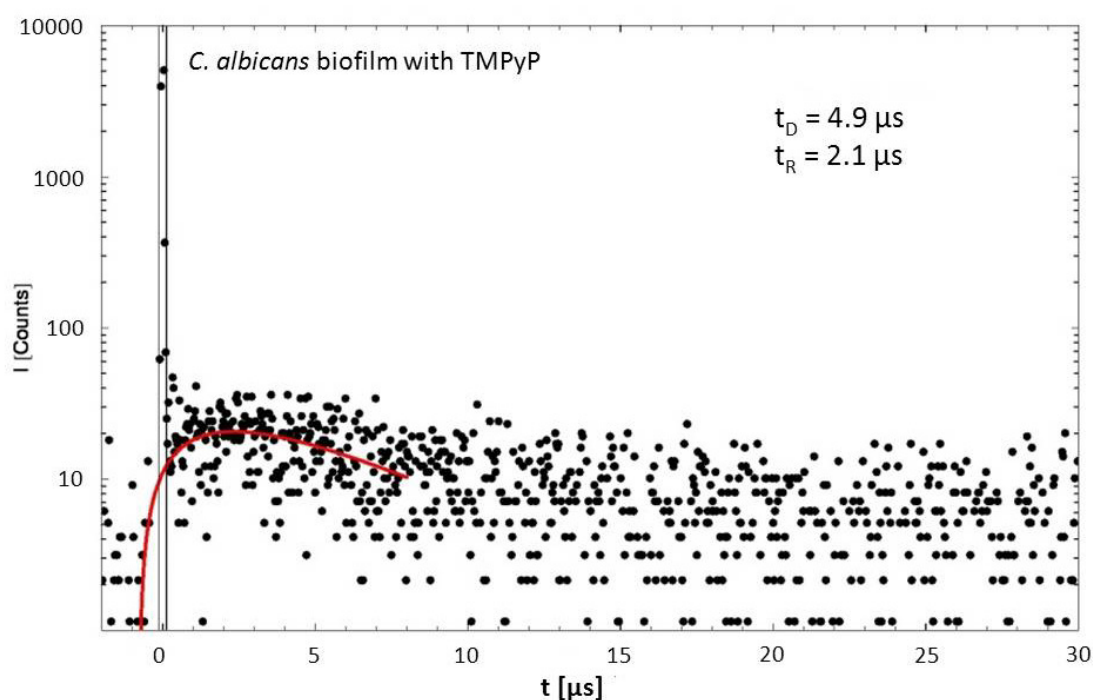
Fig. 34. Time resolved singlet oxygen luminescence: Biofilms of *C. albicans*, incubated with 100 µM of TMPyP. The biofilm was washed with H$_2$O and immediately irradiated with the Nd:YAG laser at 532 nm. The data show a decay time [61] of the $^1O_2$ luminescence signal in the typical range of µs
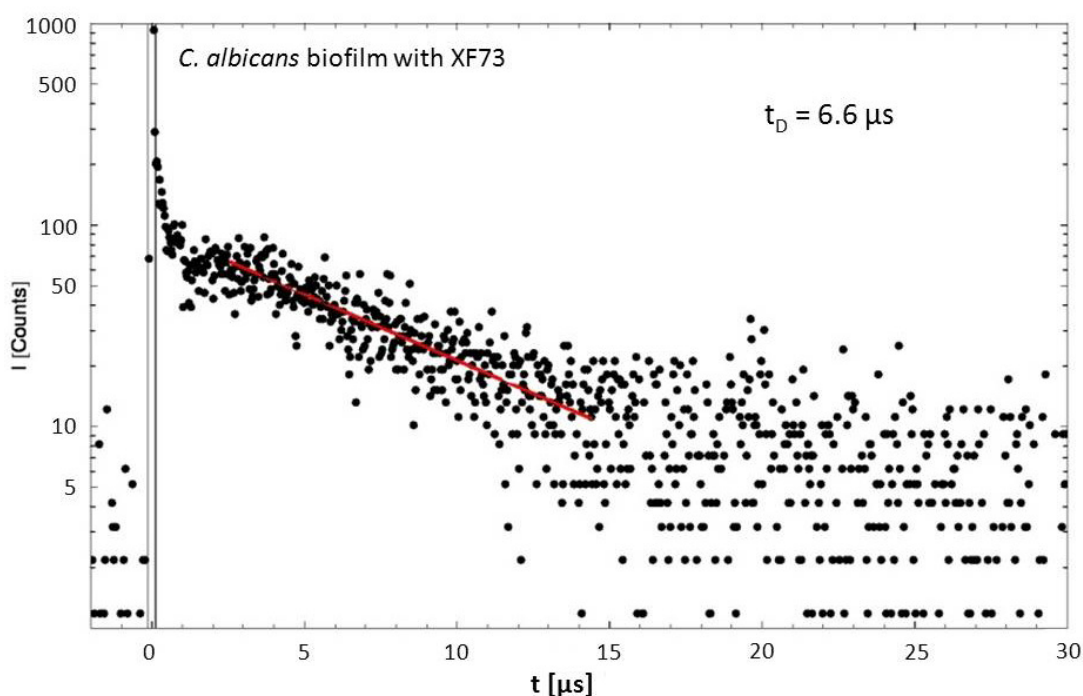
Fig. 35. Time resolved singlet oxygen luminescence: Biofilms of *C. albicans*, incubated with 100 μM of XF-73. The biofilm was washed with H$_2$O and immediately irradiated with the Nd:YAG laser at 532 nm. The data show a decay time [61] of the ^{1}O$_2$ luminescence signal in the typical range of μs

2.4 Discussion

Most manifestations of candidiasis are associated with the formation of *Candida* biofilms [147]. In addition, biofilms are less susceptible to antifungal agents, compared to its planktonic counterparts [132]. The antimicrobial drugs in current use, like AmB, have the ability to kill planktonic cells rather than biofilm cells. The problem is that over 80% of microbial infections in the human body are caused by cells growing in a biofilm state, which presents increased resistance to antimicrobial treatments, when compared to planktonic cells [140]. Biofilms present cells in different metabolic states, from rapidly proliferating to absolutely dormant. This fact frustrates efforts to control biofilms with antimicrobial agents. In addition, biofilms display some different characteristics than planktonic cells, like penetration and physiological heterogeneity.

So, it is not possible to predict the efficacy of an antimicrobial treatment against biofilm from data, collected using planktonic cells. In this way, growing microbial cells as part of a biofilm increases the relevance of test results [148].

The facts, stated above, ensure the need for effective antimicrobial therapies that can prevent and destroy biofilm of *C. albicans*. In this investigation, it was demonstrated for the first time that both TMPyP and XF-73 combined with blue light could kill 99.999% of *C. albicans* growing as a biofilm, whereas XF-73 was more efficient and acted at lower concentrations than TMPyP.

The binding of PSs by microorganisms is an important feature for the efficacy of aPDT. Demidova and Hamblin (2005) found that the efficacy of aPDT is dependent on the amount of PS binding [28]. It was already shown that TMPyP is an active PS against *C. albicans* planktonic cells [42]. Although having less positive charges, our results showed that XF-73 can bind better to both *C. albicans* phenotypes, when compared to TMPyP. Consequently, XF-73 demonstrated a greater photokilling efficacy, compared to TMPyP, regardless of planktonic or biofilm growing *Candida*. Using the same conditions as for TMPyP (incubation time and light dose), 0.5µM of XF-73 was necessary to kill >6 $\log_{10}$ of planktonic cells vs. 2 µM of TMPyP.

For biofilms, 1 µM of XF-73 were necessary to destroy >5 $\log_{10}$ cells vs. 50 µM of TMPyP upon light activation. To our knowledge, it is the first time that aPDT caused such an extensive inactivation rate of *C. albicans* biofilms. Biofilms were killed with a concentration of XF-73 two times higher than the concentration, necessary to kill planktonic cells. On the other hand, the concentration of TMPyP, necessary to kill *C. albicans* biofilm cells, was 25 times higher than the concentration, used to kill planktonic cells.

The phototoxicity of both PSs is influenced by the position of positive charges. In XF-73, the cationic groups were separated from the tetrapyrrol ring system of the PS by an alkyl chain as a spacer. Thus, the charges have a high mobility and a minimal influence on the photophysical properties of the porphyrin. Therefore, the spacer provides a high mobility of the charges, which could facilitate the interaction with *C. albicans* cell wall. TMPyP in turn possesses four positive charges, located near the tetrapyrrol rings, conferring to the drug a planar, rigid structure, making the rotation restricted on the axis of the planar structure.

Furthermore, the action of positively charged drug molecules can be retarded by the presence of negatively charged EPS [149]. Like that, TMPyP, which has more positive charges than XF-73, will form stronger electrostatic interaction with the EPS, retarding even more the diffusion of the PS within the biofilm.

Planktonic cells were eliminated more rapidly and at lower concentrations of both PSs, when compared with biofilms. There is more than one reason for the increased resistance of *Candida* biofilms to antimicrobial treatments, when compared to planktonic cells. Presence of the EPS, inhibiting drug diffusion to the cells within the biofilm and reducing the concentration of the drug reaching the cells in the biofilm [73], up regulation of multidrug resistance genes; slow growth rate leading to slow and insufficient drug uptake as result of nutrient limitation. Therefore, antimicrobial drugs with just one single mechanism of action, like AmB, are unlikely to be effective against biofilms [122]. However, aPDT acts via multihit processes and is capable of inducing oxidative damage to the whole biofilm structure during the treatment. So, in addition to the inactivation of the microorganisms within the biofilm, aPDT also disrupts the biofilm structure [55]. The high chemical reactivity of singlet oxygen ensures that aPDT has also a direct effect on extracellular molecules, like the polysaccharides, present in

the EPS. Such a dual activity of aPDT can be an advantage, because it may avoid new colonization and prevent recurrence infection [150]. If one treatment is insufficient to disrupt biofilm structures and to inactivate its cells within, repeated aPDT treatments can be conducted, since this technique does not induce resistance so far.

To investigate, whether the reduced susceptibility of biofilm could be related to the retarded diffusion or exclusion of the photosensitizer, imposed by the presence of the EPS, we tested the susceptibility of disrupted biofilms to aPDT. Resuspended biofilm cells (which presumably have lost most of their EPS) were less resistant to aPDT with XF-73 than intact biofilms. The disruption of the biofilm structure improved the accessibility of the biofilms to aPDT, suggesting that the organized structure of biofilm might play a role in the susceptibility of intact biofilm to antimicrobial drugs. It is also likely that the disruption of the biofilm structure provides new access to nutrients to the cells, which were previously starving in deep layers of the biofilm. This brings them back to the susceptible state of exponential growth [151].

The challenge in aPDT is to find a therapeutic window, in which microorganisms are killed without harming the surrounding tissue. Maisch et al. evaluated the phototoxicity of XF-73 against bacterial cells and found that, the parameters able to cause 3 $\log_{10}$ killing in a range of Gram-positive *staphylococcal* strains, including methicillin-resistant *Staphylococcus aureus* (MRSA) strains, were not toxic for human fibroblasts or keratinocytes, with $\geq 90\%$ of these cells still viable *in vitro*. Furthermore, fluorescence microscopy images showed that XF-73 is located outside of the nucleus, in the mitochondria of mammalian cells [45].. This finding corroborates the fact that PDT has a low mutagenic potential, since singlet oxygen, the main cytotoxic agent produced in photodynamic action, has a short life time in cells, less than 0.05 ps. Thereby, singlet oxygen, can diffuse less than 0.02 pm from the site of

its generation, reducing the possibility of nuclear damage [51]. The absence of genototoxic and mutagenicity to human cells is a must have of APDT that favors its long-term safety.

In a later study, fluorescence experiments showed that the distribution of the formulation XF-73 water-ethanol was restricted to the stratum corneum and no accumulation in deeper parts of the epidermis or dermis was observed, even with an incubation time of 4 h, which is the same incubation time that we have used to kill biofilm cells [45]. Localization of XF-73 in the stratum corneum indicates the existence of a therapeutic window for an efficient decolonization of pathogens without side effects for the underlying tissue. PSs, which penetrate only the stratum corneum, may be used for the treatment of *Candida* infections, since the most common type of infections, caused by *Candida* species, are superficial infections of skin and mucous membrane, which do not affect living tissues [152]. Therefore, successful treatment of superficial infections by *C. albicans* has the advantage to avoid that this microorganism reaches the bloodstream infecting internal organs.

In this study the action of AmB, the drug of choice for treating severe systemic infection, was also compared with the action of aPDT, against both cell phenotypes of *C. albicans.* Antifungal drugs, like AmB, act according the key-lock principle. This means, that they have specific action against a single component of the cell. In the case of AmB, this component is ergosterol, which is located in the cell membrane. On the other hand, aPDT acts via multihit processes, where all the putative targets in the cell are available to be damaged by the ROS, formed during the photodynamic process.

The minimum inhibitory concentrations (MIC) for AmB range from 0.06-2.0 µg mL^{-1} for planktonic cells [153]. In the present study, it was not possible to kill *C. albicans* planktonic cells, when they were treated with AmB for the same time period as

aPDT (30 min). But, when planktonic cells were treated with AmB for 24 h, it was possible to kill planktonic cells using 2.5 µg mL^{-1} of AmB. *C. albicans* isolates with MIC $\geqq$ 2 µg mL^{-1} are already considered to be resistant [154]. On the other hand, biofilms could be killed in both treatment conditions (5 and 24 h) with concentrations of 10 µg mL^{-1} and 50 µg mL^{-1} of AmB. These AmB concentrations are higher than the serum levels (0.5 to 2.0 µg mL^{-1}), used to treat patients with infections, caused by *C. albicans* and can be toxic to human cells [142, 155]. Compared to the conventional AmB treatment, aPDT was more effective. Furthermore, the damage, caused by aPDT, occurs only when light activates the drug and elicits the toxic action.

The local action of AmB to osteoblasts and fibroblasts was recently investigated. This investigation showed that 100 and 1000 µg mL^{-1} of AmB caused osteoblast cell death and 1 to 10 µg mL^{-1} caused sublethal toxicity to osteoblasts and fibroblasts. If local concentrations of 100 to 1000 times of the MIC are necessary to treat infections, caused by biofilms, cell toxicity at the site of the treatment should be considered [156].

For the first time, $^1O_2$ was detected in biofilms of *C. albicans*, indicating that this ROS was responsible for the TMPyP/XF-73 photodynamic damage to *C. albicans* biofilms cells. $^1O_2$ luminescence was detected after both PSs were washed away from the biofilms. This fact suggests that both PSs were able to penetrate the biofilm structure, since $^1O_2$ was generated by PSs, which were within the biofilm and not in the external milieu (supernatant). The luminescence intensity, detected for incubation with XF-73, is higher compared to TMPyP, which might be due to better attachment of XF-73 to the cells or the biofilm EPS. This is in agreement with the toxicity data, where a smaller amount of XF-73 is needed for the same toxic efficacy.

The results obtained in this study showed that XF-73 is a very effective PS, which is able to kill even *C. albicans* cells in the biofilm state, using very small concentrations

of the PS and low light doses that justify further investigations of XF-73 mediated aPDT in particular in clinical studies.

3 Photodynamic inactivation of *Candida albicans* coaggregated with *Staphylococcus epidermidis* in a duo-species biofilm

3.1 Introduction

Candida albicans biofilms can consist of a single microbial species or multiple microbial species. Although several infections are caused by biofilm formed solely by *C. albicans,* biofilm formed by *C. albicans* and other bacteria are predominant [157, 158]. In a biofilm formed by multiple microbial species which are closely associated, mutually beneficial interactions may arise. *Candida* species of mixed biofilms are often found with bacterial cells and are subjected to various antagonistic and synergistic interactions which may impact the virulence of *C. albicans* [159, 160]. For instance, *Pseudomonas aeruginosa* can be co-isolated with *C. albicans* thereby *Pseudomonas* can further adhere, lyse and kill *C. albicans* hyphae [161, 162]. On the other hand, *C. albicans* has a synergistic relationship with *Streptococcus gordonii*. It was showed that this bacteria enhances *C. albicans* filamentation, whereas *C. albicans* stimulates biofilm formation of *Streptococcus gordonii* [163]. Furthermore, the ability that *C. albicans* has to switch from a yeast to a hyphal morphology provide an invasion strategy to other microbial cells, like *staphylococci*, which are known to adhere in *C. albicans* hyphae [164].

A study investigating the presence of fungal pathogens in biofilms causing chronic wounds found that 3% of these wounds were positive for fungal species, predominantly *Candida sp*. which was responsible for > 50% of the microbial burden in the wounds [165]. Such polymicrobial biofilms are more extremely difficult to treat because they require a drug with activity against both fungi and bacteria cells [166].

Staphylococcus epidermidis is a commensal skin bacteria, but can cause severe infection after invasion and penetration of both epidermal and mucosal barriers [167]. Whereas *C. albicans* is by far the most frequently fungal pathogen found in biofilms, the most prevalent isolated bacterial species is *S. epidermidis*. In addition, this bacteria is the most frequent cause of nosocomial infections [168]. In patients with candidemia, *S. epidermidis* is the most commonly bacteria specie isolated [169].

Therefore, it was investigated the susceptibility of *C. albicans* co-isolated with *S. epidermidis* to XF-73-mediated aPDT. This result was compared with the results obtained in the first section, where we tested the photoactivity of XF-73 against *C. albicans* monomicrobial biofilm.

3.2 Materials and Methods

3.2.1 Strains of *C. albicans*

One to three colonies of *C. albicans* (ATCC-MYA-273, LGC Standards GmbH,
Germany) were picked up from agar plates with a sterile inoculating loop and
transferred to a culture tubes containing 5 mL of Sabouraud Dextrose Broth (SDB)
(Sigma Chemical Co., St. Louis, Mo) and grown at 37 °C on a shaker platform (200
rpm) overnight. When the cultures reached the stationary phase of growth, the cells
were harvested by centrifugation (3100 rpm, 5 min), washed once with Dulbecco's
phosphate-buffered saline (PBS without Ca^{2+} and Mg^{2+}; PAA Laboratories GmbH,
Austria) and used for further experiments.

3.2.2 Strains of *S. epidermidis* strains

One to three colonies of *S. epidermidis* (ATCC-35984) (Gentamycin-susceptible strain)
(LGC Standards GmbH, Germany) were picked up from agar plates with a sterile
inoculating loop and transferred to a culture tubes containing 5 mL of in Tryptic soy
broth (TSB) (Sigma-Aldrich-Fluka, St Louis, USA) and grown at 37 °C on a shaker
platform (200 rpm) overnight. When the cultures reached the stationary phase of
growth, the cells were harvested by centrifugation (5.000 rpm, 5 min), washed once
with PBS and used for further experiments.

3.2.3 Photosensitizer and light source

The photosensitizer used in this study was XF-73. The irradiation of samples was
performed using an incoherent light source (Omnicure Series 2000, igb-tech,
Friedelsheim, Germany) with an excitation filter set of 400–500 nm. This light source

was used because it has a higher light intensity (49.8 mW cm^{-2}) than the light used to photoinactivate *C. albicans* monomicrobial biofilms (section 2; 13.4 mW cm^{-2}). Therefore the overall period treatments could be shortened.

3.2.4 Formation of duo-species biofilm

As *C. albicans* readily forms monomicrobial biofilms in serum, duo-species biofilm formed by *C. albicans* and *S. epidermidis* were also formed in this medium. Different parameters were tested to find the optimal condition for duo-species biofilm formation. The following conditions were tested: *S. epidermidis* was added to the microplates concurrently, 2 h, 4 h and 6 h after the addition of *C. albicans*. The concentration of *C. albicans* added to the microplates in relation to *S. epidermidis* was 1:1, 1:10, 1:40. As *C. albicans* readily forms monomicrobial biofilms in serum, polymicrobial biofilms formed by *C. albicans* and *S. epidermidis* were also formed in this medium. Polymicrobial biofilms used in the experiment were formed as following: the concentration of *C. albicans* added to the microplates in relation to *S. epidermidis* was 1:40. Accordingly, *C. albicans* cells were diluted to 10^6 cells mL^{-1} in 25% of FBS and 200 μL were added to sterile flat-bottomed 96-well polystyrene plates 6 h before the addition of *S. epidermidis*. S. *epidermidis* (5 μL) were diluted in TSB to an optical density at 600 nm (OD600) of 0.5, corresponding to 10^8 cells mL^{-1}. Then they were added to the wells and mixed by pipetting up and down. The plates were incubated for 36 h at 37°C. To monitor the bacterial and fungal growth within the biofilms, CFU assay using selective plates was used to assess fungal versus bacterial numbers.

3.2.5 **Multi-channel 3D fluorescent microscopy images**

Duo-species biofilms were formed as described before, using cell culture dishes of size 35×10mm (Cellstar, Frickenhausen, Germany). Biofilms were stained with a nucleic acid intercalator membrane-permeable, the Syto-9 green-fluorescent (Molecular Probes, Eugene, OR, USA), which stain microbial cells in green. Additionally, Concanavalin A (ConA)-Texas Red conjugate (Molecular Probes, Eugene, OR, USA) was used to stain the biofilm EPS in red. The final concentrations of dyes were as follows: 0.01 mM for Syto-9 and 200 µg mL^{-1} for ConA.

Fluorescence microscopy was performed using a Zeiss Observer Z1 inverted fluorescence microscope with ApoTome (Zeiss) and AxioVision software (v 4.6.2.0, Zeiss) using appropriate filter-sets for excitation and emission of SYTO 9 (λ_{ex}485nm/λ_{em}500nm) and Con A (λ_{ex}590nm/λ_{em}615nm).

3.2.6 **Photodynamic inactivation of *C. albicans* co-isolated with *S. epidermidis***

After 36 h of incubation, biofilms were washed once to remove loosely attached cells. The cells were incubated with increasing concentrations of XF-73 (0; 0.1; 1; 10 and 100 µM) for 4 h in the dark at 37°C. Thereafter, cells were illuminated for 16.6 min (50 J cm^{-2}). The maximal fluence rate at the level of the irradiated samples was 49.8 mW cm^{-2}. Biofilms were then detached from the bottom of the well by scraping the bottom of the microplate with a pipette tip and transferred to an eppendorf tube containing 1 mL of PBS. Biofilm material scraped from the wells was homogenized by vortexing and sonicating, each for 1 min to get single cells prior a CFU assay was done.

3.2.7 **Colony forming unit assay**

Miles and Misra method was used to estimate the viable number of microbial cells after phototoxic treatments [170]. After ten-fold serial dilutions of cell suspensions in PBS, 3 x 20 μl of the dilutions were seeded onto Sabouraud Dextrose Agar supplemented with Gentamicin (0.005 mg mL^{-1}) for selective recovery of *C. albicans* and 0.1 ml onto Tryptic Soy Agar supplemented with AmB (0.5 mg mL^{-1}) for selective recovery of *S. epidermidis*, for 48 h at 37°C. A CFU assay was done to determine the number of colony forming unites per milliliter.

3.3 Results

Since *Candida* sp. are often found coaggregated with bacteria in polymicrobial biofilms *in vivo* and the susceptibility of these fungal cells to antifungal agents can be modulated by bacterial cells present in the polymicrobial biofilm, it was determined whether *C. albicans* and *S. epidermidis* could form polymicrobial biofilms *in vitro* and whether this interaction could affect the susceptibility of *C. albicans* to aPDT.

3.3.1 **Formation of duo-species biofilm**

From the different parameters tested, the best conditions to generate a duo-species biofilm formed by *C. albicans* and *S. epidermidis* were the following: *C. albicans* 10^6 cells mL^{-1} diluted in 25% of fetal bovine serum (FBS; PAN Biotech, Aidenbach, Germany) and added to the microplates 6 hours before the addition of *S. epidermidis* (OD of 0.5, corresponding to 10^8 cells mL-1). According these conditions, fungal cells could first attach to the surface of the microplates, undergo yeast-to-hyphal transition,

due to the presence of FBS. *S. epidermidis* added 6 hours later could adhere to *C. albicans* hyphaes. With these parameters it was possible to recovery 10^7 cells mL^{-1} for *C. albicans* cells and 10^{11} cells mL^{-1} for *S. epidermidis.*

3.3.2   Multi-channel 3D fluorescent microscopy images

To confirm the presence of the EPS, the duo-species biofilm was stained with ConA-Texas Red conjugate, which stained the EPS in red (Fig. 36). SYTO 9 penetrates all microbial membranes and stained microbial cells in green. Green colored area shows *C. albicans* hyphae associated with microcolonies of *S. epidermidis*. It seems that *C. albicans* acted as a scaffold for the attachment and proliferation of *S. epidermidis* (Fig. 36).
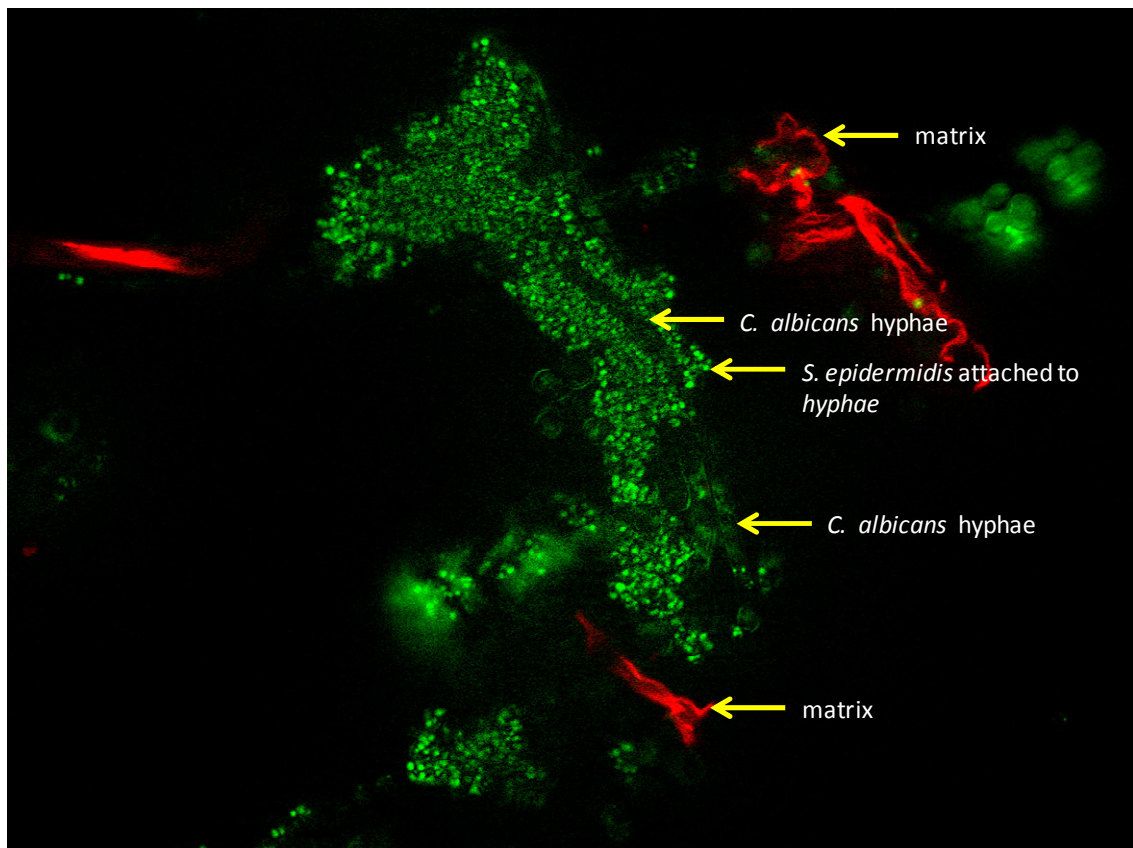
Fig. 36 Fluorescence image of *C. albicans-S. epidermidis* biofilm: 24 h biofilms were stained with Syto 9, which stained hyphae of *C. albicans* and *S. epidermidis* in green and ConA-Texas Red conjugate which stains the EPS in red (20× objective).

3.3.3 **Photodynamic inactivation of *C. albicans* co-isolated with *S. epidermidis***

The photodynamic efficacy of XF-73 in combination with blue light was investigated against *C. albicans* found as a part a duo-species biofilm of *C. albicans* and *Staphylococcus epidermidis*. These results where compared with the photoaction of XF-73 against *C. albicans* monomicrobial biofilms obtained in the first section.

C. albicans co-isolated with *S. epidermidis* showed increased resistance to XF-73 mediated aPDT even with higher concentrations of XF-73. Even concentrations as high as 100 µM of XF-73 did not cause any decrease in *C. albicans* survival (Fig. 37). *C. albicans* monomicrobial biofilms incubated with 1 µM of XF-73 for 4 h and illuminated with for 60 min (13.4 mW cm^{-2}, 48.2 J cm^{-2}) yielded 5 log$_{10}$ decrease cell survival (section 2.3.4, Fig. 27). Overall, the results showed that bacteria can affect the susceptibility of *C. albicans* to aPDT in the duo-species biofilm.
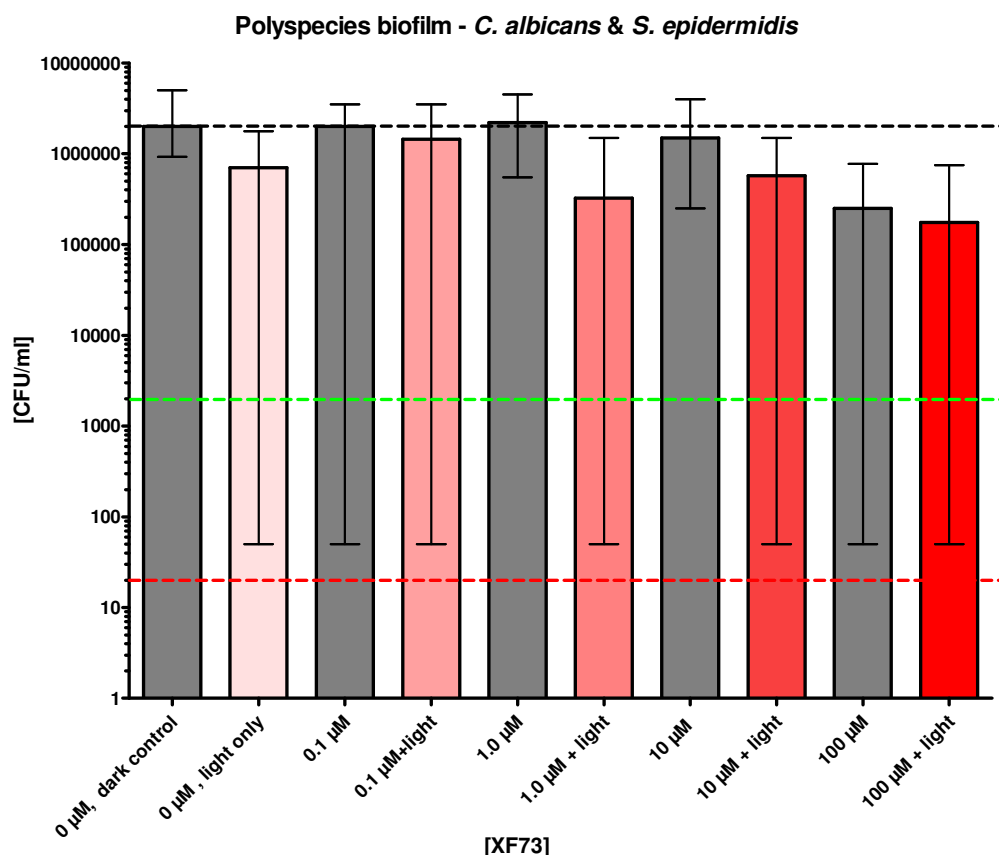
Fig. 37. APDT treatment of *C. albicans* coaggregated with *Staphylococcus epidermidis* in a duo-species biofilm. Duo-species biofilm were grown on the surface of 96 well plates for 36 h. After incubation with different concentrations of XF-73 for 4 h, the samples were irradiated with 49.8 mW cm^{-2}, 50 J cm^{-2}. A CFU assay was performed immediately after aPDT, and surviving colonies were counted 24 h later. Black dashed line: baseline CFU/ml; green dashed line: reduction of 3 log$_{10}$ steps in viable *C. albicans* (reduction 99.9%); red dashed line: reduction of 5 log$_{10}$ steps in viable *C. albicans* (reduction 99.999%). (n = 3 experiments; median ± interquartile range). The arrow marks the lower detection limit of the CFU assay.

3.4 Discussion

It is estimated that 27-56% of *C. albicans* bloodstream infections are polymicrobial [169]. The most commonly co-isolated bacterial species is *Staphylococcus epidermidis* [169]. Previous study already showed that *C. albicans* and *S. epidermidis* can extensive interact in a duo-species biofilm and that they had altered

their antimicrobial susceptibility when growing as a part of a duo-species biofilm. The EPS produced by *S. epidermidis* inhibit fluconazole penetration and *C. albicans* enhanced the growth of *S. epidermidis* and increased the resistance of *S. epidermidis* to vancomycin [159].   [159]. Therefore, we investigated whether *C. albicans* and *S. epidermidis* could form polymicrobial biofilms and the effect of *S. epidermidis* on the susceptibility of *C. albicans* to aPDT within the polymicrobial biofilm.

In accordance with already published data [159, 164], it was established a duo-species biofilm formed by *C. albicans* and *S. epidermidis*, where the bacteria were attached to the hyphal filaments of *C. albicans*. Biofilm formation by *C. albicans* mixed with bacteria occurs in a temporal manner such that the attachment of *C. albicans* becomes the scaffolding to which other microbial specie may adhere. As a result, the composition of early colonizers determines which microbes colonize at later time points of biofilm formation. This process of sequential attachment is commonly referred to as coaggregation [164].

Compared with *C. albicans* monomicrobial biofilm in the section 2, *C. albicans* in the polymicrobial biofilm was resistant to aPDT. In the section 2.3.4, *C. albicans* monomicrobial biofilms incubated with 1 µM of XF-73 for 4 h and illuminated with for 60 min (13.4 mW cm^{-2}, 48.2 J cm^{-2}) yielded 5 log$_{10}$ decrease cell survival. Here, *C. albicans* in the polymicrobial biofilm, could not be photokilled even using concentrations as high as 100 µM. Also, the light sources used in both experiments were different. Despite the same overall light doses were used in both experiments (monomicrobial×polymicrobial), the light intensity used to activate the PSs in the experiments with polymicrobial biofilms was higher (49.8 mW cm^{-2}) versus 13.4 mW cm^{-2}.

The increased resistance of *C. albicans* coaggregated with *S. epidermidis* when compared to *C. albicans* within a monomicrobial biofilm might be explained by the fact that a polymicrobial biofilm produces more EPS than a monomicrobial biofilm. Another study investigated the effects of aPDT using MB (0.1 mg mL^{-1}) and red light (100 mW cm^{-2} and 350 J cm^{-2}) on the viability of a polymicrobial biofilm formed by *C. albicans*, *S. aureus* and *Streptococcus mutans*. Single-species biofilm (2.32–3.29 log$_{10}$) were more susceptible to aPDT than the mixed-species biofilm (1.00–2.44 log$_{10}$) formed by two and three species of microorganisms, suggesting that the more complex the composition of the biofilm, the more resistant it seems to be to aPDT. The authors suggested that the interactions between the different EPS polymers in these polymicrobial biofilms, produces a more viscous EPS, increasing the antibiotic resistance further [172].

Polymicrobial biofilms are usually thicker and more stable than monomicrobial biofilms [173]. Recently it was demonstrated that the total biomass of a polymicrobial biofilm formed by *C. albicans* and *S. aureus* were greater than the biomass of each microorganism growing independently as a biofilm [174]. Such an increased biomass in a polymicrobial biofilm may enhance resistance to antimicrobial treatments.

Another point is the fact that the biofilm used in this study was older (36 h) than in the monomicrobial biofilm (24 h). The age of the biofilms might also affect it susceptibility to antimicrobial treatments. Young biofilms have a less organized structure, a more active metabolism and a less pronounced stress response than more mature biofilms [175]. Like that, young biofilms seems to be more susceptible to antimicrobial treatments than older biofilms. In contrast, some photodynamic studies already showed that aPDT is more effective in inactivating older biofilms than younger ones. MB mediated aPDT was more effective to inactivate a 48 h old biofilm of

Pseudomonas aeruginosa (>99.999%) than a 24 h old one (99.9%). *P. aeruginosa* produces larger amounts of phenazine compounds (endogenous PSs) when they are in the stationary phase, since phenazine is regulated by quorum sensing and produced under conditions of high cell density and nutrient limitation, which are the conditions present in more mature biofilms. *P. aeruginosa* secretes enzymes and EPS components that protect it from the harmful effects of its own endogenous PSs; however upon addition of an exogenous PS, their natural mechanisms of protection may become saturated, leading to the photodynamic killing of the cells. So, the authors stated that it seems that the synthesis and accumulation of higher amounts of phenazines in older biofilms than in younger ones would lead to a greater additive effect of the two PSs and result in enhanced bactericidal activity [176]. Another study also using MB as a PS, showed that "older" *Streptococcus mutans* biofilms were more susceptible to aPDT than "younger" biofilms. Two hypotheses were used to explain the increased resistance of younger biofilms to aPDT: Firstly, the channel architecture of mature biofilms permitted enhanced access for the PS within the biofilms. Secondly, younger biofilms are metabolically more active and are better able to repair damage mediated by ROS [177]. More studies to elucidate whether the biofilm age plays an important role in the susceptibility of microbial cell to aPDT are necessary.

Data obtained from the present study showed that the more complex the composition of biofilm is, the more resistant it seems to be to aPDT. If the EPS is responsible for the increased resistance of *C. albicans* in a polymicrobial biofilm when compared to the monomicrobial biofilm, an approach is necessary to weaken the EPS of a biofilm. Therefore an alternative strategy could be the combination of Polymixin B or EDTA with aPDT. Polymixin B and EDTA both agents are able to destroy bridges formed between divalent cations (calcium and magnesium) and negatively charged

polysaccharides in the biofilm EPS structure [178]. Like that is possible to disrupt the

3D-biofilm structure and consequently give access to the antimicrobial effects of aPDT.

4 Analysis of *Candida albicans* heat shock response to photodynamic inactivation-mediated oxidative stress

4.1 Introduction

The induction of heat shock proteins (Hsps) represents a potent response to oxidative stress [179]. Hsps were first identified by their elevated expression following hyperthermic cell stress. They are a highly conserved ubiquitously expressed family of stress response proteins which is expressed at low levels under normal physiological conditions [180]. However, in response to cellular stress, such as an elevation in temperature, oxidative stress or starvation - the expression of Hsps increases dramatically. These proteins have protective functions, and play a role in normal growth and development [181]. Hsps is involved in folding/unfolding of proteins, assembly of multiprotein complexes, transport/sorting of proteins into correct subcellular compartments, and protection of cells against stress/apoptosis [53, 180, 182].

The Hsp70 family is the most abundant and conserved class of stress proteins and is considered a potential biomarker of cellular toxicity, being upregulated in response to a wide range of important environmental and physiological stresses [183-185]. Hsp70 expression causes inhibition of stress-induced caspase activation and downstream events in the apoptotic cell death pathway [171]. Hsp70 is capable of binding and sequestering activated caspases in addition to its important functions in protein

refolding and transport, proteolytic degradation of unstable proteins, and control of regulatory protein activity [114, 183, 186, 187].

In response to the oxidative damage induced by aPDT, microbial cells might initiate a rescue response to allow cells to deal with the damage produced by stress. However in aPDT, the importance of cellular rescue responses is not clarified for most cellular systems and photosensitizers [179]. Therefore this study investigated whether the oxidative damage caused by TMPyP-aPDT can induce Hsp70 production in *C. albicans* and whether Hsp70 induced by thermal insult in *C. albicans* cells exerts a protective effect against aPDT.

4.2 Material and Methods

4.2.1 Strains of *C. albicans*

One to three colonies of *C. albicans* (ATCC-MYA-273, LGC Standards GmbH, Germany) were picked up from agar plates with a sterile inoculating loop and transferred to a culture tubes containing 5 mL of Sabouraud Dextrose Broth (SDB) (Sigma Chemical Co., St. Louis, Mo) and cultured overnight. When the cultures reached the stationary phase of growth, the cells were harvested by centrifugation (5000 rpm, 5 min) and washed once with Dulbecco's phosphate-buffered saline (PBS without Ca^{2+} and Mg^{2+}; PAA Laboratories GmbH, Austria). For experiments with planktonic cells, approximately 5×10^7 cells mL^{-1} were prepared in PBS.

4.2.2 **Photosensitizer and light source**

The photosensitizer used in this study was TMPyP, a standard PS used in aPDT, already known to be effective against *C. albicans* planktonic cells and a potent singlet oxygen generator. The irradiation of samples were performed using an incoherent light source (UV236) λem = 418 $^\pm$ 20 nm). The maximal fluence rate at the level of the irradiated samples was 13.4 mW cm^{-2}. Cells were irradiated for 15 min (total light dose: 12.1 J cm^{-2}).

4.2.3 **Heat shock induction prior aPDT**

To investigate whether the overexpression of Hsp70 would protect *C. albicans* cells from the oxidative damage caused by aPDT, cells adjusted at 5×10^7 cells mL^{-1} were resuspended in 5 mL of SDB and exposed to 37 °C or heated in a water bath at 45 °C for 20 min (preheat treatment) (an optimum temperature for the heat-shock response in *C. albicans*) [188]. Prior phototoxic experiments, cells were centrifugated and resuspended in PBS, since the nutrients present in the culture medium can reduce the efficiency of aPDT. Then proteins from cells heat shocked were extracted and analyzed to ensure Hsp70 overexpression (control) and simultaneously phototoxic experiments were done.

4.2.4 **Phototoxic experiments with cells pretreated at 37 °C or 45° C**

Cells exposed to 37 °C or heated at 45 °C for 20 min were incubated for 15 min with different concentrations of TMPyP (0 to 5µM) and irradiated with a light dose of 12.1 J cm^{-2}. Viable *C. albicans* cells were accessed by CFU assay.

4.2.5 **Kinetics of the Hsp70 expression process in response to sublethal doses of aPDT**

In order to determine whether aPDT caused an overexpression of Hsp70 in *C. albicans*, cells were exposed to a sublethal aPDT dose. For this, *C. albicans* cells were incubated with 1 µM of TMPyP for 15 min and irradiated with a light dose of 12.1 J cm^{-2}. These conditions caused ~1 $\log_{10}$ decrease in cell survival, in order to stress the cells, without completely killing them. These conditions were based in the phototoxic experiments from section 2.3.3 figure 24, where it was tested the photoaction of TMPyP against *C. albicans* planktonic cells. Following, cells were centrifugated and resuspended in SDB and harvested at 0, 30 min, 1 h, 2 h, 4 h, 8 h, 12 h and 24 h after aPDT exposure. The protein extracts were then analyzed for Hsp70 expression by Western blot.

4.2.6 *C. albicans* **protein extraction**

Cells were subjected to disruption after suspending in yeast-Protein extraction reagent (Y-PER$^®$, Thermo Scientific, Rockford, IL, USA). 250 mL of lysis buffer per 50 mg of wet cell pellet were added and additional 4 g of glass beads per 1 g of wet cell pellet were used. Cells were subjected to disruption 5 times, each time for 1 minute with an interval of 1 min of incubation in ice. At the end of the procedure, the pellet debris was centrifugated at 10,000 rpm for 10 min at 4°C. The supernatant was reserved for further analysis.

4.2.7 **Protein determination by the BCA method**

After proteins were extracted, protein concentration was determined by the bicinchoninic acid (BCA) assay (Thermo Scientific, Rockford, IL, USA). The BCA assay relies on two reactions. Fistly, protein reduces Cu^{2+} ions from the cupric sulfate to

Cu^{1+}. Next, BCA reacts with the newly formed Cu^{1+} ions to form a purple coloured BCA-Cu^{1+} complex that has an absorbance at 562 nm [189]. The protein content of unknown samples was determined spectrophotometrically by comparison with known diluted protein standards (albumin) (0; 0,1; 0.5; 1 and 2 mg mL^{-1}).

4.2.8 Sodium Dodecyl Sulfate – Poly Acrylamide Gel Electrophoresis (SDS – PAGE)

SDS-PAGE was carried out using Mini-Protean II (Bio-Rad,City, CA, USA). Protein extracts (2 µg total proteins per sample) were treated with reducing *Laemmli* buffer [190] and boiled at 95° C for 5 min for complete denaturation. 10 µL of cells lysates per lane (2 µg), 5 µL of prestained protein ladder (Thermo Scientific, Rockford, IL, USA) and 5 µL of a positive control recombinant protein (0,075 µg) HSP70/HSP72 (ADI-SPP-758-D, Enzo Life Sciences, Lörrach, Germany) were loaded and separated on 8% polyacrylamide SDS-PAGE gels by electrophoresis. The gel was run at 0.03A for initial 15 min until the samples travel through the stacking gel. Then, the current was turned to 0.04A until the bromophenol blue reached the anodic border of the separating gel.

4.2.9 Western blotting

After separating the proteins according to their molecular mass by SDS-PAGE, proteins were electrophoretically transferred to a nitrocellulose membrane (Hybond™-C Extra, Amerscham Biosciences, New Jersey, USA) for 50 min at 0.3 A using the SD Semi-dry Transblot Apparatus (Bio-Rad, Hercules, USA). To ensure transfer is complete, the membrane was stained with 0.1% w/v Ponceau-S in 5% acetic acid. Following, the membrane was destained by repeated washing in Tris-Buffered Saline-Tween (TBS-T; Bio-Rad, California, United States) with 0.5% Tween 20 (Carl Roth GmbH & Co,

Karlsruhe, Germany)] and blocked with fresh 5% milk (Magermilchpulver, Saliter MMP, Obergünzburg, Germany) in TBS-T for 1 h at room temperature. After bathing in blocking buffer to reduce unspecific binding, the membrane was rinsed 3 times for 5 min. each time with TBS-T. The membrane was incubated overnight with a primary monoclonal mouse antibody against HSC70/HSP70 (ADI-SPP-758-D; Enzo Life Sciences, New York, USA) diluted at 1:1000 in fresh 1% (w/v) nonfat dry milk in TBS-T, overnight at 4°C. After rinsing the membrane to remove unbound primary antibody, the membrane was again washed (3 washings for 5 min) and incubated with corresponding secondary antibody bound to horseradish peroxidase (HRP) anti-mouse IgG (Cell Signalling Technology, MA, USA) and diluted at 1:1000 in fresh 1% (w/v) nonfat dry milk in TBS-T, for 1 h in room temperature. After 3 washes of 5 minutes each with TBS-T, the membrane was incubated with ECL chemiluminescent substrate (Pierce ECL Western Blotting Substrate, Thermo Scientific, Rockford, USA). Equal volumes of reagent A (luminol) and reagent B (an enhancer) were mixed and the blot was incubated in this solution for 1 minute. The blot was immediately exposed to an X-Ray film (Amersham Hyperfilm^{TM} ECL, GE Healthcare limited, Buckinghamshire, UK) in the dark for varying periods of time ranging from 5 sec to 5 min and the reactive proteins were visualized after automatic development on an X-ray developing machine (Kodak M35, OMAT Processor, Stuttgart, Germany). To control the total protein load, the membrane was incubated with anti-GAPDH polyclonal antibody conjugated to HRP from rabbit (ab9385; Abcam, Cambridge, UK) diluted at 1:1000 with fresh 5% milk overnight at 4°C and with secondary antibody anti-rabbit IgG, HRP linked (Cell Signalling Technology, Massachusetts, USA), diluted at 1:1000 in fresh 5% milk. The signal intensities of western blot bands were analyzed by the software ImageJ [191] and the relative grey scale intensities of the samples were compared with the untreated

controls. The signal intensities were normalized to the corresponding GAPDH controls per each lane before calculating their ratios. The calculations of the signal intensities were done relatively towards the appropriate control protein band (untreated sample at 37°C), which was set as 1 (or 100%).

4.2.10 Colony forming unit assay

The Miles and Misra method was used to estimate the viable number of *C. albicans* cells after phototoxic treatments (see section 3.2.7) [170]. After ten-fold serial dilutions of cell suspensions in SBD, 3 x 20 μl were seeded onto SDA. A CFU assay was done to determine the number of colony forming unites per milliliter.

4.3 Results

4.3.1 Heat shock induction

To ensure that *C. albicans* cells were able to start a heat shock response, cells were pre heated for 20 min at 45° C, an optimum condition for the heat-shock response in *C. albicans*, and protein extracts were analyzed and compared with the protein extracts from cells kept at 37 °C (control). Cells heat shocked (45 °C) showed an increase in Hsp70 concentrations in comparison to cells left at 37 °C, as determined by the Western blot (Fig. 38 A).

Quantification of Western blot signals revealed that Hsp70 was 2.9 folds more induced in heat shocked cells (45° C) than in control ones (37° C) (Fig. 38 B).

A   **B**
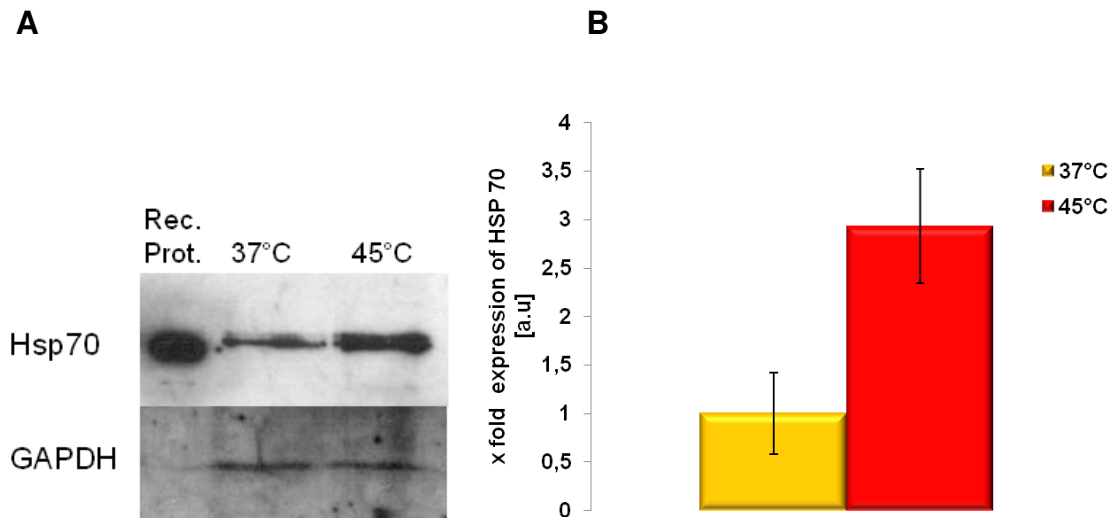
Fig. 38. Hsp70 expression by *C. albicans* . A) Westernblot of Hsp70, (Rec): positive control of the recombinant protein HSP70/HSP72 (0,075 µg). (37° C) Hsp70 expression in *C. albicans* cells kept at 37 °C (2µg protein lysates) and corresponding loading control (GAPDH). (45 °C) Hsp70 expression in *C. albicans* cells treated at 45 °C (2µg protein lysates) and corresponding loading control (GAPDH). B) Densitometric analysis of HSP 70 protein expression after Western blot. Relative density of Hsp70 protein levels in *C. albicans* were normalized to those of GAPDH. The band density for each treatment was normalized to the control value obtained in each experiment. The data represent the mean ± S.D. from three independent experiments.

4.3.2 Efficacy of aPDT upon Hsp70 upregulation

To investigate whether increased levels of Hsp70 protect cells against the oxidative damage of singlet oxygen generated by aPDT, *C. albicans* cells were pretreated for 20 min at 45° C, or kept at 37 °C (control). Thereafter *Candida* cells were submitted immediately to aPDT (15 min of incubation with TMPyP and 15 min of illumination: 12.1 J cm^{-2}, a condition which caused 1 log$_{10}$ reduction in cells viability). There was no difference in susceptibility between *C. albicans* cells kept at 37 °C (control cells) or preheated samples (Fig. 39 A and B). Like that, prior heat shock induction does not confer resistance to aPDT in *C. albicans*.

A

B
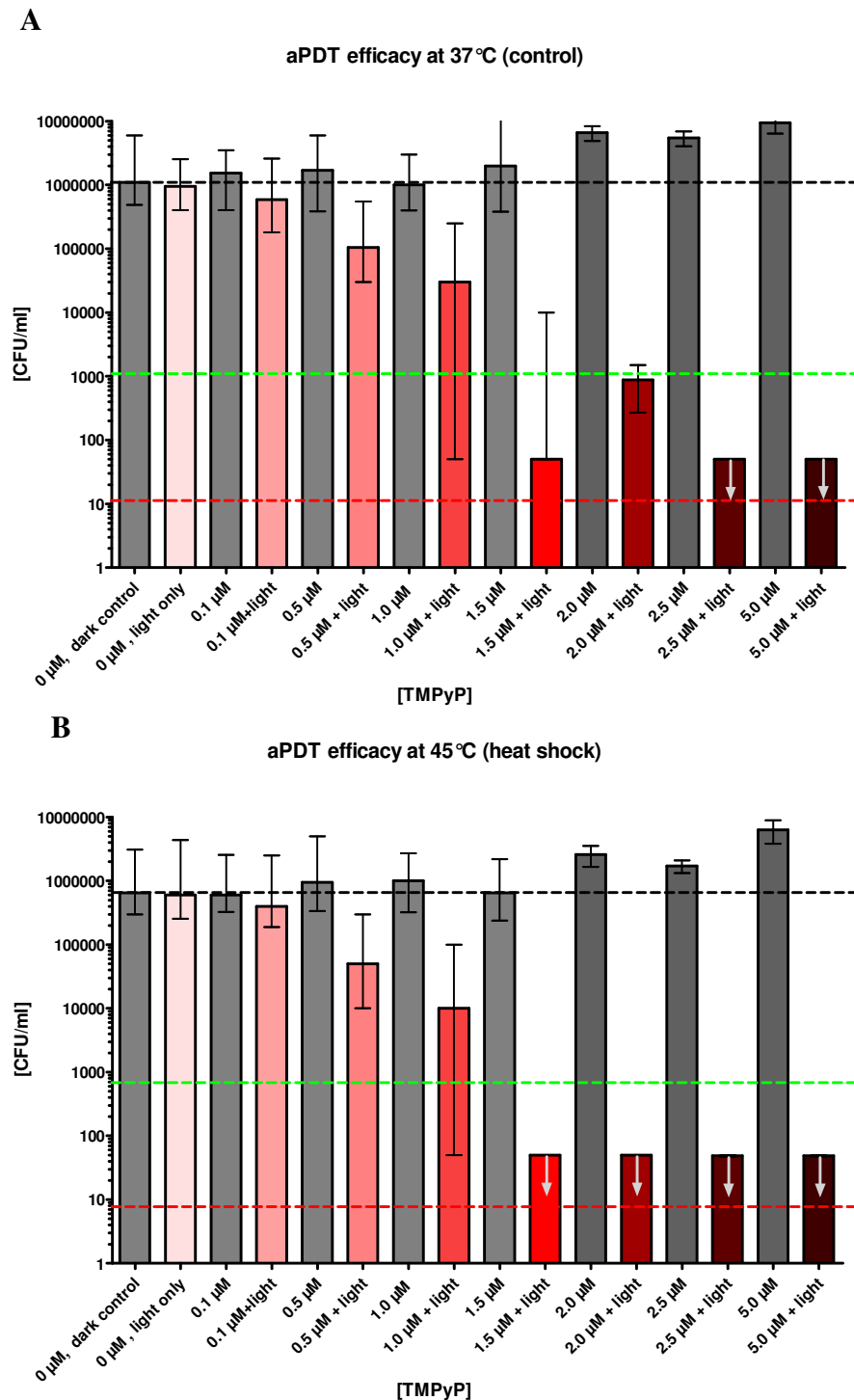
Fig. 39. *C. albicans* **planktonic cells kept at A) 37 °C and B) 45 °C and subsequently submitted to aPDT.** *C. albicans* **planktonic cells were incubated with different concentrations of TMPyP for 15 min, the samples were irradiated with 12.1 J cm^{-2}. A CFU assay was performed immediately after aPDT, and surviving colonies were counted 24 h later. Black dashed line: baseline CFU/ml; green dashed line: reduction of 3 log$_{10}$ steps in viable** *C. albicans* **(reduction 99.9%); green dashed line: reduction of 5 log$_{10}$ steps in viable** *C. albicans* **(reduction 99.999%). (n = 3 experiments; median ± interquartile range). The arrows mark the lower detection limit of the CFU assay.**

4.3.3 **Kinetics of the Hsp70 expression process in response to sublethal doses of aPDT**

C. albicans were incubated for 15 min with 1 µM of TMPyP and irradiated with a light dose of 12.1 J cm^{-2}, suffered ~1 log$_{10}$ decrease in cell survival (Fig. 40), indicating that a mild oxidative stress was induced inside the cells. Higher PS concentrations caused increased cell death, making the synthesis of protein not feasible, including heat shock proteins.
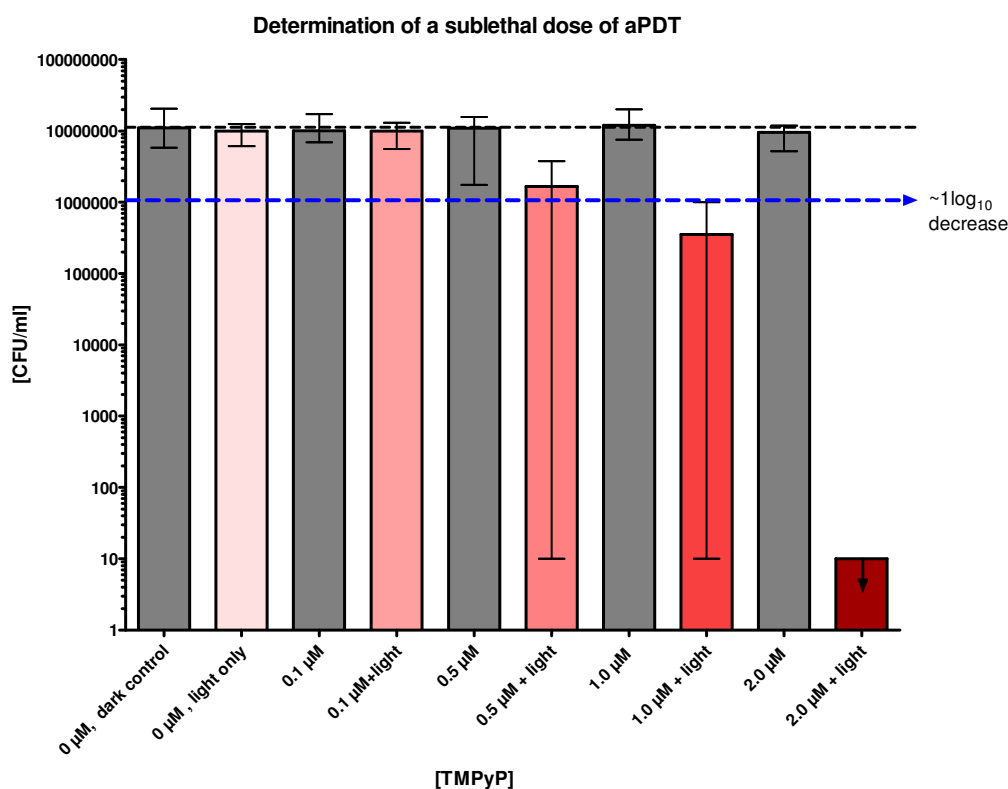
Fig. 40. Determination of sublethal condition of aPDT against *C. albicans* planktonic cells. Phototoxicity of TMPyP against *C. albicans* planktonic cells. *C. albicans* planktonic cells were incubated with different concentrations of TMPyP for 15 min, the samples were irradiated with 12.1 J cm^{-2}. A CFU assay was performed immediately after aPDT, and surviving colonies were counted 24 h later. Blue arrow shows the reduction of ~1 log cell survival caused by aPDT using 1 µM of TMPyP. (n = 3 experiments; median ± interquartile range). The arrows mark the lower detection limit of the CFU assay.

Following the sub-lethal aPDT, proteins were extracted from the cells over a 24-hour period and analyzed by Western blot. The kinetic measurements showed that the expression of Hsp70 in *C. albicans* increased at all treatment conditions with exception of the controls (proteins from *C. albicans* cells extracted immediately after aPDT, kept in the dark and not treated with TMPyP). Between each treatment and along the total observation period, there were no differences in the signal intensities observed. Same levels of Hsp70 expression was detected in *C. albicans* cells after aPDT as compared with light or PS alone for all time periods tested (Fig. 41).
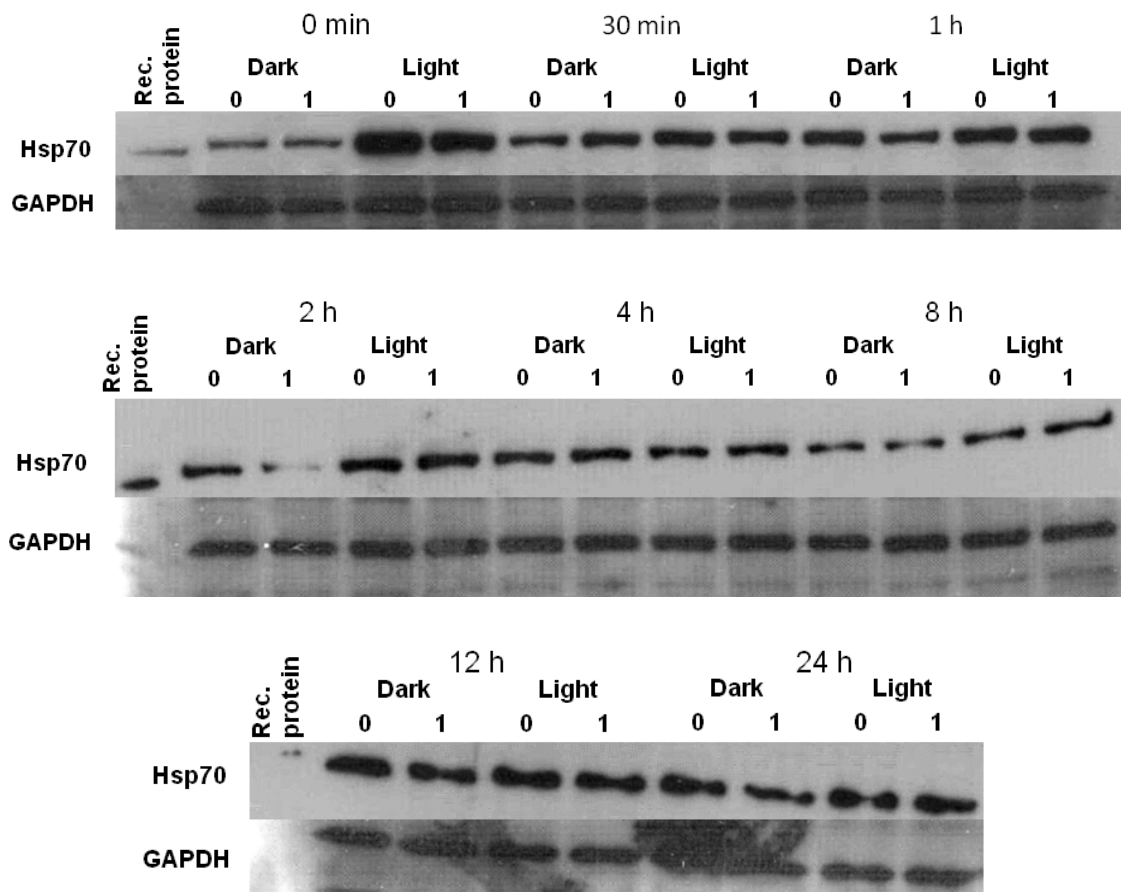
Fig. 41. Western blot analysis showing Hsp70 levels after TMPyP mediated sublethal aPDT. *C. albicans* **cells were treated with sub-lethal aPDT (1 μM TMPyP for 15 min + illumination for 15 min). Hsp70 induction was examined from 0 to 24 h after photodynamic treatment. (0) represents: 0 μM of TMPyP (proteins extracted from** *C. albicans* **which were not treated with TMPyP and either kept in the dark or exposed to the**

light. (1) represents: 1 µM of TMPyP (proteins extracted from *C. albicans* which were treated with 1 µM of TMPyP and either kept in the dark or exposed to the light.

4.4 Discussion

Hsps are rapidly induced in response to stress and likely play a major role in stress tolerance and cytoprotection [192]. However, the role of Hsp against oxidative damage is still a matter of debate, with some reports showing protection and others not [193].

A previous study showed that heat shock induction by preheat treatment prior TBO-mediated aPDT caused ~2 $\log_{10}$ less killing in *Escherichia coli* and ~4 $\log_{10}$ less killing in *Enterococcus faecalis* bacteria as compared to killing without prior heat treatment [194].

However, not all investigations on heat shock proteins show protective effect after aPDT. In this study, it was investigated whether upregulation of Hsp70 in *C. albicans* by preheat treatment (45 °C for 20 min) could protect *C. albicans* cells against the oxidative damage caused by singlet oxygen generated by TMPyP-mediated aPDT. It was observed that upegulation of Hsp70 did not protect *C. albicans* cells against the oxidative stress of singlet oxygen generated by aPDT. There was no difference in susceptibility between *C. albicans* cells kept at 37 °C (control cells) or preheated samples. The response of *C. albicans* is dependent on the oxidative stress conditions and is probably that 2,9 fold increase in Hsp70 expression got after preheat treatment was not sufficient to induce protective effects in *C. albicans* cells. Furthermore, aPDT is a multi-hit oxidative process and is likely that Hsp 70 expression is not enough to protect cells againt photodynamic damage.

In this study it was also investigated whether TMPyP-mediated aPDT was able to induce Hsp70 overexpression. Hsp70 protein levels were analyzed after sub-lethal aPDT of *C. albicans* using the porphyrin derivative, TMPyP, an already known singlet oxygen generator, generating a quantum yield of 77% singlet oxygen [40]. Here in this study Hsp70 protein levels were measured at various time intervals after aPDT and they were not increased over a period of 24 h.

For *Escherichia coli* bacterial strain, levels of Hsp60 (Groel) and Hsp70 (DnaK) were investigated after TBO-mediated aPDT. A 7-fold increase in Hsp60 and a 3-fold increase in Hsp70 were observed in *E. coli* after sub-lethal aPDT conditions [194]. Other studied showed that the expression of Hsp60 by *Streptococcus mutans* was also increased after a sub-lethal dose of aPDT with Rose Bengal, as well a singlet oxygen generator [61].

Responses to aPDT are related to both the PS which is used and the cell type which is treated by aPDT. The subcellular localization of the PS is of special importance, since it determines the localization of the primary damage. For example, hydrophobic PSs localize in the mitochondrial membranes and have there their its primary action [179]. For Hsp70 from mammalian eukaryotic cells, induction was most efficient in using PSs which localize preferentially in lysosomes. Like heat shock protein expression is a highly conserved stress defense mechanism in all eukaryotes [179], it is likely that the same happens to *C. albicans*. So far the intracellular localization of TMPyP is not known in *Candida* cells.

An investigation tested three PSs from different classes: a chlorine (mono-L-aspartyl chlorin-e6 [NPe6]), purpurin (tin etio-purpurin [SnET2] and a porphyrin PS (Photofrin [PH-II]), all of them singlet oxygen producers, were tested to investigate the

expression of Hsp70 in mouse tumor cells after photodynamic therapy (PDT). The results showed that the oxidative stress caused by singlet oxygen-PDT increased Hsp70 mRNA and protein levels in mouse cells *in vitro*, depending on the PS used in the treatment. Hsp70 expression was observed after PDT using the chlorin and the purpurin PSs. Hsp70 protein levels remained elevated 24 h after PDT. PDT using the porphyrin PS did not induce Hsp70 expression. The authors hypothesized that the expression of Hsp70 *in vitro* is dependent on the cellular localization of the PSs. Target of PH-II-PDT are both the plasma membrane and mitochondria, whereas targets for NPe6- and SnET2-PDT are the plasma membrane and lysosomes. Like that, the Hsp response after PDT may be connected to differences in lysosomal versus mitochondrial damage [195]. However, *in vivo* PDT of the same mouse cells induced Hsp70 expression for all PSs tested, including Photofrin. It is likely that secondary effect of PDT besides direct cellular oxidation may be responsible to heat shock response observed after Photofrin mediated PDT of mouse cells *in vivo* [195].

These results showed for the first time that overexpression of Hsp70 by *C. albicans* cells is not a mechanism by which microbial cells might develop resistance to TMPyP-mediated aPDT and that the expression of Hsp70 in *C. albicans* did not increase after sub-lethal TMPyP-mediated aPDT.

5 Non-invasive optical monitoring of oxygen during photodynamic inactivation of *Candida albicans* and *Staphylococcus epidermidis* biofilm

5.1 Introduction

Luminescence based sensors for oxygen can be used to monitor the efficacy of an antimicrobial treatment, since molecular oxygen is an important indicator of cell viability [196, 197]. One of the advantages of optical oxygen measurement is the possibility to evaluate oxygen concentrations in a non-invasive way, not requiring physical contact between the sensor and the optical detector. These sensors can be integrated into biocompatible matrices such as polyethylene glycol or polyurethane hydrogels, which are non toxic to the culture medium. Furthermore, optical sensors can be easily miniaturized, are not easily contaminated, can be used as disposable sensors, and do not consume oxygen in their sensing process [198]. Disadvantages include poor long term stability due to photobleaching or leaching of the immobilized indicator, and that optical sensors measure the oxygen content in an environment rather than cell activities [199].

Optical oxygen sensors are based on the mechanism of luminescence quenching by ground state oxygen (Fig. 42). When certain dye molecules (triplet emitters) absorb specific excitation light, they present long excited-state lifetimes emitting radiation at

5 Non-invasive optical monitoring of oxygen during photodynamic inactivation of Candida albicans and Staphylococcus epidermidis biofilm

91

longer wavelengths (phosphorescence). The excited triplet state of the dye can be quenched via colliding with oxygen molecules in their singlet ground states. Thereby, energy transfer from the excited indicator molecule to the oxygen molecules occurs. This results in a dye in its non-luminescent state and an electronically activated oxygen molecule that releases the energy in a manner that is not visible to the eye. This process is proportional to oxygen concentration [200]. The intensity of luminescence and its lifetime is then reduced with quenching.

Fig. 42. Principle of oxygen dependent luminescence quenching. * represents excited states of the molecules.

Oxygen concentration was monitored in a non-invasive way in *C. albicans* and *S. epidermidis* biofilms during aPDT using an optical oxygen sensor film. Knowing the concentration of oxygen during the aPDT process enables the measurement of cells viability and therefore the efficacy of the photodynamic process immediately during and after the aPDT without any time delay.

5 Non-invasive optical monitoring of oxygen during photodynamic
inactivation of Candida albicans and Staphylococcus epidermidis biofilm

92

5.2 Material and Methods

5.2.1 Preparation of the oxygen sensor film

The sensor films used in this chapter were prepared by Julia Cattani from the Institute of

Analytical Chemistry, Chemo- and Biosensors of the University of Regensburg and

described in details in her master thesis [201]. In short, the oxygen sensor (Fig. 43 A) is

based on a luminescent probe, the porphyrin dye Platinum(II)-5,10,15,20-

tetrakis(2,3,4,5,6-pentafluorophenyl porphyrin [Pt-TFPP] (Fig. 43 B). In order to

prepare a sensor cocktail for sensor fabrication, the dye was dissolved in

tetrahydrofuran (THF) (2 mg mL^{-1} w/v) along with the hydrophobic polymer

polystyrene (PS) (50 mg mL^{-1} w/v) as matrix material. The sensor cocktail is spread on

a polyethyleneterephthalate foil via a knife-coating device. After evaporation of the

THF, a 6 µm thick oxygen sensitive sensor layer is formed. Sensor spots are stamped

out of the sensor foil. These spots are the either way glued onto the bottom of microtiter

plates in order to grow the biofilm on the sensor spot or they are placed on top of a

grown biofilm inside the microtiter plate wells.
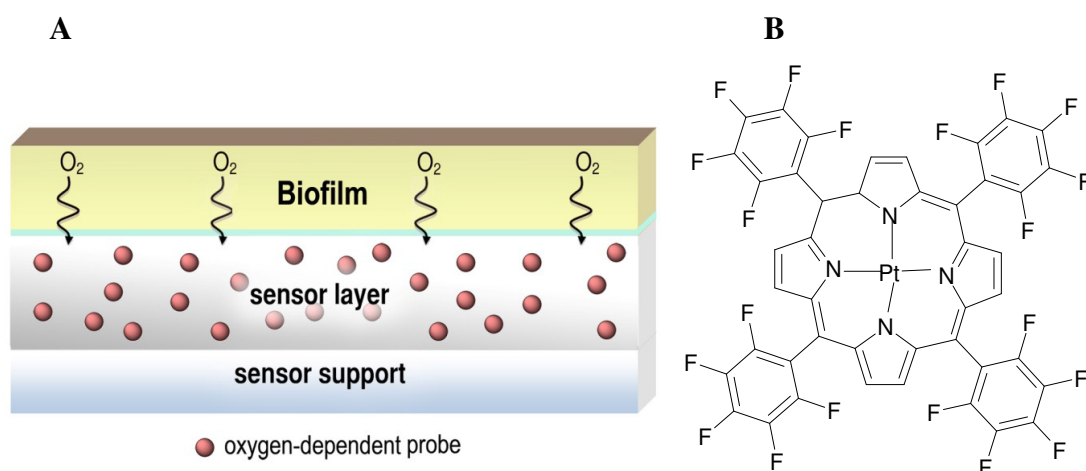
Fig. 43. A) Scheme of the oxygen sensitive sensor layer and B) Chemical structure of the oxygen dependent probe Platinum(II)-5,10,15,20-tetrakis(2,3,4,5,6-pentafluorophenyl porphyrin [Pt-TFPP]

5.2.2 **Oxygen concentration measurement**

The oxygen consumption by biofilm cells was measured by detecting the luminescence
of the dye sensor with a Tecan GENios Plus Microplate Reader multiwell microtiter
plate reader (Tecan GENios ELISA reader; Tecan Group Ltd., Männedorf, Switzerland)
at excitation/emission wavelengths of 405/635 nm. For the data evaluation, the intensity
values of the luminescence emitted by the sensor placed in microplate wells containing
biofilms submitted to different treatments (I) were divided by intensity values of the
fluorescence emitted by the sensor alone, with no biofilm (blank values, I_0) of the
respective well to obtain $I=I_0$. Wells containing biofilms (wells-biofilms) with
microorganisms consuming oxygen give values higher than 1, due to the signal increase
caused by less quenching of the fluorescent dye by oxygen. In cases where all the cells
of a biofilm were dead, the theoretical value equals 1, according to the amount of
ambient air oxygen. A total amount of 6 wells with grown biofilms per each condition
were treated with the same concentration of either an antimicrobial drug, NaN_3 or PS
and the percentage of wells containing biofilm which were not consuming oxygen was
calculated. Wells containing biofilms were classified as "breathing" (active biofilms) or
not "breathing" (non actives biofilm).

5.2.3 **Placement of sensor in the microplate**

Oxygen sensors were placed in the wells of the microplates as following (Fig. 44 A and
B):

- Sensor was glued with high vacuum grease (medium; Merck KGaA, Darmstadt,
  Germany) at the surface of the wells of the microplate and the biofilm was formed
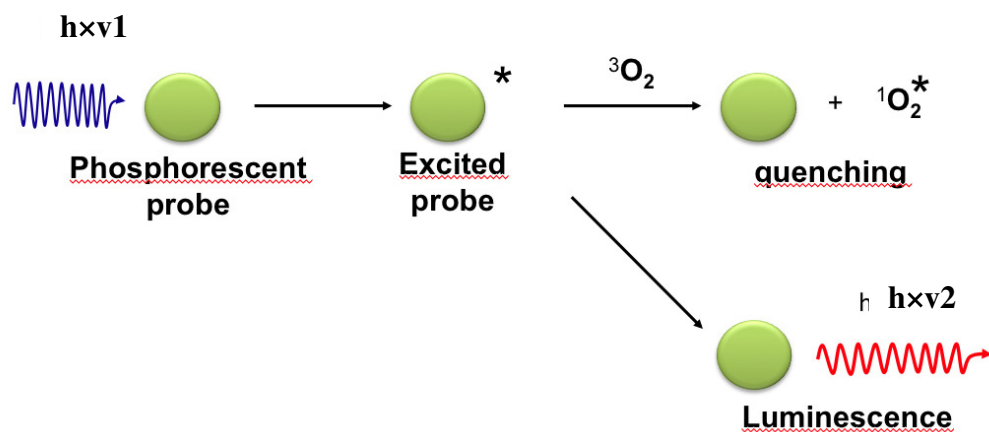
5 Non-invasive optical monitoring of oxygen during photodynamic inactivation of Candida albicans and Staphylococcus epidermidis biofilm

94

on its surface (sensor was located at the bottom of the biofilm) in 48/96 well microplates or

- Sensor was placed on the top of the biofilm in 48 well microplates
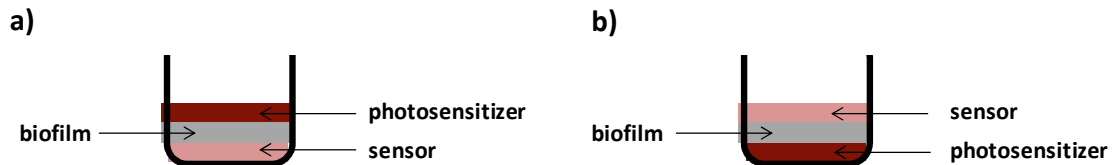
Fig. 44. Setup for oxygen measurement with sensor a) on the bottom of the biofilm and b) on the top of the microbial biofilm

5.2.4 Strains of *C. albicans*

One to three colonies of *C. albicans* (ATCC-MYA-273, LGC Standards GmbH, Germany) were picked up from agar plates with a sterile inoculating loop and transferred to a culture tubes containing 5 mL of Sabouraud Dextrose Broth (SDB) (Sigma Chemical Co., St. Louis, USA) and grown at 37 °C on a shaker platform (200 rpm) overnight. When the cultures reached the stationary phase of growth, the cells were harvested by centrifugation (5000 rpm, 5 min) and washed once with Dulbecco's phosphate-buffered saline (PBS without Ca^{2+} and Mg^{2+}; PAA Laboratories GmbH, Austria) and used for further experiments.

5.2.5 Strains of *S. epidermidis*

One to three colonies of *S. epidermidis* (ATCC-35984) (LGC Standards GmbH, Germany) were picked up from agar plates with a sterile inoculating loop and transferred to a culture tubes containing 5 mL of in Tryptic soy broth (TSB) (Sigma-Aldrich-Fluka, St Louis, USA) and grown at 37 °C on a shaker platform (200 rpm) overnight. When the cultures reached the stationary phase of growth, the cells were

harvested by centrifugation (5.000 rpm, 5 min), washed once with PBS and used for further experiments.

5.2.6 *C. albicans* biofilm formation

For *C. albicans* biofilm formation, 10^6 cells mL^{-1} cells were diluted to 10^6 cells mL^{-1} in 25% of FBS and 200 µL were added to sterile flat-bottomed 96-well polystyrene plates. Cells were then incubated at 37 °C for 24 h without shaking. Following biofilms were washed once with PBS to remove non-adhered cells and used for further experiments.

5.2.7 *S. epidermidis* biofilm formation

For *S. epidermidis* biofilm formation, cells were diluted in TSB to an optical density at 600 nm (OD600) of 0.5, corresponding to 10^8 cells mL^{-1} and 200 µL or 500 µL were added to sterile flat-bottomed 96-well or 48 well polystyrene plates, respectively. The plates were then incubated for 36 h at 37 °C. Following biofilms were washed once with PBS to remove non-adhered cells and used for further experiments.

5.2.8 Disrupted biofilms

To compare the oxygen consumption between cells growing as a biofilm with cells disrupted from the biofilm, *C. albicans* biofilms were disrupted with the tip of a pipette after aPDT and before the sensor foil was placed on the top of the biofilm. In this way, it is likely that the cells have lost most of their EPS, since the EPS is the responsible to keep the organised structure of the biofilm and all the cells which originally formed the biofilm got in contact with the sensor.

5.2.9 **Treatment of biofilms with antimicrobial drugs/sodium azide**

Penicillin-streptomycin (10.000 units of penicillin and 10 mg mL^{-1} of streptomycin in 0.9% NaCl; Sigma-Aldrich, St Louis, USA) and sodium azide (NaN$_3$, 99% purity, Acros Organics, New Jersey, USA) were used as a control to establish the set up to measure oxygen concentration of biofilms after antimicrobial treatment. Penicillin-streptomycin is a combination of antibiotics used to prevent bacterial contamination of cell cultures, showing action against Gram-positive and Gram-negative bacteria, respectively. Sodium azide inhibits the respiratory enzyme cytochrome oxidase, and as a consequence cells are asphyxiated.

Biofilms were then incubated with 100 µL (96 well microplates) or 500 µL (48 well microplates) of different concentrations of each drug. *S. epidermidis* biofilms were treated with 0; 1; 10; 100; 1000 and 5000 units of penicillin mL^{-1} together with 0; 0.3125, 0.625, 1.25, 2.5 and 5 mg mL^{-1} of streptomycin diluted in water for 3 h. Both biofilms (*C. albicans* and *S. epidermidis*) were treated with 0; 0.001; 0.01; 0.1; 0.25; 0.5; 1; 2.5; 5 and 10% w/v of NaN$_3$, diluted in distilled water for 15 min. A total amount of 6 individual biofilms were prepared per each condition and treated either with antimicrobial drugs, aPDT or left untreated.

5.2.10 **Treatment of biofilms with aPDT**

5.2.10.1 Photosensitizers and light source

The photosensitizer (PS) TMPyP was purchased from Sigma Aldrich (Taufkirchen, Germany), purity 97%. XF-73 was kindly provided by Destiny Pharma Ltd. (Brighton, UK). Both photosensitizers were dissolved in bidistilled water at a concentration of 500 µM, passed through a 0.22 µm pore-size filter and stored at 4∘C until usage. Biofilms

were incubated with 100 µL (96 well microplates) or 500 µL (48 well microplates) of different concentrations of each of the PSs for 4 h in the dark at 37°C. The irradiation of samples were performed using an incoherent light source (UV236) $\lambda_{em} = 418 \pm 20$ nm) provided by Waldmann GmbH (Schwenningen, Germany). The maximal fluence rate at the level of the irradiated samples was 13.4 mW cm^{-2}. Biofilms were illuminated for 60 min (48.2 J cm^{-2}). A total amount of 6 individual biofilms were prepared per each condition and treated with the same aPDT parameters. Oxygen measurements were made before aPDT, and then each 20 minutes during aPDT (total treatment time 60 min: 3 measurements) and once more 20 minutes after aPDT.

Controls included: biofilms kept in the dark and not treated with PS (normal control); biofilms exposed just to the light (light control) and biofilms cells treated just with the PS (dark control).

5.2.11 MTT assay (4,5-Dimethythiazol-2-yl)-2,5-diphenyltetrazolium bromide)

It was evaluated the effect of XF-73-aPDT in *S. epidermidis* biofilms measuring biofilms metabolic activity directly by the 3-(4,5-dimethylthiazol-2-yl)-2,5-diphenyl-tetrazolium bromide (MTT) test [202]. 100 μL MTT solution (stock solution of 5 mg mL^{-1} in PBS, stored at -20 °C) was added to each well containing the treated/untreated biofilms. For blank values 10 μL MTT was added to 500 μL medium. After incubation for 14 h at 37 °C, 100 μl SDS solution (20%) was added to each well and plates were again incubated at 37 °C overnight. The absorbance of the produced formazan was recorded using an EMax endpoint ELISA microplate reader (Molecular Devices, California, USA) at 540 nm. The measured OD of the untreated controls was normalized to 1, which means a viability of *S. epidermidis* of 100%.

5 Non-invasive optical monitoring of oxygen during photodynamic
inactivation of Candida albicans and Staphylococcus epidermidis biofilm

98

5.3 Results

5.3.1 Biofilm formation

Cells of *C. albicans* readily form biofilm in polystyrene microplates (section 2.2.2, Fig.
16). Therefore a sensor was prepared using polystyrene as well. Like that, oxygen
sensors were glued on the surface of 96 well microplates (surface area: 0.36 cm^2) and *C.
albicans* biofilms were formed on the surface of these sensors. Under these
circumstances, *C. albicans* biofilms did not grow homogeneously and the biofilms were
easily detached from the sensor surface without any experimental manipulations.
Therefore it was not possible to achieve a reproducible and repeatable biofilm model on
such an oxygen sensor foil (Fig. 45).

5 Non-invasive optical monitoring of oxygen during photodynamic inactivation of Candida albicans and Staphylococcus epidermidis biofilm

99

Fig. 45. *C. albicans* biofilms formed in 96 well polystyrene microplates coated with the oxygen sensitive sensor layer. The sensor was glued with high vacuum grease at the surface of the microplate wells and the biofilm was formed on its surface. Yellow arrow shows a well completely covered by the biofilm. Red arrow shows a well where the biofilm completely detached. Blue arrow shows a well partially covered by the biofilm

In a next step the surface area was increased, so that the adherence of the *C. albicans* biofilms could be better monitored visually due to a larger surface area for cell attachment. Therefore, the sensors were placed in wells of a 48 well microplate (surface area: 0,76 cm^2). Again, the biofilms were poorly adhered to the sensor surface and the biofilm was not evenly distributed over the total surface area (data not shown).

It was tested whether the dye used as an indicator in the sensor or the glue used to attach the sensor to the microplate surface could influence cell adherence to the sensor. For this, cells were put on sensor spots with different concentrations of the dye and the

glue, but no attachment difference of the cells was observed using different concentrations of the dye as well as the glue. Furthermore to control if the heterogenous distribution of a growing biofilm on such a sensor foil is a common observation, *S. epidermidis* (ATCC-MYA-273) was used, a bacteria strain forming a more robust biofilm in polystyrene microplates when compared visually to *C. albicans* (ATCC-MYA-273). *S. epidermidis* were able to form a biofilm directly on the sensor, which was homogenously distributed on the sensor foil, but when such a biofilm was washed to remove non-adherent bacteria, again the biofilm detached easily from the surface.

5.3.2 Oxygen measurement with sensor located at the bottom of the biofilms formed in 48 well microplates

5.3.2.1 Oxygen consumption of *S. epidermidis* treated with Penicillin-streptomycin and sodium azide (NaN3)

S. epidermidis biofilms grown on the sensor foil at the bottom of 48 well microplates were treated with Penicillin-streptomycin and NaN_3 in order to establish the set up for optical monitoring of oxygen consumption by biofilms. The higher concentration used of Penicilin-Streptomycin (5000 units mL^{-1} and 5 mg mL^{-1}) led to 50% of wells containing biofilms to stop consume oxygen. The lower concentrations (0, 1, 10, 1000 and 5000 Units mL^{-1}) did not cause any decrease in oxygen consuming. The higher concentration used of Penicilin-streptomycin (5000 units $mL^{-1}$and - 5 mg mL^{-1}) led to 50% of wells containing biofilms to stop consume oxygen (Fig. 46).

5 Non-invasive optical monitoring of oxygen during photodynamic
inactivation of Candida albicans and Staphylococcus epidermidis biofilm

101
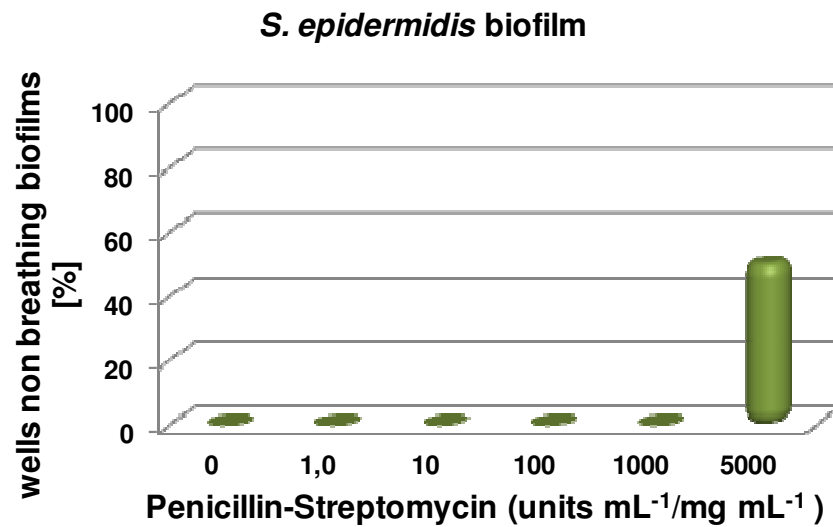
Fig. 46. O^2 measurement of *S. epidermidis* **biofilms (24 h old) treated with different
concentrations of Penicilin-streptomycin for 3 h. The optical sensor was placed on the
bottom of the biofilm.**

When biofilms were treated with NaN$_3$, 75% of the controls (biofilms not treated

with NaN$_3$) (Fig. 47) were not consuming oxygen. The data obtained does not show

consistence because wells-biofilms treated with higher concentrations (0,1; 1 and 5%)

of NaN$_3$ were breathing more than when compared to the control biofilms. Again here,

it was not possible that the biofilm covers homogenously and completely the surface

area of the sensor foil.

5 Non-invasive optical monitoring of oxygen during photodynamic inactivation of Candida albicans and Staphylococcus epidermidis biofilm

102
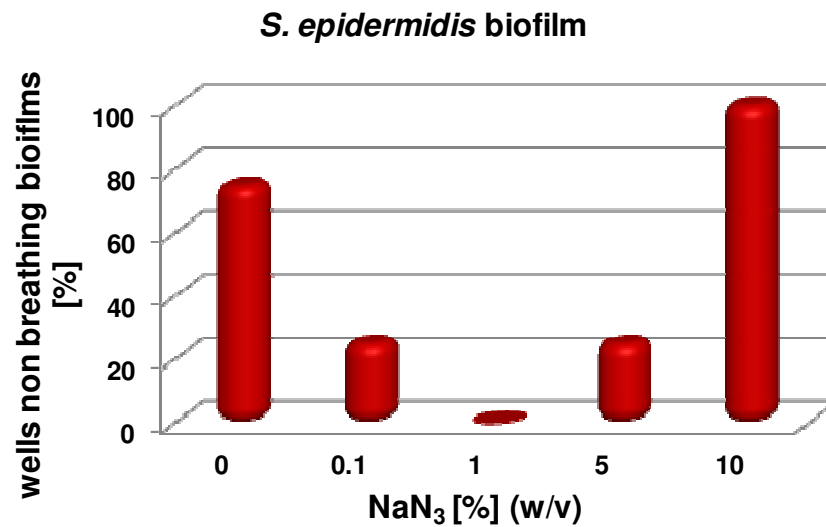
Fig. 47. O^2 measurement in *S. epidermidis* biofilms (24 h old) treated with different concentrations of NaN3 for 3 h. The optical sensor was placed on the bottom of the biofilm.

Due to the situation that in both biofilm models a homogenous distribution of the biofilms on the sensor foil could not be established, the experimental set up was changed as follows: *C. albicans* biofilms were then formed directly on the bottom of 48 well microplates and the sensor foil was placed on the top of the biofilm.

5.3.1 Oxygen measurement with sensors located at the top of *S. epidermidis* biofilms

Since the biofilms did not show optimal attachment to the sensor surface, the set up was changed. The biofilms were then formed directly at the bottom of the microplate well and the sensors were placed on the top of the biofilm. Experiments were done with intact biofilms and disrupted biofilms. The biofilms were disrupted with the tip of a pipette in order to investigate whether the EPS and the heterogeneous layers of the biofilms might interfere with oxygen measurements.

5 Non-invasive optical monitoring of oxygen during photodynamic
inactivation of Candida albicans and Staphylococcus epidermidis biofilm

103

5.3.1.1   Oxygen consumption by *S. epidermidis* biofilms submitted to TMPyP-
aPDT

The results obtained showed that control biofilms (not treated with PS and protected
from the light) were breathing and breathing decreased 20% in the end of the treatment
(Fig. 48 A). Dark control biofilms decreased breathing around 20% in the end of aPDT
(60 min) and higher concentrations (0.1 and 1 µM TMPyP) did not cause any decrease
in cell breathing. Biofilms submitted to aPDT (Fig. 48 B) showed decreased breathing
proportional to increasing TMPyP concentrations. It was also observed that biofilms
subjected to APDT started to breath less during the treatment.

Besides measuring oxygen concentration of intact biofilms, it was also measured
oxygen concentration with disrupted biofilms (Fig. 48, disrupted biofilm is marked with
*) in order to check whether the biofilm structure (presence of EPS and heterogeneous
layers of cells) affects oxygen measurement of the cells in the biofilm. When biofilms
are disrupted, the sensor can get in contact directly with all bacterial cell layers, without
interference of the EPS. In dark controls, bacteria from a disrupted biofilm, showed
100% of breathing cells in all concentrations tested during all time periods, except when
biofilms were treated with the highest TMPyP concentration (100 µM) (Fig. 48 A -
purple column). At this concentration the oxygen consumption decreased by 20% at the
end of treatment, but 20 min after treatment bacterial cells seem to recover (Fig. 48 A
red column). The decrease in oxygen consumption detected by the sensor might be due
to the fact that one control well had a biofilm which did not grow confluent (did not
grow all over the well area).

Disrupted biofilm cells showed to be more sensible to aPDT treatment than
intact biofilms (Fig. 48 B). The increased susceptibility of disrupted biofilm cells to

aPDT may be due to the detachment of the cells from the wells made with the help of

the tip of a pipette. Overall, these results show that biofilm cells kept in the dark were

breathing more than cells submitted to aPDT.
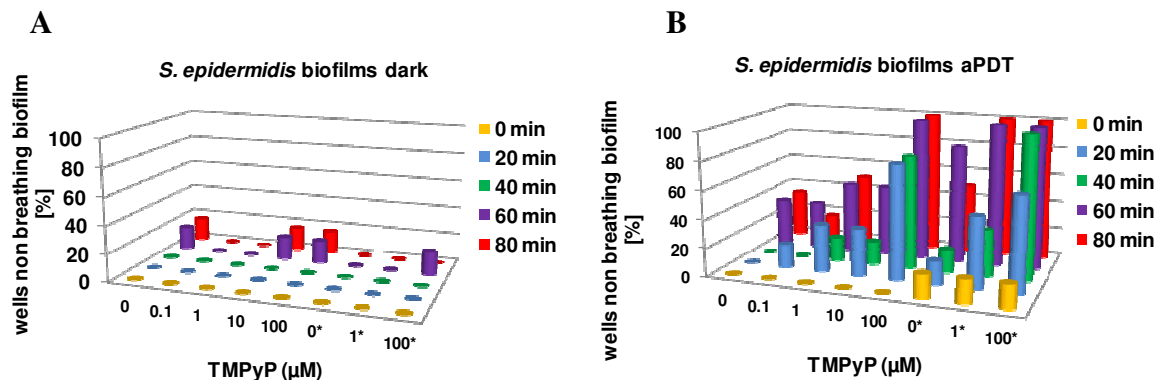
Fig. 48. Oxygen measurement in *S. epidermidis* biofilms non treated/ treated with TMPyP-aPDT placing the sensor on the top of the biofilm. Measurements were made before aPDT starts (0 min), during aPDT (20; 40 and 60 min) and 20 min after aPDT. * indicates disrupted biofilm cells. The bars represent the mean value of 6 wells grown biofilm.

5.3.1.2   Oxygen consumption by *S. epidermidis* biofilms submitted to XF-73-

aPDT

Oxygen measurements of S. *epidermidis* biofilms did not show a difference between

non-treated and treated aPDT biofilms (Fig. 49 A and B respectively).
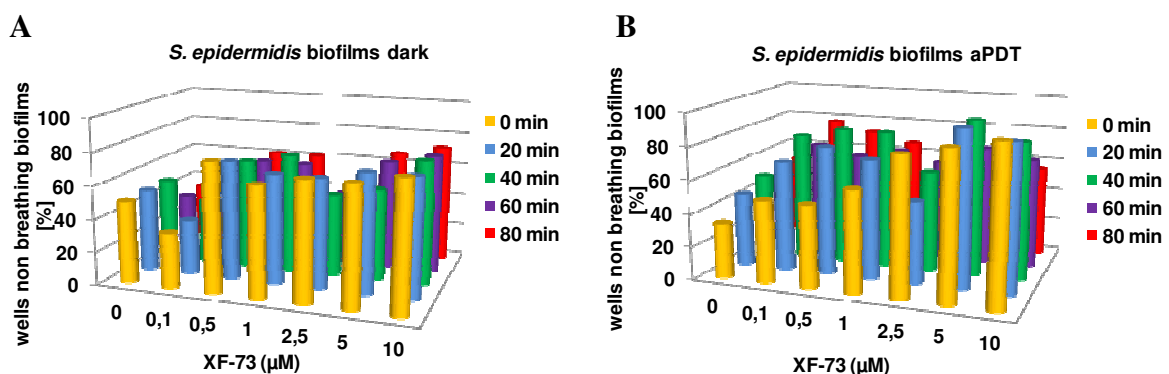
Fig. 49. Oxygen measurement of *S. epidermidis* biofilms non treated/ treated with XF-73-aPDT placing the sensor on the top of the biofilm. Measurements were made before aPDT starts (0 min), during aPDT (20; 40 and 60 min) and 20 min after aPDT. * indicates disrupted biofilm cells. The bars represent the mean value of 6 wells grown biofilm.,

5 Non-invasive optical monitoring of oxygen during photodynamic
inactivation of Candida albicans and Staphylococcus epidermidis biofilm

105

After aPDT (80 min), the metabolic activity of *S. epidermidis* biofilms was
measured by MTT assay (Fig. 50) and the results were compared with the oxygen
measurements after 80 min of aPDT. Control biofilms showed high metabolic activity
when compared to aPDT treated biofilms. APDT treated biofilms showed a decrease in
metabolic activity proportional to the increase of XF-73 concentrations (Comparison
Fig. 50×51). Oxygen measurements showed a correlation with MTT assay just with the
smallest concentrations of XF-73 used (0 and 0,1 µM of XF-73). Higher concentrations
did not show a good correlation, where the dark control biofilms were breathing less
than the aPDT treated biofilms. The biofilms of these experiments showed a confluent
grow in all the wells were they were formed.
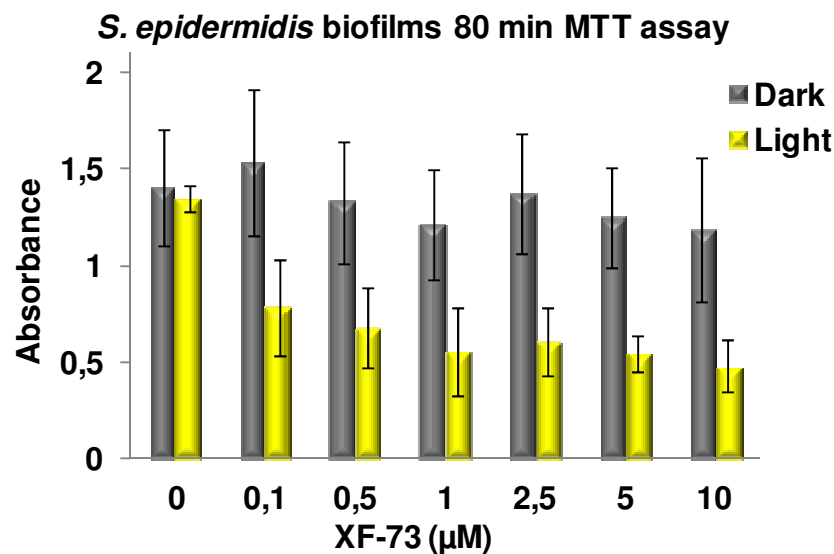
**Fig. 50. Metabolic activity of *S. epidermidis* biofilms non treated/ treated with aPDT
placing the sensor on the top of the biofilm. Measurements were made 20 min after the
end of aPDT (80 min after the beginning if the treatment). The bars represent the mean
value of 6 wells grown biofilms.**

5 Non-invasive optical monitoring of oxygen during photodynamic inactivation of Candida albicans and Staphylococcus epidermidis biofilm

106

Fig. 51. Oxygen measurement in *S. epidermidis* **biofilms non treated/ treated with XF-73-aPDTaPDT placing the sensor on the top of the biofilm. Measurements were made 20 min after the end of aPDT (80 min after the beginning of the treatment). The bars represent the mean value of 6 wells grown biofilms.**

5.3.2 Oxygen measurement with sensors located at the top of *C. albicans* biofilms

5.3.2.1 Oxygen consumption by C. *albicans* biofilms treated with sodium azide (NaN3)

C. albicans biofilms treated with NaN_3 showed a decrease in oxygen consumption with increasing NaN_3 concentrations (Fig. 52).

5 Non-invasive optical monitoring of oxygen during photodynamic
inactivation of Candida albicans and Staphylococcus epidermidis biofilm
107

**Fig. 52. Oxygen measurement in *C. albicans* biofilms treated with NaN₃ placing the sensor
on the top of the biofilm. Measurements were made 1 hour after the treatment. The bars
represent the mean value of 6 wells grown biofilms ± standard deviation.**

5.3.2.2   Oxygen measurements of *C. albicans* biofilms submitted to TMPyP-

aPDT

In the control treatment, intact biofilms were consuming more oxygen than disrupted

biofilm cells (Fig. 53 A). The same happened when biofilm were submitted to aPDT

(Fig. 53 B). Here again, the scraping of the biofilm from the microplate surface might

have caused a little damage to the cells and this coupled with the action of aPDT caused

a higher decrease in oxygen consumption when comparing intact and disrupted biofim

cells.

A

B
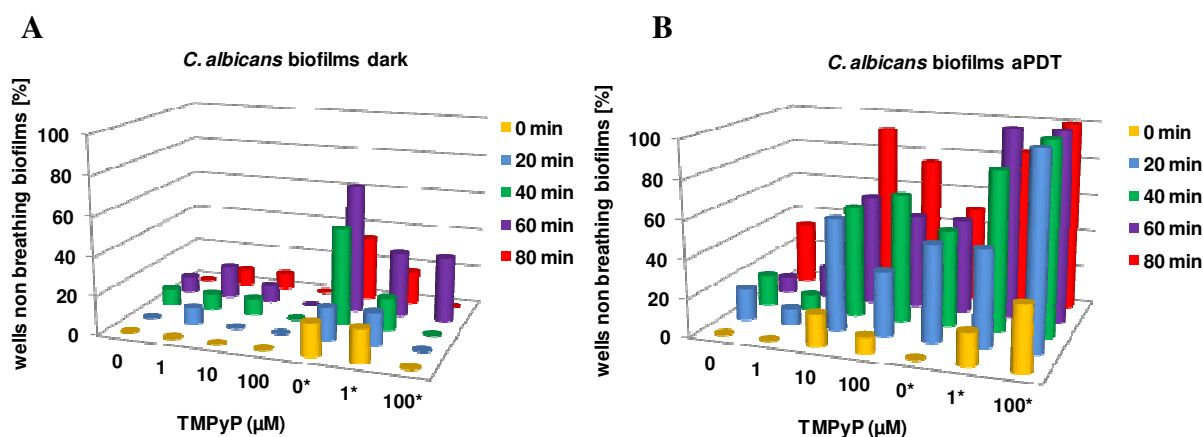
Fig. 53. Oxygen measurement in *C. albicans* biofilms non treated/ treated with TMPyP-aPDT placing the sensor on the top of the biofilm. Measurements were made before aPDT starts (0 min), during aPDT (20; 40 and 60 min) and 20 min after aPDT. * indicates disrupted biofilm cells. The bars represent the mean value of 6 wells grown biofilms.

5.3.2.3   Oxygen measurements of *C. albicans* biofilms submitted to XF-73-aPDT

Control biofilms were breathing under all PS concentrations and during the whole treatment (Fig. 54 A). With an exception of the control of the biofilm disrupted cells (0*), that showed a breathing reduction 20 min after the end of the treatment. This can be due to fact that 2 wells had no confluent biofilm growth or the tip of the pipette which was used to detach the cells from the well that killed the biofilm cells. Biofilms submitted to aPDT began to breathe less with increasing PS concentrations (Fig 54 B). Here, the higher PS concentration (100 µM XF-73) did not lead cells to reduce breathing, what can be explained by the shield effect caused by the excess of molecules of the PS in solution.

A

B
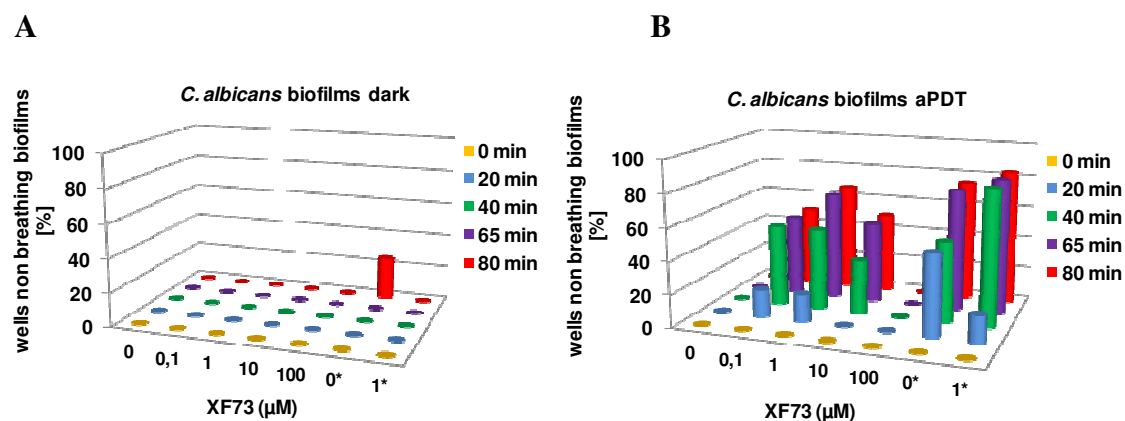
Fig. 54. Oxygen measurement in *C. albicans* biofilms non treated/ treated with XF-73-aPDT placing the sensor on the top of the biofilm. Measurements were made before aPDT starts (0 min), during aPDT (20; 40 and 60 min) and 20 min after aPDT. * indicates disrupted biofilm cells. The bars represent the mean value of 6 wells grown biofilms.
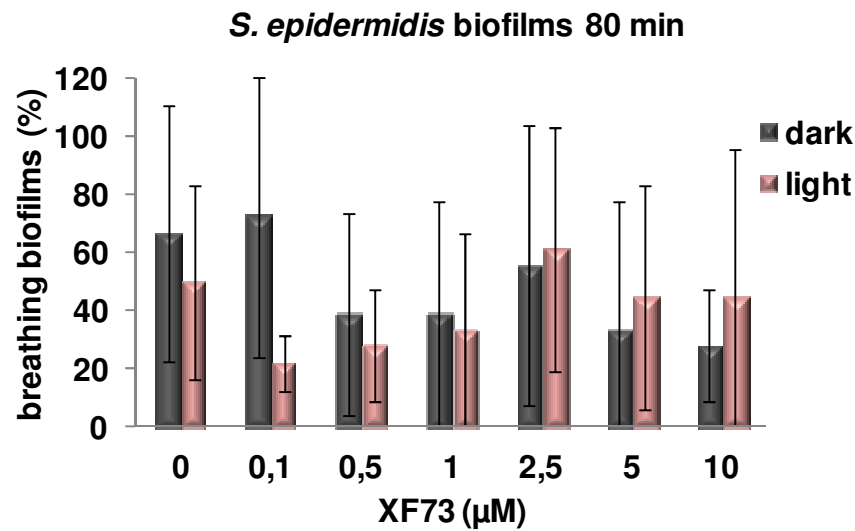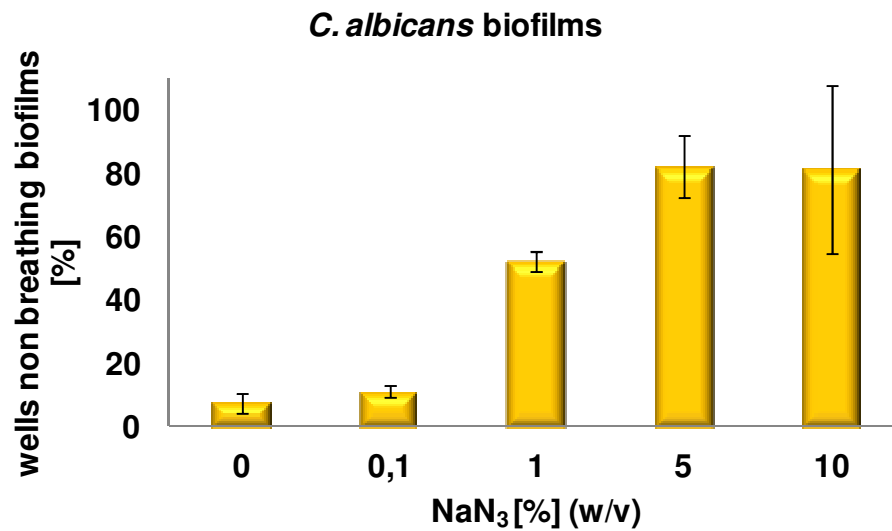
5.4 Discussion

Biofilms are complex communities of microorganisms attached to surfaces and are encased in an EPS mainly composed of carbohydrates. They can be from 10 to 1000 times more resistant to antimicrobial treatments than their planktonic counterparts. APDT can be a viable option to treat microbial cells resistant to the routinely used antimicrobial drugs since this treatment is based in the generation of singlet oxygen against which there is no cellular defense [21].

The presence and total concentration of oxygen in biological systems has a large effect on the behavior and viability of many cell types. Thereby, the integration of oxygen sensors within cell culture environments might be an efficient toll for monitoring of microbial cell survival immediately after antimicrobial treatments, with any time delay, if a correlation between survival and the corresponding oxygen concentration is possible [197]. In the section 2 it was showed that aPDT is a viable option to kill *C. albicans* biofilms. In this study, it was tried to establish a set up for the monitoring of *C. albicans* viability during and after aPDT by measuring oxygen concentration in the biofilms using a fluorescence-based sensor.

The *C. albicans* strain used in this study is able to form biofilm in polystyrene microplates as already showed (section 2.2.2, Fig. 16). The sensors used in this study were made as well of polystyrene. Therefore it was expected that *C. albicans* would also form biofilms on the sensor surface, but they were not able to cover

5 Non-invasive optical monitoring of oxygen during photodynamic
inactivation of Candida albicans and Staphylococcus epidermidis biofilm

110

homogeneously the complete surface of the well, covering just half or few parts of the sensor (Fig. 45).

One hypothesis for the weak *C. albicans* attachment to the sensor may be the differences in the surface between the microplate and the sensor regarding roughness and physicochemical properties, like hydrophobicity and polarity. Microbial adhesion to surfaces increase as the surface roughness increases. This is because shear forces are diminished, and surface area is larger on rougher surfaces. Microorganisms also adhere better to hydrophobic and non polar surfaces than to hydrophilic materials [63]. On the other hand, *S. epidermidis* could grow over the entire surface of the well microplate, but biofilm adherence was not so stable when compared with the biofilms formed on the surface of polystyrene microplates, because handling of these biofilms during the treatment (washing steps and PS treatment) made them detach very easily from the well surface.

In another set up, the biofilms were formed on the surface of the polystyrene microplates and after biofilm formation the sensors were placed on the top of the biofilms. The results achieved showed that overall, the sensor can detect differences in oxygen consumption between control biofilms and biofilms submitted to aPDT, but it was difficult to reproduce the results. When some wells were not completely covered by the biofilm, the results obtained showed that biofilms were not breathing. It is likely that the oxygen sensor could not distinguish oxygen consumption of a biofilm covering the complete well or juts part of the well.

It was then compared, the sensibility of the sensor with a cellular metabolic activity assay (MTT assay). MTT assay showed that cell metabolic activity decreased in aPDT with increasing PS concentrations. However, the oxygen measurements obtained

with the sensor did not showed a showed a correlation with MTT assay just with the smallest concentrations of XF-73 used (0 and 0,1 µM of XF-73).

The use of oxygen sensors to measure viability of cells in biofilms after antimicrobial treatment may be compromised by the fact that cells in deeper layers of biofilms might present oxygen depletion and enter in a dormant state [203]. The failure of oxygen to penetrate within the biofilm is not a physical exclusion. Water is the major component of the EPS (~97%), so that solutes that are the size of oxygen are able to diffuse in the EPS at a rate that is around 60% of the diffusion rate in pure water. Oxygen fails to penetrate and reach the cells located deep in the biofilm because it is respired by cells in the upper layers of the biofilm [204]. The size of the biofilm ranges from a few micrometers up to a few centimeters depending on the medium composition, the substrate nature and the strain. Areas located near the surface will be provided with both oxygen and substrate while deeper areas might present oxygen depletion and enter in a dormant state [205].

Furthermore, *C. albicans* and *S. epidermidis* are facultative anaerobes, which will grow aerobically in the presence of oxygen and fermentatively in the absence of oxygen. In this way, there are at least three distinct physiological states within a biofilm: 1) biofilm cells located in close proximity to the environment are in contact with both substrate and oxygen and will grow aerobically; 2) the layer below the aerated region will present just substrate and no oxygen, since oxygen will be the first metabolite to be depleted due to its moderate solubility in water; 3) deeper in the biofilm, it will be a region where both oxygen and substrate are depleted and microbial cells might become inactive and begin to die (Fig. 55) [203, 206]. Like that, there is a region within the biofilm, where oxygen is depleted, but metabolic activity is still

5 Non-invasive optical monitoring of oxygen during photodynamic
inactivation of Candida albicans and Staphylococcus epidermidis biofilm

112

present and might be measured by MTT assay. This might explain why MTT assay was
more sensible to measure biofilms viability than the oxygen sensor.

Another point would be that when the sensor was placed in the top of the
biofilm, a small quantity of water was added on the top of the biofilm for better sensor
attachment to the biofilm. The sensor could have measured also the concentration of
oxygen in the water. Or the distance between the sensor and biofilm was too big and the
overall volume of the well was gave false values. Overall, the results obtained in this
study showed that the optical oxygen sensor could detect differences between biofilms
not treated and treated with aPDT.
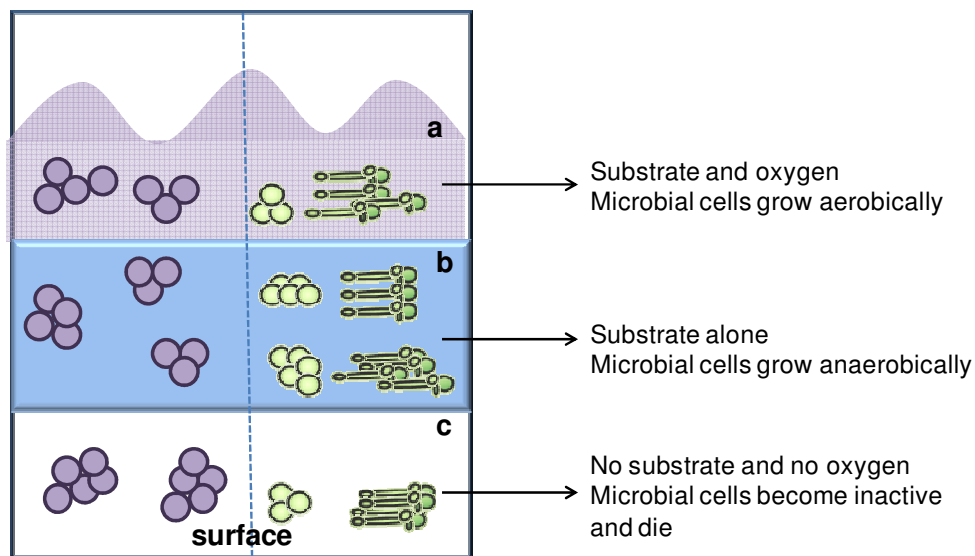
**Fig. 55. Cells within a biofilm: a) indicates active cells; b) indicates intermediate cells and
c) dormant cells. Adopted and modified from reference [203].**

6 Summary

Candida albicans is the main type of fungi able to form biofilms, which cause superficial skin and mucous membrane infections as well as invasive mycoses, particularly in immunocompromised patients. In these patients, invasive infections are often associated with high morbidity and mortality. Furthermore, the increase in antifungal resistance has decreased the efficacy of conventional therapies. The use of aPDT as an antimicrobial topical agent against superficial and cutaneous diseases represents an effective method for eliminating microorganisms.

The first chapter describes: a) the complex problem of *C. albicans* infections, b) what a biofilm is, why they are so resistant to antimicrobial agents and their importance in infections. In addition the first chapter describes the antimicrobial Photodynamic Therapy (aPDT) and suggests it as an effective approach for killing of microbial cells.

The second chapter shows for the first time the use of XF-73, a new porphyrine derivative, combined with blue light to inactivate *C. albicans* biofilms, causing 5 $\log_{10}$ cell killing. The results were compared to TMPyP, an already known PS The efficacy of aPDT was also compared with the efficacy of Amphotericin B (AmB), the gold standard for the treatment of fungal infections. The presence of extracellular polymeric substance (EPS), which is a hallmark characteristic of microbial biofilms, was also detected. Besides, for the first time, singlet oxygen ($^1O_2$) was directly detected in biofilms treated by XF-73-aPDT.

In chapter 3, a model of duo-species biofilm, formed by *C. albicans* and *S. epidermidis,* was developed. The susceptibility of *C. albicans,* co-aggregated in this duo- species biofilm, was evaluated using XF-73-aPDT. Duo-species biofilms were less

susceptible to XF-73-aPDT than monomicrobial *C. albicans* biofilms. The results showed that the susceptibility to aPDT decreases with the increase of the complexity of the biofilms composition.

Since the over expression of heat shock proteins is a mechanism, whereby cells can become resistant to aPDT, in chapter 4 it was examined, whether the heat shock protein 70 (Hsp70) over expression after thermal stress protects *C. albicans* cells against the oxidative damage caused by aPDT. In addition, it was investigated, whether *C. albicans* cells, treated by aPDT, might over express Hsp70. For this, the kinetics of Hsp70 expression in *C. albicans* cells, treated with a sub lethal dose of aPDT, were determined over a period of 24 h. The results, obtained, showed that the over expression of Hsp70 by *C. albicans* cells is not a mechanism, by which microbial cells might develop resistance to TMPyP-mediated aPDT. Also, the expression of Hsp70 in *C. albicans* did not increase after sub-lethal TMPyP-mediated aPDT.

Chapter 5 reports the use of a luminescence based oxygen-sensitive sensor for monitoring oxygen concentration of *C. albicans* and *S. epidermidis* biofilms during aPDT. The knowledge of oxygen concentration during aPDT is important to improve the efficacy of aPDT.

7 Zusammenfassung

Candida albicans ist die wichtigste Pilzart, welche fähig ist, Biofilme zu bilden. Sie verursachen vor allem bei immunsupprimierten Patienten oberflächliche Haut- und Schleimhautentzündungen sowie invasive Mykosen. Bei solchen Patienten werden invasive Infektionen oft mit einer erhöhten Morbidität und Mortalität in Verbindung gebracht. Zudem hat die verstärkte antimykotische Resistenz die Wirksamkeit konventioneller Therapien verringert. Die Nutzung von aPDT als antimikrobielle Behandlung gegen oberflächliche Krankheiten und Hautkrankheiten stellt eine effektive Methode zur Eliminierung von Mikroorganismen dar.

Das erste Kapitel beschreibt: a) die Problematik von *C. albicans* Infektionen, b) was Biofilme sind, warum sie so resistent gegen antimikrobielle Behandlungen sind und welche Bedeutung sie bei Infektionen haben. Zusätzlich wird im ersten Kapitel die antimikrobielle Photodynamische Therapie (aPDT) beschrieben und als eine effektive Methode zum Abtöten mikrobieller Zellen vorgestellt.

Das zweite Kapitel zeigt erstmals den Einsatz des neuen Porphyrin Derivates XF-73 in Verbindung mit blauem Licht zur Inaktivierung von *C. albicans* Biofilmen, wobei eine Zellabtötung von 5 $\log_{10}$ erreicht wurde. Die Ergebnisse wurden mit TMPyP, welcher einen bereits bekannten Photosensitizer darstellt, sowie mit der Wirksamkeit von Amphotericin B (AmB), dem Standardmedikament für die Behandlung von Pilzinfektionen, verglichen. Es konnte außerdem gezeigt werden, dass die Existenz extrazellulärer polymerer Substanzen (EPS), welche eine zentrale Charakteristik mikrobieller Biofilme ist, einen Einfluss auf die Effizienz der Wirksamkeit von aPDT- und AmB-Behandlungen hat. Weiterhin konnte erstmals

Singulett-Sauerstoff ($^1O_2$) direkt in Biofilmen, welche mit XF-73-aPDT behandelt wurden, gemessen werden.

In Kapitel 3 wurde ein Modell eines Biofilms, welcher aus *C. albicans* und *S. epidermidis* gebildet wurde, entwickelt. Die Empfindlichkeit der *C. albicans* innerhalb dieses Biofilms gegenüber XF-73-aPDT wurde evaluiert. Dabei zeigte sich, dass die Biofilme, welche aus diesen beiden Spezies bestanden, weniger empfindlich gegenüber XF-73-aPDT waren als monomikrobielle *C. albicans*-Biofilme. Die Ergebnisse zeigten, dass die Empfindlichkeit gegenüber aPDT mit steigender Komplexität der Biofilme abnimmt.

Da die übermäßige Bildung von Hitzeschock-Proteinen ein Mechanismus ist, durch welchen Zellen resistent gegen aPDT werden können, wurde in Kapitel 4 untersucht, ob das durch eine thermische Stresssituation induzierte Hitzeschock-Protein 70 (Hsp70) *C. albicans* gegen die oxidative Wirkung der aPDT schützt. Zusätzlich wurde untersucht, ob *C. albicans*-Zellen, welche einer aPDT ausgesetzt werden, übermäßig Hsp70 bilden. Hierfür wurde der Verlauf der Hsp70-Bildung in *C. albicans*-Zellen, welche mit einer subletalen Dosis aPDT behandelt wurden, für eine Dauer von 24 Stunden bestimmt. Die Ergebnisse zeigten, dass die übermäßige Bildung von Hsp70 durch *C. albicans*-Zellen kein Mechanismus ist, durch welchen die mikrobiellen Zellen eine Resistenz gegen TMPyP-aPDT entwickeln können. Auch zeigte sich durch die Behandlung mit subletaler TMPyP-aPDT keine vermehrte Bildung von Hsp70 durch *C. albicans*.

Kapitel 5 beschreibt den Einsatz eines lumineszenzbasierten Sauerstoffsensors, durch welchen die Sauerstoffkonzentration in den *C. albicans*- und *S. epidermidis*-Biofilmen während der aPDT gemessen werden kann. Das Wissen über die

Sauerstoffkonzentration während der aPDT ist wichtig, um in der Zukunft die Wirksamkeit der aPDT zu verbessern.

8 References

1.   Zeina, B., et al., *Killing of cutaneous microbial species by photodynamic therapy.* Br J Dermatol, 2001. 144(2): p. 274-8.

2.   Vandeputte, P., S. Ferrari, and A.T. Coste, *Antifungal resistance and new strategies to control fungal infections.* Int J Microbiol, 2012. 2012: p. 713687.

3.   Garber, G., *An overview of fungal infections.* Drugs, 2001. 61 Suppl 1: p. 1-12.

4.   Martin, G.S., et al., *The epidemiology of sepsis in the United States from 1979 through 2000.* New England Journal of Medicine, 2003. 348(16): p. 1546-1554.

5.   Sifuentes-Osornio, J., D.E. Corzo-Leon, and L.A. Ponce-de-Leon, *Epidemiology of Invasive Fungal Infections in Latin America.* Curr Fungal Infect Rep, 2012. 6(1): p. 23-34.

6.   Espinel-Ingroff, A., *Novel antifungal agents, targets or therapeutic strategies for the treatment of invasive fungal diseases: a review of the literature (2005-2009).* Revista Iberoamericana De Micologia, 2009. 26(1): p. 15-22.

7.   Groll, A.H. and A. Tragiannidis, *Recent Advances in Antifungal Prevention and Treatment.* Seminars in Hematology, 2009. 46(3): p. 212-229.

8.   Vandeputte, P., S. Ferrari, and A.T. Coste, *Antifungal resistance and new strategies to control fungal infections.* Int J Microbiol. 2012: p. 713687.

9.   Kauffman, C.A., *Systemic antifungal agents. What is in the pipeline?* Drugs R D, 1999. 1(2): p. 153-9.

10.   Lui, H. and R.R. Anderson, *Photodynamic therapy in dermatology. Shedding a different light on skin disease.* Arch Dermatol, 1992. 128(12): p. 1631-6.

11.   Dai, T., Y.Y. Huang, and M.R. Hamblin, *Photodynamic therapy for localized infections--state of the art.* Photodiagnosis Photodyn Ther, 2009. 6(3-4): p. 170-88.

12.   Raab, O., *Ueber die Wirkung fluorizierender Stoffe auf Infusorien.* Z. Biol., 1900. 39: p. 524-546.

13.   H. v. J. Tappeiner; Jesionek, A., *Therapeutische Versuche mit fluoreszierenden Stoffen.* Münch. Med. Wochenschr., 1903. 50: p. 2042-2044.

14.   Davies, J., *Where have All the Antibiotics Gone?* Can J Infect Dis Med Microbiol, 2006. 17(5): p. 287-90.

15.   Hahn, F.E., *Acquired resistance and natural insensitivity to chemotherapeutic drugs.* Antibiot Chemother, 1975. 20: p. 1-7.

16.   Administration:, U.S.F.a.D. March 27, 2002, Antibiotic resistance.

17.   Huber, H., *Weitere Versuche mit photodynamischen sensibilisie- renden Farbstoffen.* Arch. f. Hyg., 1905. 54.

18.   Prates, R.A., et al., *Influence of multidrug efflux systems on methylene blue-mediated photodynamic inactivation of Candida albicans.* J Antimicrob Chemother, 2011. 66(7): p. 1525-32.

19.   Dougherty, T.J., et al., *Photodynamic therapy.* J Natl Cancer Inst, 1998. 90(12): p. 889-905.

20.   Konan, Y.N., R. Gurny, and E. Allemann, *State of the art in the delivery of photosensitizers for photodynamic therapy.* J Photochem Photobiol B, 2002. 66(2): p. 89-106.

21.   Donnelly, R.F., P.A. McCarron, and M.M. Tunney, *Antifungal photodynamic therapy.* Microbiol Res, 2008. 163(1): p. 1-12.

22.   Kalka, K., H. Merk, and H. Mukhtar, *Photodynamic therapy in dermatology.* J Am Acad Dermatol, 2000. 42(3): p. 389-413; quiz 414-6.

23.   Foote, C.S., *Definition of type I and type II photosensitized oxidation.* Photochem Photobiol, 1991. 54(5): p. 659.

24.   Schafer, M., C. Schmitz, and G. Horneck, *High sensitivity of Deinococcus radiodurans to photodynamically-produced singlet oxygen.* Int J Radiat Biol, 1998. 74(2): p. 249-53.

25.   Bertoloni, G., et al., *Factors influencing the haematoporphyrin-sensitized photoinactivation of Candida albicans.* J Gen Microbiol, 1989. 135(4): p. 957-66.

26.   Minnock, A., et al., *Mechanism of uptake of a cationic water-soluble pyridinium zinc phthalocyanine across the outer membrane of Escherichia coli.* Antimicrobial Agents and Chemotherapy, 2000. 44(3): p. 522-527.

27.   Maisch, T., et al., *Antibacterial photodynamic therapy in dermatology.* Photochemical & Photobiological Sciences, 2004. 3(10): p. 907-917.

28.   Demidova, T.N. and M.R. Hamblin, *Effect of cell-photosensitizer binding and cell density on microbial photoinactivation.* Antimicrob Agents Chemother, 2005. 49(6): p. 2329-35.

29.   Kharkwal, G.B., et al., *Photodynamic therapy for infections: clinical applications.* Lasers Surg Med, 2011. 43(7): p. 755-67.

30.   Maisch, T., *A new strategy to destroy antibiotic resistant microorganisms: antimicrobial photodynamic treatment.* Mini Rev Med Chem, 2009. 9(8): p. 974-83.

31.   Mroz, P., et al., *Photodynamic therapy with fullerenes.* Photochemical & Photobiological Sciences, 2007. 6(11): p. 1139-1149.

32.   Wainwright, M., *'Safe' photoantimicrobials for skin and soft-tissue infections.* Int J Antimicrob Agents. 36(1): p. 14-8.

33.   Longo, J.P.F., Muehlmann, L.A., Azevedo, R.B., *Nanostructured Carriers for Photodynamic Therapy Applications in microbiology*, in *Science against microbial pathogens: communicating current research and technological advances*, A. Méndez-Vilas, Editor. 2011. p. 189-196.

34.   Redmond, R.W. and J.N. Gamlin, *A compilation of singlet oxygen yields from biologically relevant molecules.* Photochem Photobiol, 1999. 70(4): p. 391-475.

35.   Mohr, H., et al., *Virus inactivation of blood products by phenothiazine dyes and light.* Photochemistry and Photobiology, 1997. 65(3): p. 441-445.

36.   Wainwright, M., *The emerging chemistry of blood product disinfection.* Chemical Society Reviews, 2002. 31(2): p. 128-136.

37.   Lin, J., et al., *Toluidine blue-mediated photodynamic therapy of oral wound infections in rats.* Lasers Med Sci, 2010. 25(2): p. 233-8.

38.   Josefsen, L.B. and R.W. Boyle, *Unique Diagnostic and Therapeutic Roles of Porphyrins and Phthalocyanines in Photodynamic Therapy, Imaging and Theranostics.* Theranostics, 2012. 2(9): p. 916-966.

39.   Maestrin, A.P.J., et al., *Synthesis, spectroscopy and photosensitizing properties of hydroxynitrophenylporphyrins.* Journal of the Brazilian Chemical Society, 2004. 15(5): p. 708-713.

40.   Baier, J., et al., *Time dependence of singlet oxygen luminescence provides an indication of oxygen concentration during oxygen consumption.* Journal of Biomedical Optics, 2007. 12(6).

41.   Cormick, M.P., et al., *Photodynamic inactivation of Candida albicans sensitized by tri- and tetra-cationic porphyrin derivatives.* Eur J Med Chem, 2009. 44(4): p. 1592-9.

42.   Quiroga, E.D., M.G. Alvarez, and E.N. Durantini, *Susceptibility of Candida albicans to photodynamic action of 5,10,15,20-tetra(4-N-methylpyridyl)porphyrin in different media.* FEMS Immunol Med Microbiol, 2010. 60(2): p. 123-31.

43.   Cormick, M.P., et al., *Mechanistic insight of the photodynamic effect induced by tri- and tetra-cationic porphyrins on Candida albicans cells.* Photochem Photobiol Sci, 2011. 10(10): p. 1556-61.

44.   Pereira Gonzales, F. and T. Maisch, *XF drugs: A new family of antibacterials.* Drug News Perspect, 2010. 23(3): p. 167-74.

45.   Maisch, T., et al., *Photodynamic effects of novel XF porphyrin derivatives on prokaryotic and eukaryotic cells.* Antimicrob Agents Chemother, 2005. 49(4): p. 1542-52.

46.   Lukyanets, E.A., *Phthalocyanines as photosensitizers in the photodynamic therapy of cancer.* Journal of Porphyrins and Phthalocyanines, 1999. 3(6-7): p. 424-432.

47.   Siejak, A., et al., *Triplet behavior in weakly coupled chromophors in covalent pyridyl porphyrin-polymer systems.* Spectrochim Acta A Mol Biomol Spectrosc, 2009. 74(1): p. 148-53.

48.   Mantareva, V., et al., *Non-aggregated Ga(III)-phthalocyanines in the photodynamic inactivation of planktonic and biofilm cultures of pathogenic microorganisms.* Photochem Photobiol Sci, 2011. 10(1): p. 91-102.

49.   Maisch, T., *Anti-microbial photodynamic therapy: useful in the future?* Lasers in Medical Science, 2007. 22(2): p. 83-91.

50.   Wainwright, M., *Photodynamic antimicrobial chemotherapy (PACT).* Journal of Antimicrobial Chemotherapy, 1998. 42(1): p. 13-28.

51.   Moan, J. and K. Berg, *The Photodegradation of Porphyrins in Cells Can Be Used to Estimate the Lifetime of Singlet Oxygen.* Photochemistry and Photobiology, 1991. 53(4): p. 549-553.

52.   Kim, S.Y., O.J. Kwon, and J.W. Park, *Inactivation of catalase and superoxide dismutase by singlet oxygen derived from photoactivated dye.* Biochimie, 2001. 83(5): p. 437-44.

53.   Casas, A., et al., *Mechanisms of resistance to photodynamic therapy.* Curr Med Chem, 2011. 18(16): p. 2486-515.

54.   Tegos, G.P. and M.R. Hamblin, *Phenothiazinium antimicrobial photosensitizers are substrates of bacterial multidrug resistance pumps.* Antimicrob Agents Chemother, 2006. 50(1): p. 196-203.

55.   Kishen, A., et al., *Efflux pump inhibitor potentiates antimicrobial photodynamic inactivation of Enterococcus faecalis biofilm.* Photochem Photobiol. 86(6): p. 1343-9.

56.   Giuliani, F., et al., *In Vitro Resistance Selection Studies of RLP068/Cl, a New Zn(II) Phthalocyanine Suitable for Antimicrobial Photodynamic Therapy.* Antimicrobial Agents and Chemotherapy, 2010. 54(2): p. 637-642.

57.   Tyedmers, J., A. Mogk, and B. Bukau, *Cellular strategies for controlling protein aggregation.* Nat Rev Mol Cell Biol, 2010. 11(11): p. 777-88.

58.   Casas, A., et al., *Mechanisms of resistance to photodynamic therapy.* Curr Med Chem. 18(16): p. 2486-515.

59.   Shackley, D.C., et al., *Comparison of the cellular molecular stress responses after treatments used in bladder cancer.* BJU Int, 2002. 90(9): p. 924-32.

60.   St Denis, T.G., et al., *Analysis of the bacterial heat shock response to photodynamic therapy-mediated oxidative stress.* Photochem Photobiol. 87(3): p. 707-13.

61.   Bolean, M., et al., *Photodynamic therapy with rose bengal induces GroEL expression in Streptococcus mutans.* Photomed Laser Surg, 2010. 28 Suppl 1: p. S79-84.

62.   ten Cate, J.M., et al., *Molecular and Cellular Mechanisms That Lead to Candida Biofilm Formation.* Journal of Dental Research, 2009. 88(2): p. 105-115.

63.   Donlan, R.M., *Biofilms: microbial life on surfaces.* Emerg Infect Dis, 2002. 8(9): p. 881-90.

64.   Chandra, J., P.K. Mukherjee, and M.A. Ghannoum, *In vitro growth and analysis of Candida biofilms.* Nat Protoc, 2008. 3(12): p. 1909-24.

65.   Williams, P., *Quorum sensing, communication and cross-kingdom signalling in the bacterial world.* Microbiology-Sgm, 2007. 153: p. 3923-3938.

66.   Ramage, G., et al., *Candida biofilms: an update.* Eukaryotic Cell, 2005. 4(4): p. 633-638.

67.   Molero, G., et al., *Candida albicans: genetics, dimorphism and pathogenicity.* Int Microbiol, 1998. 1(2): p. 95-106.

68.   (NIH), D.o.H.a.H.S.-N.I.o.H. *Immunology of Biofilms.* 2007; Available from: http://grants.nih.gov/grants/guide/pa-files/PA-07-288.html.

69.   Jefferson, K.K., *What drives bacteria to produce a biofilm?* Fems Microbiology Letters, 2004. 236(2): p. 163-173.

70.   Lewis, K., *Riddle of biofilm resistance.* Antimicrobial Agents and Chemotherapy, 2001. 45(4): p. 999-1007.

71.   Ramage, G., J.P. Martinez, and J.L. Lopez-Ribot, *Candida biofilms on implanted biomaterials: a clinically significant problem.* FEMS Yeast Res, 2006. 6(7): p. 979-86.

72.   Ramage, G., et al., *Fungal biofilm resistance.* Int J Microbiol. 2012: p. 528521.

73.   Donlan, R.M. and J.W. Costerton, *Biofilms: survival mechanisms of clinically relevant microorganisms.* Clin Microbiol Rev, 2002. 15(2): p. 167-93.

74.   Baillie, G.S. and L.J. Douglas, *Effect of growth rate on resistance of Candida albicans biofilms to antifungal agents.* Antimicrobial Agents and Chemotherapy, 1998. 42(8): p. 1900-1905.

75.   Lewis, K., *Multidrug tolerance of biofilms and persister cells.* Bacterial Biofilms, 2008. 322: p. 107-131.

76.   Mukherjee, P.K., et al., *Mechanism of fluconazole resistance in Candida albicans biofilms: Phase-specific role of efflux pumps and membrane sterols.* Infection and Immunity, 2003. 71(8): p. 4333-4340.

77.   Cortes , E.M., J.C. Bonilla, and R.D. Sinisterra, *Biofilm formation,control and novel strategies for eradication.* Science against Microbial Pathogens: Communicating Current Research and Technological Advances, ed. A. Mendez-Vilas. Vol. 2. 2011.

78.   Loeffler, J. and D.A. Stevens, *Antifungal drug resistance.* Clinical Infectious Diseases, 2003. 36: p. S31-S41.

79.   Kuhn, D.M. and M.A. Ghannoum, *Candida biofilms: antifungal resistance and emerging therapeutic options.* Curr Opin Investig Drugs, 2004. 5(2): p. 186-97.

80.   Sardi, J.C., et al., *Candida species: current epidemiology, pathogenicity, biofilm formation, natural antifungal products and new therapeutic options.* J Med Microbiol, 2013. 62(Pt 1): p. 10-24.

81.   Montejo, M., *[Epidemiology of invasive fungal infection in solid organ transplant].* Rev Iberoam Micol, 2011. 28(3): p. 120-3.

82.   Gruszecki, W.I., et al., *Organization of antibiotic amphotericin B in model lipid membranes. A mini review.* Cellular & Molecular Biology Letters, 2003. 8(1): p. 161-170.

83.   Ellis, D., *Amphotericin B: spectrum and resistance.* J Antimicrob Chemother, 2002. 49 Suppl 1: p. 7-10.

84.   Mesa-Arango, A.C., L. Scorzoni, and O. Zaragoza, *It only takes one to do many jobs: Amphotericin B as antifungal and immunomodulatory drug.* Front Microbiol, 2012. 3: p. 286.

85.   Shapiro, R.S., N. Robbins, and L.E. Cowen, *Regulatory Circuitry Governing Fungal Development, Drug Resistance, and Disease.* Microbiology and Molecular Biology Reviews, 2011. 75(2): p. 213-267.

86.   Schaffner, A. and A. Bohler, *Amphotericin B refractory aspergillosis after itraconazole: evidence for significant antagonism.* Mycoses, 1993. 36(11-12): p. 421-4.

87.   Kanafani, Z.A. and J.R. Perfect, *Resistance to antifungal agents: Mechanisms and clinical impact.* Clinical Infectious Diseases, 2008. 46(1): p. 120-128.

88.   Fanos, V. and L. Cataldi, *Amphotericin B-induced nephrotoxicity: A review.* Journal of Chemotherapy, 2000. 12(6): p. 463-470.

89.   Dismukes, W.E., *Introduction to antifungal drugs.* Clin Infect Dis, 2000. 30(4): p. 653-7.

90.   Robbins, N., et al., *Hsp90 governs dispersion and drug resistance of fungal biofilms.* PLoS Pathog. 7(9): p. e1002257.

91.   Shalini, K., et al., *Advances in synthetic approach to and antifungal activity of triazoles.* Beilstein J Org Chem. 7: p. 668-77.

92.   Achkar, J.M. and B.C. Fries, *Candida infections of the genitourinary tract.* Clin Microbiol Rev, 2010. 23(2): p. 253-73.

93.   Lupetti, A., et al., *Molecular basis of resistance to azole antifungals.* Trends Mol Med, 2002. 8(2): p. 76-81.

94.   Ostrosky-Zeichner, L., et al., *An insight into the antifungal pipeline: selected new molecules and beyond.* Nature Reviews Drug Discovery, 2010. 9(9): p. 719-727.

95.   Onyewu, C., et al., *Ergosterol biosynthesis inhibitors become fungicidal when combined with calcineurin inhibitors against Candida albicans, Candida glabrata, and Candida krusei.* Antimicrobial Agents and Chemotherapy, 2003. 47(3): p. 956-964.

96.   Johnson, E.M., et al., *Emergence of Azole Drug-Resistance in Candida Species from Hiv-Infected Patients Receiving Prolonged Fluconazole Therapy for Oral Candidosis.* Journal of Antimicrobial Chemotherapy, 1995. 35(1): p. 103-114.

97.   Albengres, E., H. Le Louet, and J.P. Tillement, *Systemic antifungal agents. Drug interactions of clinical significance.* Drug Saf, 1998. 18(2): p. 83-97.

98.   Hsueh, P.R., et al., *Antifungal susceptibilities of clinical isolates of Candida species, Cryptococcus neoformans, and Aspergillus species from Taiwan: surveillance of multicenter antimicrobial resistance in Taiwan program data from 2003.* Antimicrob Agents Chemother, 2005. 49(2): p. 512-7.

99.   Kothavade, R.J., et al., *Candida tropicalis: its prevalence, pathogenicity and increasing resistance to fluconazole.* J Med Microbiol, 2010. 59(Pt 8): p. 873-80.

100.   Mathew, B.P. and M. Nath, *Recent approaches to antifungal therapy for invasive mycoses.* ChemMedChem, 2009. 4(3): p. 310-23.

101.   Eschenauer, G., D.D. Depestel, and P.L. Carver, *Comparison of echinocandin antifungals.* Ther Clin Risk Manag, 2007. 3(1): p. 71-97.

102.   Ostrosky-Zeichner, L., et al., *Amphotericin B: time for a new "gold standard".* Clin Infect Dis, 2003. 37(3): p. 415-25.

103.   Denning, D.W., *Echinocandin antifungal drugs.* Lancet, 2003. 362(9390): p. 1142-1151.

104.   Petrikkos, G. and A. Skiada, *Recent advances in antifungal chemotherapy.* International Journal of Antimicrobial Agents, 2007. 30(2): p. 108-117.

105.   Manzoni, P., et al., *Echinocandins for the nursery: an update.* Curr Drug Metab, 2012.

106.   Morris, M.I. and M. Villmann, *Echinocandins in the management of invasive fungal infections, part 1.* Am J Health Syst Pharm, 2006. 63(18): p. 1693-703.

107.   Chen, S.C.A., M.A. Slavin, and T.C. Sorrell, *Echinocandin Antifungal Drugs in Fungal Infections A Comparison.* Drugs, 2011. 71(1): p. 11-41.

108.   Gow, N.A., et al., *Candida albicans morphogenesis and host defence: discriminating invasion from colonization.* Nat Rev Microbiol, 2012. 10(2): p. 112-22.

109.   Wachtler, B., et al., *From attachment to damage: defined genes of Candida albicans mediate adhesion, invasion and damage during interaction with oral epithelial cells.* PLoS One, 2011. 6(2): p. e17046.

110.   Wisplinghoff, H., et al., *Nosocomial bloodstream infections in US hospitals: analysis of 24,179 cases from a prospective nationwide surveillance study.* Clin Infect Dis, 2004. 39(3): p. 309-17.

111.   Hajjeh, R.A., et al., *Incidence of bloodstream infections due to Candida species and in vitro susceptibilities of isolates collected from 1998 to 2000 in a population-based active surveillance program.* J Clin Microbiol, 2004. 42(4): p. 1519-27.

112.   Lockhart, S.R., et al., *Natural defenses against Candida colonization breakdown in the oral cavities of the elderly.* J Dent Res, 1999. 78(4): p. 857-68.

113.   Pappas, P.G., et al., *A prospective observational study of candidemia: epidemiology, therapy, and influences on mortality in hospitalized adult and pediatric patients.* Clin Infect Dis, 2003. 37(5): p. 634-43.

114.   *What is Candida?* . Available from: http:/www.thehealthsuccesssite.com/candida-candidiasis.html

115.   Leroy, O., et al., *Epidemiology, management, and risk factors for death of invasive Candida infections in critical care: a multicenter, prospective, observational study in France (2005-2006).* Crit Care Med, 2009. 37(5): p. 1612-8.

116.   Pfaller, M.A. and D.J. Diekema, *Epidemiology of invasive candidiasis: a persistent public health problem.* Clin Microbiol Rev, 2007. 20(1): p. 133-63.

117.   Colombo, A.L., et al., *Epidemiology of candidemia in Brazil: a nationwide sentinel surveillance of candidemia in eleven medical Centers.* Journal of Clinical Microbiology, 2006. 44(8): p. 2816-2823.

118.   rfums, M. 2012; Available from: http://www.studyblue.com/notes/note/n/soft-tissue-infections/deck/4054056.

119.   Thompson, G.R., 3rd, J. Cadena, and T.F. Patterson, *Overview of antifungal agents.* Clin Chest Med, 2009. 30(2): p. 203-15, v.

120.   Samaranayake, L.P., W. Keung Leung, and L. Jin, *Oral mucosal fungal infections.* Periodontol 2000, 2009. 49: p. 39-59.

121.   Ninane, J., *A multicentre study of fluconazole versus oral polyenes in the prevention of fungal infection in children with hematological or oncological malignancies. Multicentre Study Group.* Eur J Clin Microbiol Infect Dis, 1994. 13(4): p. 330-7.

122.   Biel, M.A., *Photodynamic therapy of bacterial and fungal biofilm infections.* Methods Mol Biol, 2010. 635: p. 175-94.

123.   Phillips, P., et al., *Itraconazole cyclodextrin solution for fluconazole-refractory oropharyngeal candidiasis in AIDS: correlation of clinical response with in vitro susceptibility.* AIDS, 1996. 10(12): p. 1369-76.

124.   Ovchinnikova, E.S., et al., *Evaluation of adhesion forces of Staphylococcus aureus along the length of Candida albicans hyphae.* BMC Microbiol, 2012. 12: p. 281.

125.   Akcaglar, S., B. Ener, and O. Tore, *Acid proteinase enzyme activity in Candida albicans strains: a comparison of spectrophotometry and plate methods.* Turkish Journal of Biology, 2011. 35(5): p. 559-567.

126.   Sturtevant, J. and R. Calderone, *Candida albicans adhesins: Biochemical aspects and virulence.* Rev Iberoam Micol, 1997. 14(3): p. 90-7.

127.   Wang, Y.C., et al., *Global screening of potential Candida albicans biofilm-related transcription factors via network comparison.* Bmc Bioinformatics, 2010. 11.

128.   van der Meer, J.W.M., et al., *Severe Candida spp. infections: new insights into natural immunity.* International Journal of Antimicrobial Agents, 2010. 36: p. S58-S62.

129.   Tampakakis, E., A.Y. Peleg, and E. Mylonakis, *Interaction of Candida albicans with an Intestinal Pathogen, Salmonella enterica Serovar Typhimurium.* Eukaryotic Cell, 2009. 8(5): p. 732-737.

130.   Uppuluri, P., et al., *Characteristics of Candida albicans biofilms grown in a synthetic urine medium.* J Clin Microbiol, 2009. 47(12): p. 4078-83.

131.   d'Enfert, C., *Hidden killers: persistence of opportunistic fungal pathogens in the human host.* Curr Opin Microbiol, 2009. 12(4): p. 358-64.

132.   Ramage, G., et al., *Characteristics of biofilm formation by Candida albicans.* Rev Iberoam Micol, 2001. 18(4): p. 163-70.

133.   Chandra, J., P.K. Mukherjee, and M.A. Ghannoum, *Candida biofilms associated with CVC and medical devices.* Mycoses, 2012. 55: p. 46-57.

134.   Harriott, M.M. and M.C. Noverr, *Candida albicans and Staphylococcus aureus form polymicrobial biofilms: effects on antimicrobial resistance.* Antimicrob Agents Chemother, 2009. 53(9): p. 3914-22.

135.   Chandra, J., et al., *Biofilm formation by the fungal pathogen Candida albicans: development, architecture, and drug resistance.* J Bacteriol, 2001. 183(18): p. 5385-94.

136.   Nett, J. and D. Andes, *Candida albicans biofilm development, modeling a host-pathogen interaction.* Curr Opin Microbiol, 2006. 9(4): p. 340-5.

137.   Kumamoto, C.A. and M.D. Vinces, *Contributions of hyphae and hypha-co-regulated genes to Candida albicans virulence.* Cell Microbiol, 2005. 7(11): p. 1546-54.

138.   Garcia-Sanchez, S., et al., *Candida albicans biofilms: a developmental state associated with specific and stable gene expression patterns.* Eukaryot Cell, 2004. 3(2): p. 536-45.

139.   Nett, J., et al., *Putative role of beta-1,3 glucans in Candida albicans biofilm resistance.* Antimicrob Agents Chemother, 2007. 51(2): p. 510-20.

140.   Donlan, R.M., *Biofilm formation: a clinically relevant microbiological process.* Clin Infect Dis, 2001. 33(8): p. 1387-92.

141.   Sternberg, E.D., D. Dolphin, and C. Bruckner, *Porphyrin-based photosensitizers for use in photodynamic therapy.* Tetrahedron, 1998. 54(17): p. 4151-4202.

142.   Phillips, A.J., I. Sudbery, and M. Ramsdale, *Apoptosis induced by environmental stresses and amphotericin B in Candida albicans.* Proc Natl Acad Sci U S A, 2003. 100(24): p. 14327-32.

143.   Parker, J.G. and W.D. Stanbro, *Optical Determination of the Rates of Formation and Decay of O-2(1-Delta-G) in H2o, D2o and Other Solvents.* Journal of Photochemistry, 1984. 25(2-4): p. 545-547.

144.   Boyce, J.M. and D. Pittet, *Guideline for Hand Hygiene in Health-Care Settings. Recommendations of the Healthcare Infection Control Practices Advisory Committee and the HIPAC/SHEA/APIC/IDSA Hand Hygiene Task Force.* Am J Infect Control, 2002. 30(8): p. S1-46.

145.   Gebel, J. and D.-K.d. DGHM, *Anforderungskatalog für die Aufnahme von chemischen Desinfektionsverfahren in die Desinfektionsmittel-Liste der DGHM.* mhp-Verlag GmbH, 2002: p. 9-16.

146.   Bolton, J.R., et al.,, *Light-induced intramolecular electron transfer from a porphyrin linked to a p-benzoquinone by a rigid spacer group* J. Chem. Soc., Chem. Commun.,, 1985: p. 559-560.

147.   Perezous, L.F., et al., *Colonization of Candida species in denture wearers with emphasis on HIV infection: a literature review.* J Prosthet Dent, 2005. 93(3): p. 288-93.

148.   Costerton, J.W., et al.,, *The problem not just bacteria ? bacterial biofilms.* The Analyst, 1999. 6(3): p. 18-25

149.   Davey, M.E. and A. O'Toole G, *Microbial biofilms: from ecology to molecular genetics.* Microbiol Mol Biol Rev, 2000. 64(4): p. 847-67.

150.   Wainwright, M. and K.B. Crossley, *Photosensitising agents - circumventing resistance and breaking down biofilms: a review.* International Biodeterioration & Biodegradation, 2004. 53(2): p. 119-126.

151.   Mayers, D.L., et al.,, *Antimicrobial Drug Resistance.* Vol. 2. 2009, New York: Springer.

152.   Raz-Pasteur, A., Y. Ullmann, and I. Berdicevsky, *The pathogenesis of Candida infections in a human skin model: scanning electron microscope observations.* ISRN Dermatol, 2011. 2011: p. 150642.

153.   Doctor, F. *Amphotericin B deoxycholate.* [cited 2013 28.02.]; Available from: http://www.doctorfungus.org/.

154.   Yang, Y.L., et al., *The trend of susceptibilities to amphotericin B and fluconazole of Candida species from 1999 to 2002 in Taiwan.* BMC Infect Dis, 2005. 5: p. 99.

155.   Chabrier-Rosello, Y., et al., *Sensitivity of Candida albicans germ tubes and biofilms to photofrin-mediated phototoxicity.* Antimicrob Agents Chemother, 2005. 49(10): p. 4288-95.

156.   Harmsen, S., et al., *Amphotericin B Is Cytotoxic at Locally Delivered Concentrations.* Clinical Orthopaedics and Related Research, 2011. 469(11): p. 3016-3021.

157.   O'Toole, G., H.B. Kaplan, and R. Kolter, *Biofilm formation as microbial development.* Annual Review of Microbiology, 2000. 54: p. 49-79.

158.   El-Azizi, M.A., S.E. Starks, and N. Khardori, *Interactions of Candida albicans with other Candida spp. and bacteria in the biofilms.* J Appl Microbiol, 2004. 96(5): p. 1067-73.

159.   Adam, B., G.S. Baillie, and L.J. Douglas, *Mixed species biofilms of Candida albicans and Staphylococcus epidermidis.* J Med Microbiol, 2002. 51(4): p. 344-9.

160.   Douglas, L.J., *Medical importance of biofilms in Candida infections.* Rev Iberoam Micol, 2002. 19(3): p. 139-43.

161.   Brand, A., et al., *Cell wall glycans and soluble factors determine the interactions between the hyphae of Candida albicans and Pseudomonas aeruginosa.* Fems Microbiology Letters, 2008. 287(1): p. 48-55.

162.   Hogan, D.A. and R. Kolter, *Pseudomonas-Candida interactions: an ecological role for virulence factors.* Science, 2002. 296(5576): p. 2229-32.

163.   Diaz, P.I., et al., *Synergistic Interaction between Candida albicans and Commensal Oral Streptococci in a Novel In Vitro Mucosal Model.* Infection and Immunity, 2012. 80(2): p. 620-632.

164.   Peters, B.M., et al., *Microbial interactions and differential protein expression in Staphylococcus aureus -Candida albicans dual-species biofilms.* Fems Immunology and Medical Microbiology, 2010. 59(3): p. 493-503.

165.   Dowd, S.E., et al., *Survey of fungi and yeast in polymicrobial infections in chronic wounds.* J Wound Care, 2011. 20(1): p. 40-7.

166.   Harriott, M.M. and M.C. Noverr, *Importance of Candida-bacterial polymicrobial biofilms in disease.* Trends Microbiol, 2011. 19(11): p. 557-63.

167.   Yao, Y., et al., *Factors characterizing Staphylococcus epidermidis invasiveness determined by comparative genomics.* Infect Immun, 2005. 73(3): p. 1856-60.

168.   Otto, M., *Staphylococcus epidermidis--the 'accidental' pathogen.* Nat Rev Microbiol, 2009. 7(8): p. 555-67.

169.   Klotz, S.A., et al., *Polymicrobial bloodstream infections involving Candida species: analysis of patients and review of the literature.* Diagn Microbiol Infect Dis, 2007. 59(4): p. 401-6.

170.   Miles, A.A., *Citation Classic - Estimation of the Bactericidal Power of the Blood.* Current Contents/Life Sciences, 1979(37): p. L12-L12.

171.   Chen, Y.C., et al., *Alternative activation of extracellular signal-regulated protein kinases in curcumin and arsenite-induced HSP70 gene expression in human colorectal carcinoma cells.* European Journal of Cell Biology, 2001. 80(3): p. 213-221.

172.   Pereira, C.A., et al., *Susceptibility of Candida albicans, Staphylococcus aureus, and Streptococcus mutans biofilms to photodynamic inactivation: an in vitro study.* Lasers Med Sci, 2011. 26(3): p. 341-8.

173.   Blaschek, H.P.W., H.H.; Agle, M.E., *Biofilms in the Food Environment.* 2007: Wiley-Blackwell.

174.   Peters, B.M., et al., *Efficacy of Ethanol against Candida albicans and Staphylococcus aureus Polymicrobial Biofilms.* Antimicrobial Agents and Chemotherapy, 2013. 57(1): p. 74-82.

175.   Wolcott, R.D., et al., *Biofilm maturity studies indicate sharp debridement opens a time- dependent therapeutic window.* J Wound Care, 2010. 19(8): p. 320-8.

176.   Street, C.N., et al., *In vitro photodynamic eradication of Pseudomonas aeruginosa in planktonic and biofilm culture.* Photochem Photobiol, 2009. 85(1): p. 137-43.

177.   Wood, S., et al., *Erythrosine is a potential photosensitizer for the photodynamic therapy of oral plaque biofilms.* Journal of Antimicrobial Chemotherapy, 2006. 57(4): p. 680-684.

178.   Mulcahy, H., L. Charron-Mazenod, and S. Lewenza, *Extracellular DNA chelates cations and induces antibiotic resistance in Pseudomonas aeruginosa biofilms.* PLoS Pathog, 2008. 4(11): p. e1000213.

179.   Moor, A.C.E., *Signaling pathways in cell death and survival after photodynamic therapy.* Journal of Photochemistry and Photobiology B-Biology, 2000. 57(1): p. 1-13.

180.   Kalmar, B. and L. Greensmith, *Induction of heat shock proteins for protection against oxidative stress.* Adv Drug Deliv Rev, 2009. 61(4): p. 310-8.

181.   Lindquist, S., *The heat-shock response.* Annu Rev Biochem, 1986. 55: p. 1151-91.

182.   Mayer, M.P. and B. Bukau, *Hsp70 chaperones: Cellular functions and molecular mechanism.* Cellular and Molecular Life Sciences, 2005. 62(6): p. 670-684.

183.   Kim, Y.H., et al., *Arsenic trioxide induces Hsp70 expression via reactive oxygen species and JNK pathway in MDA231 cells.* Life Sciences, 2005. 77(22): p. 2783-2793.

184.   van der Weerd, L., et al., *Neuroprotective effects of HSP70 overexpression after cerebral ischaemia - An MRI study.* Experimental Neurology, 2005. 195(1): p. 257-266.

185.   Young, J.C., J.M. Barral, and F.U. Hartl, *More than folding: localized functions of cytosolic chaperones.* Trends in Biochemical Sciences, 2003. 28(10): p. 541-547.

186.   Mayer, M.P., *Recruitment of Hsp70 chaperones: a crucial part of viral survival strategies.* Rev Physiol Biochem Pharmacol, 2005. 153: p. 1-46.

187.   Ramirez, C.A., J.M. Requena, and C.J. Puerta, *Identification of the HSP70-II gene in Leishmania braziliensis HSP70 locus: genomic organization and UTRs characterization.* Parasit Vectors, 2011. 4: p. 166.

188.   Zeuthen, M.L. and D.H. Howard, *Thermotolerance and the Heat-Shock Response in Candida-Albicans.* Journal of General Microbiology, 1989. 135: p. 2509-2518.

189.   Smith, P.K., et al., *Measurement of Protein Using Bicinchoninic Acid.* Analytical Biochemistry, 1985. 150(1): p. 76-85.

190.   Laemmli, U.K., *Cleavage of structural proteins during the assembly of the head of bacteriophage T4.* Nature, 1970. 227(5259): p. 680-5.

191.   Schneider, C.A., W.S. Rasband, and K.W. Eliceiri, *NIH Image to ImageJ: 25 years of image analysis.* Nat Methods, 2012. 9(7): p. 671-5.

192.   Guo, S., et al., *Heat shock protein 70 regulates cellular redox status by modulating glutathione-related enzyme activities.* Cell Stress Chaperones, 2007. 12(3): p. 245-54.

193.   van der Weerd, L., et al., *Neuroprotective effects of HSP70 overexpression after cerebral ischaemia--an MRI study.* Exp Neurol, 2005. 195(1): p. 257-66.

194.   St Denis, T.G., et al., *Analysis of the bacterial heat shock response to photodynamic therapy-mediated oxidative stress.* Photochem Photobiol, 2011. 87(3): p. 707-13.

195.   Gomer, C.J., et al., *Photodynamic therapy-mediated oxidative stress can induce expression of heat shock proteins.* Cancer Research, 1996. 56(10): p. 2355-2360.

196.   Bunn, H.F. and R.O. Poyton, *Oxygen sensing and molecular adaptation to hypoxia.* Physiol Rev, 1996. 76(3): p. 839-85.

197.   Grist, S.M., L. Chrostowski, and K.C. Cheung, *Optical oxygen sensors for applications in microfluidic cell culture.* Sensors (Basel), 2010. 10(10): p. 9286-316.

198.   Quaranta, M., S.M. Borisov, and I. Klimant, *Indicators for optical oxygen sensors.* Bioanal Rev, 2012. 4(2-4): p. 115-157.

199.   Weidgans, B.M., *New Fluorescent Optical pH Sensors with Minimal Effects of Ionic Strength*, in *Institut für Analytische Chemie, Chemo- und Biosensorik.* 2004, Universität Regensburg: Regensburg.

200.   Ramamoorthy, R., P.K. Dutta, and S.A. Akbar, *Oxygen sensors: Materials, methods, designs and applications.* Journal of Materials Science, 2003. 38(21): p. 4271-4282.

201.   Cattani, J.T., *Design of a Luminescent Sprayable pH-Sensor for use in dermatology and a Optical Oxygen Sensor for Studying Fungal and Bacterial Biofilms*, in *Fakultät für Chemie und Pharmazie* 2012, Universität Regensburg: Regensburg. p. 83.

202.   Mosmann, T., *Rapid colorimetric assay for cellular growth and survival: application to proliferation and cytotoxicity assays.* J Immunol Methods, 1983. 65(1-2): p. 55-63.

203.   Stewart, P.S. and M.J. Franklin, *Physiological heterogeneity in biofilms.* Nat Rev Microbiol, 2008. 6(3): p. 199-210.

204.   Zhang, T.C., Y.C. Fu, and P.L. Bishop, *Competition for substrate and space in biofilms.* Water Environment Research, 1995. 67(6): p. 992-1003.

205.   Lehaitre, M., et al., *Biofouling and Underwater measurements*. 2008, Paris: UNESCO Publishing.

206.   Rani, S.A., et al., *Spatial patterns of DNA replication, protein synthesis, and oxygen concentration within bacterial biofilms reveal diverse physiological states.* Journal of Bacteriology, 2007. 189(11): p. 4223-4233.

9 Acknowledgement

10 Curriculum vitae

Personal data

Name: Fernanda Pereira Gonzales
Date of birth: November 13th 1979
Place of birth: Campo Grande; Mato Grosso do Sul
Nationality: Brazilian
Marital status: unmarried
Address: Schikaneder Straße, 3, 93053 Regensburg

Education

1994-1997: High school at the Salesiano Dom Bosco School

Studies

1997-2001: Graduation in Pharmacy Biochemistry at the UNIDERP University, Campo
Grande, Mato Grosso do Sul, Brazil.
Title of diploma thesis: "Risk factors for enteroparasites genesis/Boa
Sorte, city of Corguinho, state Mato Grosso do Sul/Brazil", Supervisor:
Prof. Dra. Vania Lucia Brandao Nunes.

2005-2007: Master degree in Bioscience Applied to Pharmacy at the Department of
Clinical, Toxicological, and Bromatological Analysis, Faculty of
Pharmaceutical Sciences of Ribeirão Preto, University of São Paulo,
Ribeirão Preto, SP, Brazil.
Title of thesis: "Selection, identification and determination of functional
parameters of photosensitizers with antifungal action". Supervisor: Prof.
Dr. Gilberto Úbida Leite Braga.

2009-2013: Ph.D. student at the Institute of Analytical Chemistry, Chemo-and
Biosensors, University of Regensburg, Germany.
Title of thesis: "Photodynamic inactivation of microbial biofilms: impact
of Hsp70 expression and non-invasive optical monitoring of oxygen
during photodynamic inactivation", Supervisor: Prof. Dr. Otto Wolfbeis
and PD Dr. Tim Maisch

11 List of publications (peer-reviewed journals) and presentations

Publications

Fungicidal photodynamic effect of a two positively charged porphyrin against *Candida albicans* biofilm cells. Gonzales, F.P., Felgenträger, A., Bäumler, W., Maisch, T.; *Future Microbiology*. (2013) 8, p. 785-797.

Ion induced stacking of photosensitizer molecules can remarkably affect the luminescence detection of singlet oxygen in *Candida albicans* cells. Felgenträger, A., Gonzales, F.P., Maisch, T., Bäumler, W.; *Journal of Biomedical Optics*. (2013) 18, p. 045002-1-045002-8.

Dirty hands: photodynamic killing of human pathogens like EHEC, MRSA and Candida within seconds. Eichner, A., Gonzales, F.P., Felgenträger, A., Regensburger, J., Holzmann, T., Schneider, W., Bäumler, W., Maisch, T.; *Photochemical & Photobiological Sciences*. (2012) 1, p. 135-147.

Photodynamic inactivation for controlling *Candida albicans* infections. Pereira Gonzales F. and Maisch T. *Fungal Biology*. (2011) 116, p. 1-10.

XF drugs: A new family of antibacterials. Pereira Gonzales F. and Maisch T. *Drug News & Perspectives*. (2010) 23, p. 167-174.

Photodynamic inactivation of microorganisms as an innovative approach to kill mucocutaneous and skin microorganisms. Pereira Gonzales F. and Maisch T. *Giornale italiano di dermatologia e venereologia*. (2010) 145, p. 477-489.

Oral presentations

Photodynamic effect of a two-fold positively charged porphyrin-derivative against *Candida albicans* **biofilm in vitro.** Gonzales, F.P., Felgenträger, A., Regensburger, J.; Bäumler, W. Maisch, T.; 9th International Symposium on Photodynamic Therapy and Photodiagnosis in Clinical Practice, Brixen, Brixen-Bressanone, Italy. (October 16-20, 2012).

Photodynamic inactivation of *Candida albicans* **in planktonic and biofilm-grown cells by a two-fold positive charged porphyrine-derivative and visible light.** Gonzales, F.P., Felgenträger, A., Maisch, T. 35th Meeting of the American Society for Photobiology, Providence, RI, USA (June 12-16, 2010).

Poster presentations

Role of *Candida albicans* **Heat Shock Protein 70 (HSP70) to Photodynamic Therapy.** Gonzales, F.P., Maisch, T. 36th meeting of the American Society for Photobiology **(ASP),** Montreal, Canada. (June 23-27, 2012).

Investigation of *Candida albicans* **Heat Shock Response to Photodynamic Therapy.** Gonzales, F.P., Maisch, T. 39th Annual Meeting of the European Society for Dermatological Research (ADF), Marburg, Germany (March, 1-3, 2012).

Susceptibility of *Candida albicans* **biofilm to photodynamic therapy with a porphyrin derivative and visible light.** Gonzales, F.P., Felgenträger, A., Maisch, T. 8th International Symposium on Photodynamic Therapy and Photodiagnosis in Clinical Practice, Brixen-Bressanone, Italy. (October 6-9, 2010).

Photodynamic inactivation of *Candida albicans* **biofilm: detection of singlet oxygen luminescence and phototoxic efficacy.** Felgenträger, A., Gonzales, F.P., Maisch, T. 35th Meeting of the American Society for Photobiology, Providence, RI, USA. (June 12-16, 2010).

Photodynamic fungicidal effect of a two-fold positive charged porphyrine derivative and visible light against *Candida albicans.* Gonzales, F.P., Felgenträger, A., Lehner, K., Maisch, T. 37th Annual Meeting of the European Society for Dermatological Research (ADF) Lübeck, Germany**.** (February, 6-10, 2010).

12 Lectures

Seminar about „Aktuelle Themen zur Inaktivierung von Mikroorganismen" by PD. Dr.
Tim Maisch.
Winter and sommer semester 2010, 2011 and 2012.

Seminar about „Photodynamisch-mikrobielles Seminar" by PD. Dr. Tim Maisch.
Winter and summer semester 2010, 2011 and 2012.

Bioanalytical Chemistry II by Prof. Otto Wolfbeis.
Summer semester 2011.

Bioanalytical Chemistry I by Prof. Otto Wolfbeis.
Winter semester 2011.

13 Eidesstattliche Erklärung

Ich erkläre hiermit an Eides statt, dass ich die vorliegende Arbeit ohne unzulässige Hilfe Dritter und ohne Benutzung anderer als der angegebenen Hilfsmittel angefertigt habe; die aus anderen Quellen direkt oder indirekt übernommenen Daten und Konzepte sind unter Angabe des Literaturzitats gekennzeichnet. Weitere Personen waren an der inhaltlich materiellen Herstellung der vorliegenden Arbeit nicht beteiligt. Insbesondere habe ich hierfür nicht die entgeltliche Hilfe eines Promotionsberaters oder anderer Personen in Anspruch genommen. Niemand hat von mir weder unmittelbar noch mittelbar geldwerte Leistungen für Arbeiten erhalten, die im Zusammenhang mit dem Inhalt der vorgelegten Dissertation stehen. Diese Arbeit wurde bisher weder im In- noch im Ausland in gleicher oder ähnlicher Form einer anderen Prüfungsbehörde vorgelegt.

Regensburg, den 08.04.2013

Fernanda Pereira Gonzales